



LUND UNIVERSITY

Endogenous modulators of hyperexcitability in epilepsy: electrophysiological and optogenetic delineation of neuropeptide Y mechanisms in interneurons

Ledri, Marco

2012

[Link to publication](#)

Citation for published version (APA):

Ledri, M. (2012). *Endogenous modulators of hyperexcitability in epilepsy: electrophysiological and optogenetic delineation of neuropeptide Y mechanisms in interneurons*. [Doctoral Thesis (compilation), Neurology, Lund]. Experimental Epilepsy Group, Division of Neurology, Department of Clinical Sciences.

Total number of authors:

1

General rights

Unless other specific re-use rights are stated the following general rights apply:

Copyright and moral rights for the publications made accessible in the public portal are retained by the authors and/or other copyright owners and it is a condition of accessing publications that users recognise and abide by the legal requirements associated with these rights.

- Users may download and print one copy of any publication from the public portal for the purpose of private study or research.
- You may not further distribute the material or use it for any profit-making activity or commercial gain
- You may freely distribute the URL identifying the publication in the public portal

Read more about Creative commons licenses: <https://creativecommons.org/licenses/>

Take down policy

If you believe that this document breaches copyright please contact us providing details, and we will remove access to the work immediately and investigate your claim.

LUND UNIVERSITY

PO Box 117
221 00 Lund
+46 46-222 00 00

Endogenous modulators of hyperexcitability in epilepsy:

*electrophysiological and optogenetic delineation of
neuropeptide Y mechanisms in interneurons*



LUND
UNIVERSITY

av

Marco Ledri

Fakultetsopponent:

Prof. Dimitri Kullmann
UCL Institute of Neurology
Queen Square, London, UK

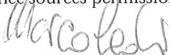
AKADEMISK AVHANDLING

som för avläggande av filosofie doktorsexamen
vid Medicinska fakulteten, Lunds universitet,
kommer att offentligen försvaras i Segerfalksalen, Wallenberg Neurocentrum, Lund,
fredagen den 27 april 2012, kl. 9.15

Organization LUND UNIVERSITY Department of Clinical Sciences Division of Neurology Lund, Sweden	Document name DOCTORAL DISSERTATION	
	Date of issue April 27, 2012	
	Sponsoring organization	
Author(s) Marco Ledri		
Title and subtitle Endogenous modulators of hyperexcitability in epilepsy: electrophysiological and optogenetic delineation of neuropeptide Y mechanisms in interneurons		
Abstract <p>Epilepsy is one of the most common neurological disorders worldwide, affecting 1% of the general population, and is characterized by a predisposition for the generation of epileptic seizures. Despite having several different aetiologies, a common underlying cause of epilepsy seems to be an acquired imbalance between excitatory and inhibitory circuits in the brain, which leads to hyperexcitability and appearance of seizures. Current treatment relies on the use of antiepileptic drugs (AEDs), but these only treat the symptoms, not affect the causes of the disease, and trigger undesirable side effects because of their systemic administration. Recent advancements in drug discovery have led to the development of new AEDs that are better tolerated and with improved pharmacokinetics, but 30-40% of all patients with epilepsy, and particularly those with temporal lobe epilepsy (TLE) remain resistant to the treatment. Thus, there is an urgent need for developing new antiepileptic treatment strategies.</p> <p>In the last years, research on novel antiepileptic treatments has identified several endogenous molecules as potential new targets for therapeutic intervention. Among these, neuropeptide Y (NPY) seems to be a particularly promising target, as it plays an important role in controlling neuronal excitability in different brain areas, including the hippocampus. Indeed, overexpression of NPY via gene therapy approaches in animal models of epilepsy has profound effects on seizure generation and suppression, providing proof of principle evidence that such approach could be successfully used to reduce and control seizures. The actions of NPY are mediated by various receptors, and their activation predominantly causes suppression of glutamatergic synaptic transmission, which leads to decreased excitability. However, little is known about the effect NPY has on GABAergic inhibitory cell populations, and NPY mechanisms of action have to be carefully determined if such an approach could be used in humans.</p> <p>There are several different subtypes of inhibitory cell populations in all cortical areas, and each of them serve a different function with distinct roles in controlling network activity. Perisomatic-targeting interneurons comprise those inhibitory cell types that form synapses onto the perisomatic region of target cells, an area including the cell soma, proximal dendrites and axon initial segment. Thanks to the strategic location of their targets, perisomatic interneurons are particularly suited to control the output of large numbers of excitatory principal cells, with major impact on the network excitability. Two main subclasses, called basket cells, make up the majority of perisomatic interneurons, and their classification is based on the expression of either the neuropeptide Cholecystokinin (CCK) or the calcium binding protein Parvalbumin (PV). PV-basket cells are thought to be important for the generation of gamma-frequency oscillations, while CCK-basket cells are proposed to modulate this activity. Since gamma oscillations can convert into higher frequency epileptiform activity, and NPY strongly modulates network excitability, this thesis aimed to investigate the effects of NPY on CCK- and PV- basket cells, to understand if actions of NPY on perisomatic interneurons could contribute to its seizure-suppressant effects.</p> <p>Using transgenic mice, electrophysiological and optogenetic techniques, the evidence provided in this thesis demonstrates that NPY strongly modulates excitatory and inhibitory incoming synaptic transmission onto CCK-basket cells, but does not directly affect PV cell output onto principal cells. These effects could alter the way CCK-basket cells react to network activity, and have potential impacts on network excitability. In addition, we show that hyperexcitability enhances GABAergic output from PV cells, uncovering a potential mechanism that could increase principal cell synchrony and contribute to the generation of seizures.</p>		
Key words: Epilepsy, Neuropeptide Y, interneurons, synaptic transmission, synaptic plasticity, optogenetics, electrophysiology, hippocampus		
Classification system and/or index terms (if any):		
Supplementary bibliographical information:		Language English
ISSN and key title: 1652-8220		ISBN 978-91-86871-95-6
Recipient's notes	Number of pages 133	Price
	Security classification	

Distribution by (name and address)

I, the undersigned, being the copyright owner of the abstract of the above-mentioned dissertation, hereby grant to all reference sources permission to publish and disseminate the abstract of the above-mentioned dissertation.

Signature 

Date **2012-03-19**

Endogenous modulators of hyperexcitability in epilepsy:

electrophysiological and optogenetic delineation of
neuropeptide Y mechanisms in interneurons

Marco Ledri

Experimental Epilepsy Group
Division of Neurology
Department of Clinical Sciences
Lund University Hospital
Sweden



LUND
UNIVERSITY

Academic Dissertation
Lund 2012

Cover picture

Drawing illustrating CCK- (red) and PV- (green) basket cells morphology in the dentate gyrus, and NPY application

Cover artwork by Marco Ledri and Bengt Mattsson

ISSN 1652-8220

ISBN 978-91-86871-95-6

Lund University, Faculty of Medicine Doctoral Dissertation Series 2012:33

© Marco Ledri and the respective publishers

Printed by Media Tryck, Lund University

to both my grandads

Don't look for problems but find solutions.
Everybody is good at complaining.

Index

Summary	13
Riassunto in italiano	15
Original papers and manuscripts	17
Publications not included in the thesis	18
List of abbreviations	19
1 Introduction	21
1.1 Epilepsy	21
1.1.1 Definition of epilepsy	21
1.1.2 Current treatment	22
1.2 The hippocampal formation	23
1.2.1 Anatomy and organization	23
1.2.2 Interneurons	23
1.2.3 Basket cells	25
1.2.4 Alterations of hippocampal networks in epilepsy	27
1.3 Neuropeptide Y	28
1.3.1 NPY and its receptors	28
1.3.2 NPY in epilepsy and seizures	29
1.3.3 NPY and basket cells	30
1.4 Optogenetics	32
1.4.1 Channelrhodopsin-2	32
1.4.2 Targeting and delivery strategies	33
2 Aims of the thesis.....	37
3 Experimental procedure.....	39
3.1 Animals	39
3.2 Viral vector production	39
3.3 Electrode implantation and virus injection.....	40
3.4 Rapid kindling and test stimulations.....	41
3.4.1 Test stimulations	41
3.5 Slice preparation.....	42
3.6 Electrophysiology.....	42
3.6.1 Principles of whole-cell electrophysiology.....	42
3.6.2 Whole-cell electrophysiology	43

3.6.3	Stimulation protocols	45
3.6.4	NPY application.....	46
3.6.5	Data acquisition	46
3.7	Immunohistochemical procedures.....	46
3.7.1	Immunostaining.....	46
3.7.2	Axonal arbour reconstruction.....	47
3.7.3	Y2 immunohistochemistry and optical density measurements.....	48
3.8	Statistics	48
4	Results and comments	51
4.1	Effects of NPY on CCK-basket cells.....	51
4.1.1	Identification of CCK-basket cells.....	51
4.1.2	Intrinsic membrane properties	52
4.1.3	Spontaneous excitatory synaptic transmission.....	52
4.1.4	Evoked excitatory synaptic transmission and short-term plasticity	52
4.1.5	Spontaneous inhibitory synaptic transmission	54
4.1.6	Differential effects of NPY on perisomatic and dendritic inhibitory synapses	54
4.1.7	Evoked inhibitory synaptic transmission.....	55
4.1.8	Expression of Y2 receptors	56
4.2	Effects of NPY on PV cells.....	56
4.2.1	Expression of ChR2 in PV cells.....	56
4.2.2	NPY does not affect PV-GC synapses	57
4.2.3	Hyper-excitability alters GABA release at PV-GC synapses	58
5	General discussion.....	59
5.1	NPY and CCK-basket cells	59
5.1.1	Identification of CCK-basket cells.....	59
5.1.2	Generation of hyper-excitability.....	60
5.1.3	Excitatory input onto CCK-basket cells	60
5.1.4	Inhibitory input onto CCK-basket cells.....	61
5.1.5	Functional implications	62
5.2	NPY and PV cells	65
5.2.1	Stimulation of PV cells.....	65
5.2.2	NPY on PV-GC synapses	66

5.2.3	Enhanced GABA release at PV-GC synapses	66
5.2.4	Functional implications	67
6	Concluding remarks.....	69
	Acknowledgements.....	71
	References.....	75
	Appendix.....	83
	Paper I.....	83
	Paper II	99
	Paper III.....	119

Summary

Epilepsy is one of the most common neurological disorders worldwide, affecting 1% of the general population, and is characterized by a predisposition for the generation of epileptic seizures. Despite having several different aetiologies, a common underlying cause of epilepsy seems to be an acquired imbalance between excitatory and inhibitory circuits in the brain, which leads to hyperexcitability and appearance of seizures. Current treatment relies on the use of antiepileptic drugs (AEDs), but these only treat the symptoms, not affect the causes of the disease, and trigger undesirable side effects because of their systemic administration. Recent advancements in drug discovery have led to the development of new AEDs that are better tolerated and with improved pharmacokinetics, but 30–40% of all patients with epilepsy, and particularly those with temporal lobe epilepsy (TLE) remain resistant to the treatment. Thus, there is an urgent need for developing new antiepileptic treatment strategies.

In the last years, research on novel antiepileptic treatments has identified several endogenous molecules as potential new targets for therapeutic intervention. Among these, neuropeptide Y (NPY) seems to be a particularly promising target, as it plays an important role in controlling neuronal excitability in different brain areas, including the hippocampus. Indeed, overexpression of NPY via gene therapy approaches in animal models of epilepsy has profound effects on seizure generation and suppression, providing proof of principle evidence that such approach could be successfully used to reduce and control seizures. The actions of NPY are mediated by various receptors, and their activation predominantly causes suppression of glutamatergic synaptic transmission, which leads to decreased excitability. However, little is known about the effect NPY has on GABAergic inhibitory cell populations, and NPY mechanisms of action have to be carefully determined if such an approach could be used in humans.

There are several different subtypes of inhibitory cell populations in all cortical areas, and each of them serve a different function with distinct roles in controlling network activity. Perisomatic-targeting interneurons comprise those inhibitory cell types that form synapses onto the perisomatic region of target cells, an area including the cell soma, proximal dendrites and axon initial segment. Thanks to the strategic location of their targets, perisomatic interneurons are particularly suited to control the output of large numbers of excitatory principal cells, with major impact on the network excitability. Two main subclasses, called basket cells, make up the majority of perisomatic interneurons, and their classification is based on the expression of either the neuropeptide Cholecystokinin (CCK) or the calcium binding protein Parvalbumin (PV). PV-basket cells are thought to

be important for the generation of gamma-frequency oscillations, while CCK-basket cells are proposed to modulate this activity. Since gamma oscillations can convert into higher frequency epileptiform activity, and NPY strongly modulates network excitability, this thesis aimed to investigate the effects of NPY on CCK- and PV- basket cells, to understand if actions of NPY on perisomatic interneurons could contribute to its seizure-suppressant effects.

Using transgenic mice, electrophysiological and optogenetic techniques, the evidence provided in this thesis demonstrates that NPY strongly modulates excitatory and inhibitory incoming synaptic transmission onto CCK-basket cells, but does not directly affect PV cell output onto principal cells. These effects could alter the way CCK-basket cells react to network activity, and have potential impacts on network excitability. In addition, we show that hyperexcitability enhances GABAergic output from PV cells, uncovering a potential mechanism that could increase principal cell synchrony and contribute to the generation of seizures.

Riassunto in italiano

L'epilessia, caratterizzata dalla predisposizione a generare attacchi epilettici, è uno dei disturbi neurologici più comuni, e colpisce l'uno per cento della popolazione mondiale. Pur avendo diverse eziologie, la causa comune sembra essere uno squilibrio tra i circuiti eccitatori e inibitori cerebrali, con conseguente ipereccitabilità e manifestazione di attacchi epilettici. Attualmente, il trattamento più utilizzato si basa sull'uso di farmaci antiepilettici (AEDs), pur essendo solamente sintomatico e presentando effetti collaterali a causa della somministrazione sistemica. Recenti progressi nella ricerca hanno portato alla scoperta di nuovi farmaci, più tollerabili e con migliori proprietà farmacocinetiche, ma il 30-40% dei pazienti, e in particolare quelli con epilessia del lobo temporale (TLE), rimane resistente al trattamento. Per questi motivi quindi, è necessario sviluppare nuove strategie terapeutiche in questo campo.

Negli ultimi anni, la ricerca di nuove terapie antiepilettiche ha portato all'identificazione di diverse molecole endogene come nuovi potenziali bersagli per l'intervento terapeutico. Tra questi, il neuropeptide Y (NPY) sembra essere particolarmente promettente, svolgendo un ruolo importante nel controllo dell'eccitabilità in diverse aree cerebrali, tra cui l'ippocampo. Infatti, la sovraespressione di NPY tramite approcci di terapia genica in modelli animali di epilessia, ha effetti profondi sulla generazione di attacchi epilettici, e sembra essere particolarmente promettente per ridurre e controllare le convulsioni. Le azioni di NPY sono mediate da diversi recettori, la cui attivazione provoca una soppressione della trasmissione sinaptica glutamatergica, con conseguente diminuzione dell'eccitabilità del sistema. Tuttavia, la conoscenza riguardo gli effetti di NPY sulle popolazioni di cellule inibitorie GABAergiche è ancora molto limitata, ed è quindi necessario uno studio approfondito sui meccanismi di azione di NPY per determinare se tale approccio possa essere usato in clinica.

Esistono diversi sottotipi di cellule inibitorie in tutte le aree corticali, ognuna con diverse funzioni e ruoli nel controllo dell'attività cerebrale. Gli interneuroni perisomatici formano sinapsi nella regione perisomatica di altri neuroni, in un'area che comprende il corpo cellulare, i dendriti prossimali e il segmento iniziale dell'assone. Grazie alla collocazione strategica delle loro sinapsi, gli interneuroni perisomatici sono particolarmente adatti al controllo dell'output di un gran numero di cellule eccitatorie principali, ed esercitano un notevole impatto sull'eccitabilità generale dell'intero circuito. I due sottotipi principali di cellule basket comprendono la maggior parte degli interneuroni perisomatici, e la loro suddivisione è basata sull'espressione del neuropeptide Colecistochinina (CCK) o della Parvalbumina (PV), proteina che lega il calcio. Le cellule PV-

basket sono ritenute importanti per la generazione di oscillazioni a frequenza gamma, mentre le cellule CCK-basket sembrano avere un ruolo modulatorio. Poiché le oscillazioni gamma possono trasformarsi in attività epilettica ad alta frequenza e NPY modula fortemente l'eccitabilità del network, la presente tesi ha lo scopo di studiare gli effetti di NPY sulle cellule CCK e PV, per capire se le azioni di NPY sugli interneuroni perisomatici possano contribuire ai suoi effetti di soppressione degli attacchi epilettici.

Mediante l'utilizzo di topi transgenici, tecniche elettrofisiologiche e optogenetiche, i risultati riportati in questa tesi dimostrano che NPY modula fortemente la trasmissione sinaptica afferente, eccitatoria e inibitoria, sulle cellule CCK-basket, ma non modifica direttamente l'output da cellule PV sulle cellule principali. Tali effetti potrebbero alterare la reattività delle cellule CCK-basket all'attività del circuito circostante, e potenzialmente modificare l'eccitabilità del sistema. Inoltre, gli studi presentati in questa tesi dimostrano che, in condizioni di ipereccitabilità, la trasmissione sinaptica GABAergica delle cellule PV è potenziata, svelando un possibile meccanismo in grado di aumentare la sincronia di gruppi di cellule principali, contribuendo in tal modo alla generazione di attacchi epilettici.

Original papers and manuscripts

The present thesis is based on the following papers, which will be referred to by their roman numerals:

I. **Ledri M**, Sørensen AT, Erdelyi F, Szabo G, Kokaia M, *Tuning afferent synapses of hippocampal interneurons by neuropeptide Y*, Hippocampus 2011 Feb;21(2):198-211

II. **Ledri M**, Nikitidou L, Erdelyi F, Szabo G, Kirik D, Deisseroth K, Kokaia M, *Altered profile of basket cell afferent synapses in hyper-excitable dentate gyrus revealed by optogenetic and two-pathway stimulations*, Eur J Neuroscience, *in press*

III. **Ledri M**, Nikitidou L, Madsen M, Kirik D, Deisseroth K, Kokaia M, *Optogenetics reveal enhanced GABA release at perisomatic inhibitory synapses of dentate gyrus granule cells in hyper-excitable hippocampus*, Manuscript

Publications not included in the thesis

Kanter-Schlifke I, Toft Sørensen A, **Ledri M**, Kuteeva E, Hökfelt T, Kokaia M, *Galanin gene transfer curtails generalized seizures in kindled rats without altering hippocampal synaptic plasticity*, Neuroscience. 2007 Dec 19;150(4):984-92

Sørensen AT, Nikitidou L, **Ledri M**, Lin EJ, During MJ, Kanter-Schlifke I, Kokaia M, *Hippocampal NPY gene transfer attenuates seizures without affecting epilepsy-induced impairment of LTP*, Exp Neurol. 2009 Feb;215(2):328-33

Kokaia M, Andersson M, **Ledri M**, *An optogenetic approach to epilepsy*, Neuropharmacology, invited review, submitted

List of abbreviations

AAV	Adeno-Associated Virus
ACh	Acetylcholine
AD	Afterdischarge
AED	Antiepileptic Drug
AMPA	Alpha-amino-3-hydroxy-5-methyl-4-isoxazolepropionic Acid
CA	Cornus Ammonis
CaMKIIα	Calcium/Calmodulin Kinase 2 alpha
CCK	Cholecystokinin
ChR2	Channelrhodopsin-2
CR-IS	Calretinin-positive Interneuron Specific (interneuron)
DAB	D-Amino Benzidine
DIO	Double Inverted Open Reading frame
EEG	Electroencephalogram
EF1α	Elongation Factor 1 alpha
GABA	Gamma-AminoButyric Acid
GAD65	Glutamate Acid Decarboxylase 65
GC	Granule cell
GFP	Green Fluorescent Protein
GIRK	G-protein coupled Inward Rectifier Potassium (current)
HICAP	Hilar Commissural-Associational Pathway related cell
HIPP	Hilar Perforant-Path Associated cell
ISI	Inter Stimulus Interval
leE(I)PSC	light-evoked Excitatory (Inhibitory) Post-synaptic Current
mEPSC	miniature Excitatory Post-synaptic Current
mIPSC	miniature Inhibitory Post-synaptic Current
NMDA	N-Methyl-D-Aspartic Acid
NPY	Neuropeptide Y
PPD	Paired Pulse Depression

- PPF** Paired Pulse Facilitation
PTX Picrotoxin
PV Parvalbumin
RRP Readily Releasable Pool
sEPSC spontaneous Excitatory Post-synaptic Current
sIPSC spontaneous Inhibitory Post-synaptic Current
SS Somatostatin
STIB Stimulation-Induced Bursting
TLE Temporal Lobe Epilepsy
VGCC Voltage-Gated Calcium Channel

1 Introduction

1.1 Epilepsy

1.1.1 Definition of epilepsy

Epilepsy is one of the most common neurological disorders worldwide, and is defined by the International League Against Epilepsy as “*a disorder of the brain characterized by an enduring predisposition to generate epileptic seizures and by the neurobiologic, cognitive, psychological and social consequences of this condition*” (Fisher et al., 2005). It affects about 1% of the general population, can occur at all ages, although it is most common in children and the elderly, and represent an enormous financial burden for society, with almost 10 billion dollars spent yearly in the United States alone. Epilepsy is not one single disease, but rather a family of disorders of several different aetiologies. Epilepsy can develop from head injuries, brain tumors, stroke, infections, but can also be the result of inherited genetic mutations in genes important for controlling neuronal excitability, or have no apparent cause (idiopathic epilepsy). Regardless of the cause, epilepsy manifests with the appearance of epileptic seizures, defined as “*a transient occurrence of signs and/or symptoms due to abnormal excessive or synchronous neuronal activity in the brain*” (Fisher et al., 2005). Seizures can have diverse symptomatic appearances: they can vary from a momentary loss of awareness, to short periods of unconsciousness, to highly generalized convulsions. The classification of seizures is a continuously evolving topic, but it recognizes two main categories, partial and generalized (Seino, 2006). Partial seizures involve one confined brain area, at least initially, while generalized seizures are produced by abnormal activity throughout the entire brain.

The most common form of epilepsy in humans is temporal lobe epilepsy (TLE), characterized by the appearance of partial complex seizures, often with secondary generalization. In TLE, seizures usually start from a confined brain

area within limbic structures such as the amygdala, temporal neocortex or hippocampal formation, and eventually generalize and involve the entire brain (Engel, 2001). Approximately two thirds of patients with TLE have hippocampal sclerosis as the pathological substrate, consisting of cell loss in certain regions of the hippocampal formation (Engel, 2001). Due to the complex aetiology of epilepsy in general and TLE in particular, it is difficult to isolate a single cause underlying the cell loss, but it is thought that the original insult triggers a cascade of events that result in network reorganization and development of hyper-excitability, reducing the threshold for seizure generation, ultimately making the network more prone to develop abnormal activity.

1.1.2 Current treatment

The treatment for epilepsy is largely dependent on the frequency, severity and types of seizures, but the use of anti-epileptic drugs (AEDs) is the first and most common therapeutic approach. In general, AEDs are designed to counteract the hyper-excitability that has developed in the epileptic environment, and to restore the normal balance between excitation and inhibition of the network by increasing the net inhibitory drive. Such drugs rely on increasing GABAergic transmission, limiting GABA uptake, decreasing glutamatergic excitatory transmission, interfering with the function of sodium channels important for action potential generation, or by generally reducing neurotransmission by blocking calcium channels. However, AEDs efficiency is widely variable, and up to 40% of patients, and particularly those with TLE, fail to respond significantly to the treatment and develop pharmaco-resistant epilepsy. Surgical resection of an identified seizure focus remains the last treatment option, but can only be performed on a well-selected cohort of candidates, which represent a minority (Engel et al., 2003).

One of the main problems with AEDs is the fact that they do not modify the disease process, but can only control the symptoms, while inevitably giving rise to several side effects due to the systemic administration. Recent development of new AEDs classes has provided some advantages in terms of simpler pharmacokinetics, fewer interactions and better tolerance, but their efficacy has not been demonstrated to be superior to older drugs, leaving a significant amount of patients still with intractable epilepsy. Therefore, the development of novel treatment strategies is highly needed. Ideally, the treatment should be administered only where needed, by targeting specific regions involved in seizure generation or propagation, and only affect cell types responsible for seizure control, leaving others unaltered to limit potential side effects. The nature of TLE makes it particularly suitable as a target for such treatment, since the seizure focus is mostly confined to specific brain regions (e.g. the hippocampal formation).

1.2 The hippocampal formation

1.2.1 Anatomy and organization

The hippocampal formation is a structure located within the medial temporal lobe, and comprises the hippocampus proper, the dentate gyrus and the subiculum. The hippocampus proper (also known as Cornus Ammonis, or CA) is further divided in three main subfields (CA1, CA2 and CA3), while the dentate gyrus also includes the hilar region (Witter and Amaral, 2004). The principal cells in the hippocampus proper and subiculum are the pyramidal cells, and the principal cells in the dentate gyrus are the granule cells (Witter and Amaral, 2004). The hippocampal formation has a central role in the sensory integration system, thanks to the variety of inputs it receives from cortical regions, including visual, somatosensory, olfactory and auditory cortices (Lavenex and Amaral, 2000).

The sensory input from these various regions, carrying information about the external world, is conveyed to the entorhinal cortex, which represents the main excitatory afferent of the hippocampal formation. Entorhinal cortex axons enter the dentate gyrus via the perforant pathway. Afferents from the lateral entorhinal cortex terminate in the outer-third, and those from the medial terminate in the middle-third of the molecular layer, where they contact the dendritic trees of granule cells. Granule cells axons, the so-called mossy fibers, originate from the opposite pole of the granule cell somas and enter the hilus. Here they give rise to several collaterals, before travelling to the CA3 region and contacting proximal dendrites of pyramidal cells. Pyramidal cells in CA3 then project via Schaffer collateral fibers to CA1 pyramidal neurons, which in turn connect to pyramidal cells of the subiculum via the alveus. Finally, projections from pyramidal neurons of the subiculum exit the hippocampus and reach the deep layers of the entorhinal cortex, completing the circuit (Figure 1). This particular and largely unidirectional arrangement of hippocampal connectivity has been referred to as *feed-forward tri-synaptic circuit* (Andersen et al., 1969).

Besides receiving input from the entorhinal cortex, the hippocampal formation also receives a variety of extrinsic inputs from projections of cholinergic, noradrenergic, serotonergic and dopaminergic nuclei (Witter and Amaral, 2004). Intrinsic input is mediated by local GABAergic interneurons and several modulating neuropeptides (Carnahan and Nawa, 1995). Both intrinsic and extrinsic inputs to the hippocampal formation are believed to be important for controlling its proper function, such as spatial coding and memory.

1.2.2 Interneurons

In the hippocampal formation, two main cell types account for the vast majority of cells present in all regions: principal cells and interneurons. Principal

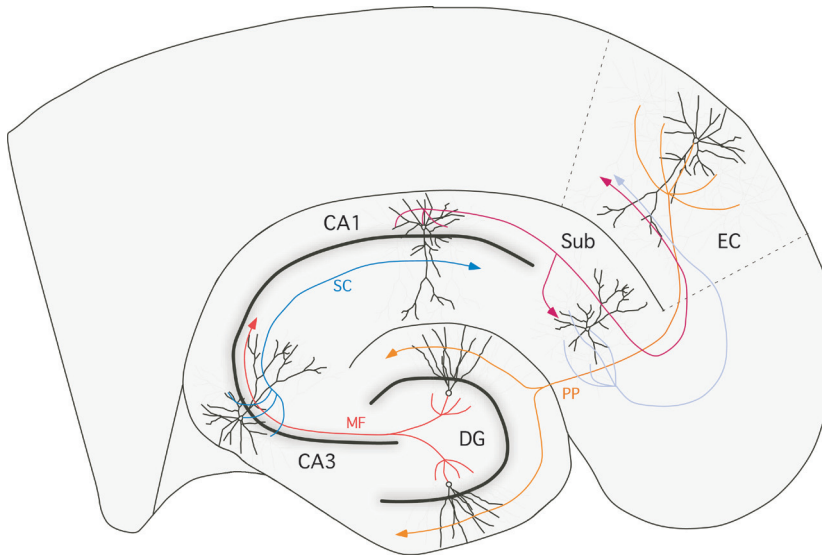


Figure 1: Main glutamatergic pathways connecting principal cell subfields of the hippocampal formation. EC, Entorhinal Cortex; Sub, Subiculum; DG, Dentate Gyrus; PP, Perforant Pathway; MF, Mossy Fibers; SC, Schaffer Collaterals

cells use glutamate as their main neurotransmitter, are excitatory, and are typically organized in tightly packed cell layers, with the exception of the subiculum. On the other hand, interneurons use GABA as principal neurotransmitter, are inhibitory, do not form layers but are rather dispersed throughout all regions of the hippocampal formation. Despite the common feature of using GABA as inhibitory neurotransmitter, interneurons in the hippocampus are remarkably heterogeneous. There are at least 16 distinct types of GABAergic interneurons identified in all major areas of the hippocampus (Freund and Buzsaki, 1996; Somogyi and Klausberger, 2005; Houser, 2007), and their classification is based on their molecular expression profile, firing pattern and innervation of distinct subcellular domains of principal cells (a representation of interneuron diversity is depicted in Figure 2). GABAergic synapses cover almost the entire membrane surface of principal cells, from the axon initial segment to the tip of basal and apical dendritic shafts. Synapses on different domains of principal cells are provided by different classes of interneurons, and although a complete understanding of interneuron diversity has not yet been achieved, an important dichotomy in the inhibitory control of principal cells has been established. Based on the targeted domain of principal cells, interneurons can be broadly divided into two main populations: those that contact principal cells in the perisomatic or the dendritic region (Freund and Buzsaki, 1996).

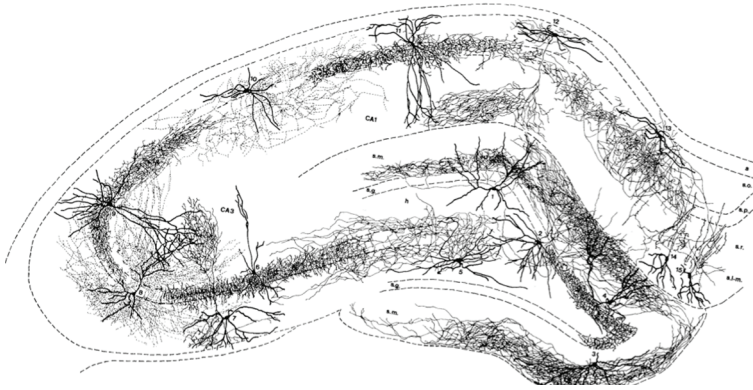


Figure 2: Composite drawing of characteristic interneuron subtypes exemplifying the diversity of hippocampal GABAergic cells. Reprinted with permission from Freund and Buzsaki, 1996

The function of GABAergic interneurons is to provide basic inhibition, but also to shape the spatial and temporal profile of principal cell activity. In this context, dendritic inhibition is thought to be important for regulating plasticity of glutamatergic excitatory dendritic inputs from other principal cells and remote excitatory afferents (Miles et al., 1996). On the other hand, perisomatic inhibition is strategically located to control the output of principal cells, and seem to be important for coordinating and synchronizing the activity of large numbers of principal cells (Miles et al., 1996).

1.2.3 Basket cells

Two types of perisomatic inhibitory cells have been identified in the hippocampus: chandelier (or axo-axonic) cells and basket cells (Freund and Buzsaki, 1996). Chandelier cells are highly specialized in innervating the axon initial segment of principal cells, while basket cell axons form synapses in a region including the cell soma and proximal dendrites of target cells (Freund and Buzsaki, 1996).

Basket cells are the most abundant perisomatic inhibitory cell type of the hippocampus. There are two major subtypes of basket cells in all main regions of the hippocampus, and their classification is based primarily on the expression of either the calcium binding protein Parvalbumin (PV), or the neuropeptide Cholecystokinin (CCK) (Freund and Katona, 2007). These two types of basket cells represent remarkable examples of how the diversity of GABAergic interneurons has evolved to serve specific tasks in complex neuronal networks. Although their location and somatodendritic morphology are extremely similar, their electrical properties and especially their role in the hippocampal network are very different.

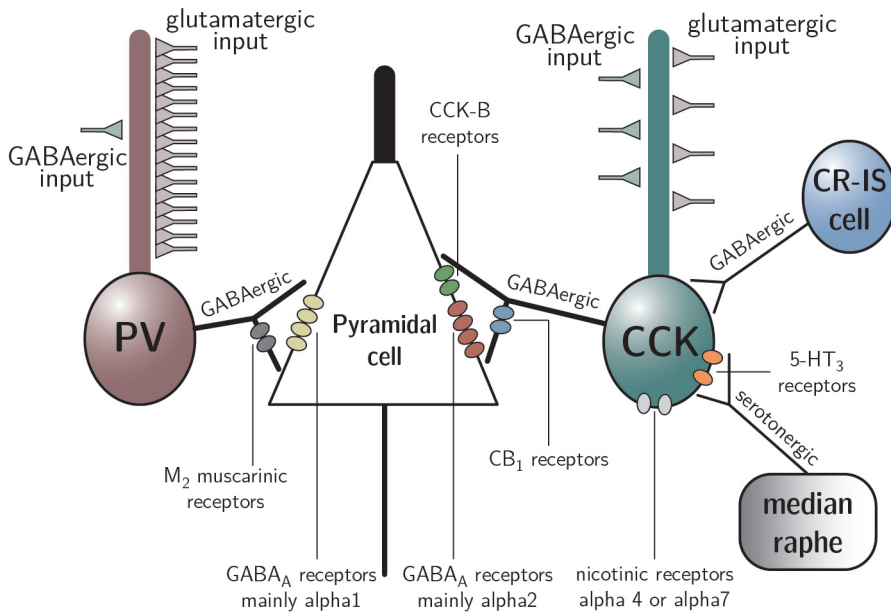


Figure 3: Major differences between PV- and CCK-basket cells in their connectivity and receptor expression patterns, underlying the different network integration and function. The modulatory function of CCK-basket cells is provided by the expression of a variety of modulatory receptors (CB1, nicotinic and 5-HT₃) that are absent on PV-basket cells. Adapted from Freund, 2003.

PV-basket cells are capable of firing high-frequency action potential without accommodation, release GABA with high synchrony (Hefft and Jonas, 2005) and are thought to act as clockworks for cortical network oscillations (Freund, 2003), by functioning as an ensemble inter-connected via both electrical and chemical synapses (Galarreta and Hestrin, 1999; Traub et al., 2001). On the other hand, CCK-basket cells fire accommodating action potential trains, express a variety of modulatory receptors on their membranes (5-HT₃, nicotinic alpha4 and alpha7, and CB1 receptors, Figure 3) (Freedman et al., 1993; Katona et al., 1999; Porter et al., 1999; Ferezou et al., 2002), and are thought to act as fine-tuning devices that modulate network oscillations generated by PV-basket cells (Freund, 2003; Freund and Katona, 2007). Further supporting the evidence of this functional dichotomy is the difference in the synaptic afferent profile of the two basket cell types. PV-basket cells receive three times more glutamatergic input (Gulyas et al., 1999), but CCK-basket cells seem to be more extensively innervated by local GABAergic synapses (Matyas et al., 2004), including innervation from the Calretinin-containing interneuron-selective interneurons (Gulyas et al., 1996). In addition, CCK-basket cells also selectively receive serotonergic innervation

from the median raphe nucleus (Freund et al., 1990; Papp et al., 1999), while PV-basket cells and principal cells in the hippocampus do not (Figure 3).

Basket cells are integrated in both the feed-forward and feedback inhibitory mechanisms of the network. In the dentate gyrus, as part of their feed-forward function, they receive excitatory input from the perforant path, allowing them to limit incoming activity from the entorhinal cortex (Kneisler and Dingledine, 1995a). At the same time, they are extensively innervated by mossy fiber collaterals in the hilus (Ribak and Peterson, 1991), and their feedback innervation onto granule cells establishes a loop that is necessary for the generation of fast network oscillations. In particular, basket cells are involved in the generation and modulation of gamma-frequency (30-90 Hz) oscillations, which are associated with higher cognitive functions, including selective visual attention (Fries et al., 2001), auditory memory tasks (Lutzenberger et al., 2002), and dreaming during REM sleep (Llinas and Ribary, 1993). However, in some clinical settings, EEG recordings from epilepsy patients have shown the appearance of high-frequency activity before seizure onset, suggesting that gamma oscillations may play a role in the generation of epileptiform activity (Fisher et al., 1992). Moreover, in several experimental models, network oscillations at gamma frequency have been shown to coexist with epileptiform bursts that can precede, superimpose, or follow the oscillations (Traub et al., 2005). The mechanism by which network oscillations convert into higher-frequency epileptiform activity is not completely understood, but it is likely that alterations in the synaptic integration and function of basket cells could play an important role in the conversion process.

1.2.4 Alterations of hippocampal networks in epilepsy

The most accepted hypothesis aiming to explain the causes underlying the hyper-excitability of epileptic networks, and the occurrence of recurrent seizures, is an acquired imbalance between glutamatergic excitation and GABAergic inhibition, in favour of an increased excitation (Avoli, 1983; Mody et al., 1992). This imbalance is thought to occur in part for the sprouting of existing excitatory principal cell axons, together with a concurrent reduction in inhibition. Consistent with this hypothesis, many studies have reported an increase in functional recurrent excitatory circuits, in both tissue isolated from patients and animal models of TLE. One of these synaptic reorganizations is the sprouting of mossy fibers, a process that involves the growth of granule cell axons into the inner third of the molecular layer (Tauck and Nadler, 1985; Cronin and Dudek, 1988; Sutula et al., 1989; Houser et al., 1990), where they form recurrent connections to other granule cells (Kotti et al., 1997; Molnar and Nadler, 1999) and contribute to an increase in dentate gyrus excitability (Cronin et al., 1992; Scharfman et al., 2003). Interestingly, collaterals of sprouted mossy fibers have been shown to contact not only granule cells, but also PV-basket cells (Kotti

et al., 1997; Sloviter et al., 2006). In addition, CA1 pyramidal cells have also been shown to undergo axonal sprouting, and form recurrent CA1-CA1 synaptic contacts that may increase CA1 pyramidal cell excitability (Perez et al., 1996; Smith and Dudek, 2001; Bausch and McNamara, 2004).

In parallel to the sprouting of excitatory connections, several alterations involving GABAergic interneurons have also been reported in TLE, as various interneuron subtypes undergo cell death and others alter their connectivity. Somatostatin- (SS) and Neuropeptide Y- (NPY) positive interneurons seem to be the most vulnerable (Robbins et al., 1991; Sperk et al., 1992; Mathern et al., 1995; Schwarzer et al., 1995), although some degree of cell loss has been reported in other subtypes as well (Sloviter, 1989; Maglóczy and Freund, 1993; Maglóczy et al., 2000). However, recent evidence suggests that perisomatic inhibition, and particularly that provided by PV-basket cells, is to some extent preserved in TLE. A selective reduction in CA1 pyramidal cell innervation from CCK-, but not from PV-basket cells has been observed in animal models of epilepsy (Wyeth et al., 2010). Similarly, PV-positive axons are maintained in CA1 and dentate gyrus of tissue from epileptic patients (Wittner et al., 2001; Wittner et al., 2005). Nevertheless, some studies reported an increase of CCK-immunoreactive fibers in the dentate gyrus of animal models of epilepsy (Gruber et al., 1993; Schwarzer et al., 1995), indicating that these plastic changes might be dependent on the model and the detection method used.

As perisomatic inhibition provided by PV-basket cells is extremely efficient in controlling the generation of action potential by principal cells, preservation of PV-basket cell innervation might compensate the increased excitability and limit the generation/propagation of seizures. However, the ability of PV-basket cells to generate synchronous and oscillatory activity in large principal cell populations could also indicate that preservation of PV-basket cell axons might contribute to the generation of abnormal synchrony and maintenance of epileptic seizures (Wittner et al., 2005; Marchionni and Maccaferri, 2009).

1.3 Neuropeptide Y

1.3.1 NPY and its receptors

Neuropeptide Y (NPY) is a 36 amino acid peptide expressed by neurons in many brain regions and by other secretory cells of the body. In the brain, the actions of NPY have been associated with different physiological processes, such as regulation of energy balance, learning and memory, feeding, anxiety and epilepsy (Wahlestedt et al., 1993; Balasubramaniam, 1997). In the hippocampus, NPY is contained within a subpopulation of GABAergic interneurons, which often co-express somatostatin (Hendry et al., 1984; Freund and Buzsaki, 1996),

where it is expressed as a precursor peptide (prepro-NPY) in the cell soma. It is then transported in dendrites and axons via large dense core vesicles (Thureson-Klein et al., 1986; De Potter et al., 1988), where it is finally converted into its biologically active form and released during periods of high-frequency activity (Hokfelt, 1991; Hokfelt et al., 2003).

Five NPY receptor subtypes (Y1, Y2, Y4, Y5 and Y6) have been identified so far, all belonging to the G-protein coupled receptor superfamily (Michel et al., 1998). Three of these receptors (Y1, Y2 and Y5) are widely expressed in the CNS and hippocampus (Redrobe et al., 1999), and have been shown to mediate different effects on neuronal excitability and synaptic transmission. In the hippocampus, NPY has been shown to reduce glutamate release in Schaffer-collateral-to-CA1 and in mossy fiber-to-CA3 synapses in the hippocampus, via activation of Y2 receptors (Colmers et al., 1987; Klapstein and Colmers, 1993) leading to reduction of Ca^{2+} influx through pre-synaptic voltage-gated calcium channels (Qian et al., 1997). On GABAergic cells, NPY has been shown to activate G-protein coupled inward rectifier potassium currents (GIRK) in hilar interneurons via Y1 receptors (Paredes et al., 2003), and to decrease the amplitude of stimulation-induced inhibitory post-synaptic currents in cortical interneurons (Bacci et al., 2002).

1.3.2 NPY in epilepsy and seizures

Several studies have demonstrated how NPY plays a critical role in the modulation of hippocampal excitability and seizure activity in the brain, both *in vitro* and *in vivo*. Inter-ictal bursting induced *in vitro* by removal of extracellular magnesium or by application of the GABA_A receptor antagonist Picrotoxin (PTX) were markedly decreased following NPY application. Similarly, ictal activity induced by Stimulation Train Induced Bursting (STIB) was sensitive to effects of NPY (Klapstein and Colmers, 1993, 1997). *In vivo*, removal of NPY in knock-out animals results in increased susceptibility and death following kainate-induced seizures (Baraban et al., 1997), while overexpression of NPY in transgenic rats confers increased resistance (Vezzani et al., 2002). In the kainic acid model of epilepsy, infusion of NPY into the lateral ventricle suppresses motor seizure activity and shortens the kainate-induced ictal EEG recorded in granule cells and CA3 pyramidal cells, and similar effects have been reported in the hippocampal rapid kindling model (Woldbye et al., 1996; Woldbye et al., 1997). In addition, in animal models of epilepsy, and in human tissue from temporal lobe epilepsy patients, the expression of NPY and its receptors undergo considerable changes (Vezzani et al., 1999). After induction of seizures, NPY and Y2 receptor expression have been found to be up-regulated in hilar interneurons, dentate granule cells and mossy fibers (Marksteiner et al., 1990; Gruber et al., 1994; Schwarzer et al., 1998; Vezzani et al., 1999), while Y1 receptor expression

in dentate granule cell dendrites is down-regulated (Kofler et al., 1997).

Together, these observations have led to the concept that NPY could represent a potential new target for developing alternative treatment strategies for pharmacoresistant epilepsy. The first studies using NPY-based gene therapy approaches for epilepsy have demonstrated a wide range of seizure-suppressant effects exerted by the overexpression of NPY via injection of recombinant Adeno-Associated viral vectors (Richichi et al., 2004). Injection of rAAV-NPY in the hippocampus of rats significantly suppressed kainate-induced seizures and delayed kindling epileptogenesis (Richichi et al., 2004). More recently, overexpression of Y2 receptor (Woldbye et al., 2010), or of a combination of NPY and Y5 receptor (Gotzsche et al., 2012), have also been shown to delay electrical kindling and the time spent in kainate-induced motor seizures. In addition, NPY overexpression in the hippocampus of animals with chronic epilepsy (induced by electrical status epilepticus) significantly decreases the progression and frequency of spontaneous seizures (Noe et al., 2008). Taken together, these studies indicate that NPY-based gene therapy for epilepsy could represent a very promising approach.

1.3.3 NPY and basket cells

Details on the mechanisms of action of NPY and its function as a seizure suppressant agent have mostly been investigated in principal cells with regards to glutamatergic synaptic transmission. However, when using gene therapy approaches involving overexpression of NPY in large brain areas, inhibitory cell populations and inhibitory synaptic transmission could also be potentially affected. Although NPY expression could be directed selectively in glutamatergic principal cells, its release during high frequency activity could still influence neighbouring inhibitory synapses. It has been shown that NPY acts as a volume transmitter, and when released from synaptic terminals can affect synaptic transmission of separate sets of synapses (Sorensen et al., 2008a). Therefore, it becomes important to investigate whether NPY could alter inhibitory networks as well. Moreover, since single GABAergic interneurons innervate large numbers of principal cells, NPY-induced alterations in inhibitory synaptic transmission could have major consequences in network function and activity.

As discussed above (paragraph 1.2.3), perisomatic inhibitory interneurons, and basket cells in particular, play crucial roles in generating, maintaining and modulating network activity. Their function during gamma frequency oscillations, and the fact that gamma oscillations could convert into epileptiform activity, suggest that basket cells could be centrally involved in the generation of seizures. Therefore, alterations of basket cells afferent and efferent synapses by NPY could have strong significance in regards to its seizure-suppressant effects.

In the dentate gyrus, CCK- and PV- basket cells are part of a very complex network. They receive a wide variety of excitatory and inhibitory inputs, and in

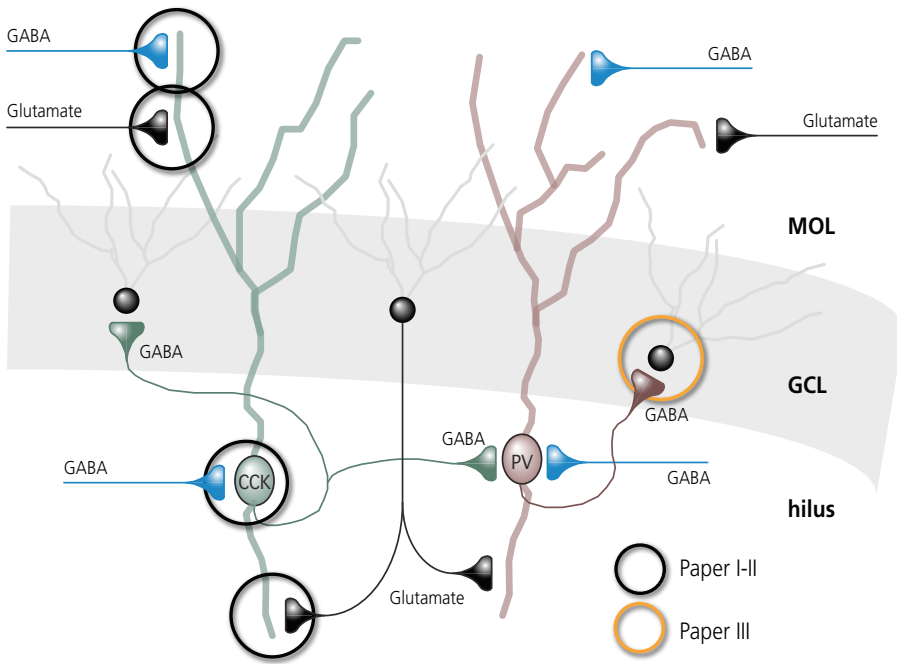


Figure 4: Schematic diagram illustrating the integration of CCK- and PV-basket cells in the dentate gyrus circuit. In *paper I-II* we asked whether afferent synapses onto CCK-basket cells (*black circles*) could be affected by NPY, while in *paper III* we evaluated the effects of NPY and hyperexcitability on PV cell output onto granule cells (*orange circle*).

turn project most of their output to granule cells, but also to other basket cells (Figure 4). All these different synapses could potentially be modulated by NPY. We started by evaluating whether NPY could affect afferent synapses onto CCK-basket cells, since alterations in their afferents might alter the way CCK-basket cells exert their modulatory role (Figure 4, *black circles*). Conversely, PV-basket cells are more efficient in inhibiting and synchronizing granule cells, therefore we were interested in investigating whether NPY could directly modulate their synapses onto granule cells (Figure 4, *orange circle*). Delineating the mechanisms of action of NPY on basket cell circuitry would help understanding how NPY exerts its antiepileptic actions, and might improve the specificity of potential future gene therapy approaches, with particular regards to reducing side effects, such as impairment of memory and learning processes (Sorensen et al., 2008b). In this light, the use of newly developed tools for probing and dissecting neuronal networks, such as optogenetics, can prove very useful.

1.4 Optogenetics

One of the major challenges in neuroscience has always been the need to control specific cell populations while leaving others unaltered, at a speed that is relevant to the physiological processes of the brain. Until very recently, such a precise and fast tool was not available to neuroscientists, as electrodes do not allow the precise targeting of specific cell types and drugs are too slow. However, the advent of optogenetic tools made possible what once was extremely difficult to achieve.

The term *optogenetics* refers to the combination of optical and genetic methods designed to control well-defined events in specific cells of living tissue. In general, it requires the introduction of genes encoding light-sensitive proteins in the genome of target cells, which then become easily controllable by exposure to different wavelengths of light. Since the work from Karl Deisseroth's group in 2005, where such genes were first introduced into neurons and proved effective in controlling neuronal excitability (Boyden et al., 2005), the field has seen an exponential growth in terms of flexibility and variety of the available tools. In general, the most widely used optogenetic tools available are engineered versions of natural opsins, transmembrane proteins capable of translocating ions across the cell membrane upon exposure to specific wavelengths of light. Depending on the type and direction of the ion movement, the effect on the membrane potential can either be depolarizing (activating) or hyperpolarizing (silencing).

1.4.1 Channelrhodopsin-2

Channelrhodopsin-2 (ChR2) belongs to the depolarizing family of optogenetic tools, and is a non-selective cation channel normally expressed by the algae *Chlamydomonas reinhardtii*. Upon exposure to blue light (activation maximum at 470 nm), it allows the passive movement of Na^+ , H^+ , Ca^{2+} and K^+ (Nagel et al., 2003). When expressed in neurons, it causes depolarization of the membrane potential and generation of action potentials (Figure 5) (Boyden et al., 2005). The major attractive feature of ChR2 is its very rapid activation/deactivation kinetics, which allows generation of single action potentials by brief (1–2 ms) light exposure (Figure 5).

Despite its remarkable properties, the degree of neuronal activation mediated by ChR2 presented some limitations with regards to fidelity of generation of action potential trains at higher frequencies. Therefore, much effort has been spent on mutagenesis approaches to develop ChR2 mutants with improved characteristics. As a result, several modifications to the original ChR2 sequence have been generated, with the aim of enhancing expression levels in neurons and increasing photocurrent amplitudes. Human codon optimization and substitution of histidine for arginine at codon 134 resulted in the development

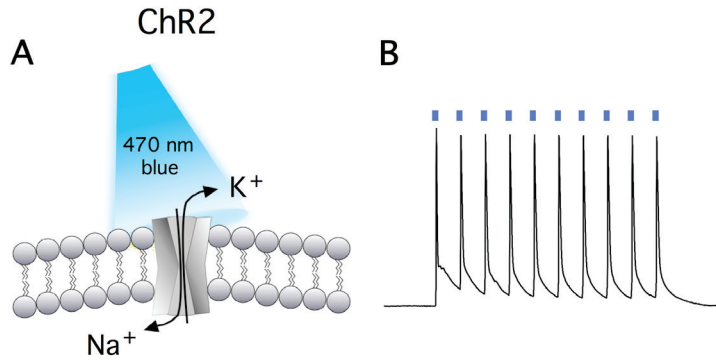


Figure 5: *A*, When activated by blue light, Channelrhodopsin-2 (ChR2) permits the passive movement of Na^+ and K^+ ions. *B*, When expressed in neurons, it allows the generation of action potentials by brief blue light exposure. Adapted from Kokaia and Sørensen, 2011

of ChR2(H134R), a ChR2 variant showing improved expression levels and photocurrent amplitudes (Nagel et al., 2005), overcoming some of the limitation of wild-type ChR2. Other ChR2 variants with improved kinetics and expression include ChIEF (Lin et al., 2009), ChETA (Gunaydin et al., 2010) and ChR2(ET/TC) (Berndt et al., 2011).

1.4.2 Targeting and delivery strategies

The most common methods to deliver optogenetic tools to the tissue or area of interest rely on Lenti- or AAV viral vectors. Lentiviral vectors have the advantage of being able to incorporate large transgenic constructs (9–10 kb), are easy to produce, and are the method of choice for *in vitro* preparations. On the other hand, AAVs can only accommodate much smaller constructs (4.7 kb), but are much more efficient *in vivo*, thanks to their smaller size and ability to cover much larger brain areas from single injection sites. The specificity of expression of the desired optogenetic construct is determined by the choice of the promoter placed upstream to the transgene. For targeting principal (excitatory) cell populations, optogenetic transgenes are usually driven by the *CamKII α* promoter, which in cortical areas is selectively expressed by glutamatergic cells (Liu and Jones, 1996), and provides high enough expression levels to achieve effective optogenetic neuronal control. However, cell specific promoters for GABAergic interneurons are usually less efficient in driving expression of their gene, e.g. Parvalbumin promoter, and could potentially be too weak to allow efficient opsin expression. To overcome this issue, researchers have used the Cre/loxP expression strategy.

Cre is the product of the *cre* (cyclization recombination) gene of the

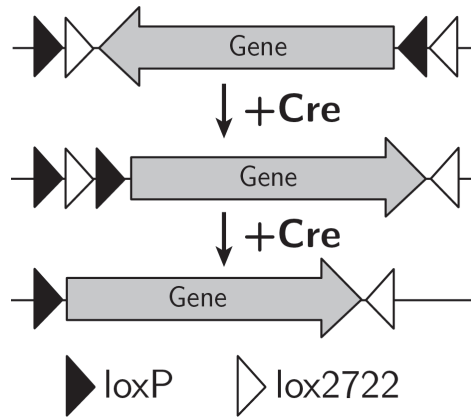


Figure 6: Schematic illustration of the Cre-dependent Double Inverted Open Reading Frame (DIO) construct. In the presence of Cre, the gene is first inverted into the sense orientation. The subsequent excision between lox pair sites prevents further recombination.

bacteriophage P1, and is a site-specific DNA recombinase. Cre recognizes a 34-bp site on the P1 genome called loxP (locus of X-over of P1) and efficiently catalyses reciprocal conservative DNA recombination between pairs of loxP sites (Hoess and Abremski, 1990). The loxP site consists of two 13-bp inverted repeats flanking an 8-bp nonpalindromic core region that gives the loxP site an overall directionality. Cre-mediated recombination between two directly repeated loxP sites results in excision of the DNA between them, while Cre-mediated recombination between pairs of loxP sites in inverted orientation will result in inversion of the intervening DNA rather than excision. A number of transgenic mice expressing Cre under the control of many different cell- or tissue-specific promoters are already commercially available (Jackson Laboratories, jaxmice.jax.org). Because each of the 13-bp repeats of the loxP site binds only one Cre monomer, and because Cre acts stoichiometrically (Mack et al., 1992), only four Cre monomers are needed to achieve full recombination, an expression level that the weaker cell-specific promoters can also drive. Therefore, once the Cre-mediated recombination has taken place, the expression levels of the transgenes are only dependent on the promoter driving them, which in this case can be strong and general, granting high levels of transgene in the target tissues.

Taking advantage of this strategy, transgenic constructs for the Cre-dependent expression of opsins have been developed, where the direction of the transgene is inverted, and flanked by two nested pairs of incompatible lox sites (loxP and lox2722) (Atasoy et al., 2008). In Cre-expressing cells, the transgene is first reversibly flipped into the sense orientation using either pair of lox sites (Figure 6), allowing gene expression; subsequently, an irreversible excision occurs

between the other lox site pair, preventing further recombination (Figure 5).

These constructs (named DIO, Double Inverted Open Reading Frame) are now available for most opsin variants, and are usually incorporated in Adeno-Associated viruses for in vivo delivery. In particular, expression of ChR2 in PV-positive cells has been previously accomplished in the barrel and infralimbic pre-frontal cortices (Cardin et al., 2009; Sohal et al., 2009), where it proved instrumental in demonstrating how direct activation of PV-cells facilitates gamma-frequency oscillations.

2 Aims of the thesis

The work presented in this thesis was conducted to extend the current knowledge on the mechanisms of action of NPY on hippocampal GABAergic interneurons, and to determine whether effects of NPY on inhibitory cell populations could contribute to its seizure-suppressant effects. The specific aims were:

- To investigate whether NPY affects synaptic transmission onto CCK-basket cells in normal conditions (*paper I*)
- To explore the effects of NPY on CCK-basket cells in hyper-excitabile conditions (*paper II*)
- To examine whether NPY affects inhibition from PV cells onto dentate gyrus granule cells (*paper III*)
- To determine whether hyper-excitability alters PV-to-granule cell synaptic transmission (*paper III*)

3 Experimental procedure

3.1 Animals

All experimental procedures were approved by the local Ethical Committee for Experimental Animals, and followed guidelines in accordance with European Community Council Directive for the Care and Use of Laboratory Animals. Animals were kept in standard cages on a 12-h light/dark cycle with *ad libitum* access to laboratory food and water.

For experiments requiring recordings from CCK-basket cells (*papers I and II*), Glutamic Acid Decarboxylase 65-Green Fluorescent Protein (GAD65-GFP) animals were used. In this line, GFP is expressed under the control of the GAD65 promoter, allowing prospective identification of different populations of GABAergic interneurons, including CCK-basket cells (Brager et al., 2003). Animals were 2-4 weeks (*paper I*) or 6-8 weeks (*paper II*) at the beginning of the experimental procedures.

For experiments where synaptic transmission from PV-cells to granule cells was evaluated (*paper III*), PV-Cre (Hippenmeyer et al., 2005) mice were used, 6-8 weeks old at the beginning of the experimental procedures. Control experiments where the effect of NPY was tested in afferent synapses onto PV-positive cells were conducted in 17-23 day old PV-tdTomato mice, generated by crossing homozygote PV-Cre mice with homozygote CAG-lox-STOP-lox-tdTomato (Ai14) mice (Madisen et al., 2010).

3.2 Viral vector production

AAV-CaMKII α -Chr2-mCherry (*paper II*) and AAV-DIO-Ef1 α -Chr2(H134R)-mCherry (*paper III*) viral vectors (Figure 7 represents the design of the transgenic constructs) were produced as previously described (Eslamboli et al., 2005), with minor modifications. Briefly, the transfer vector and the packaging plasmid, pDG5, were transfected into 293 cells. Seventy hours after

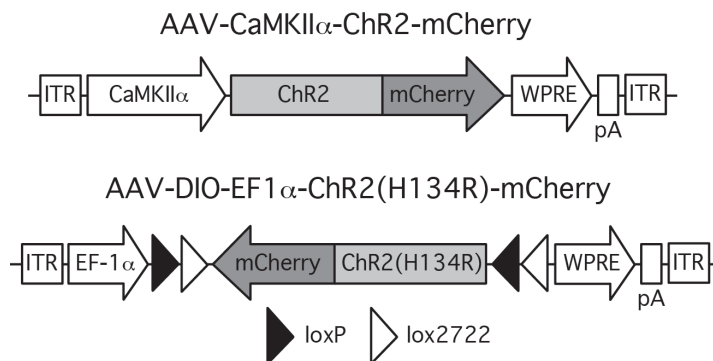


Figure 7: AAV-CaMKII α -ChR2-mCherry (*paper II*) and AAV-DIO-Ef1 α -ChR2(H134R)-mCherry (*paper III*) viral constructs used for inducing ChR2 expression

transfection the cells were harvested and lysed using one freeze–thaw cycle. The crude lysate was clarified by centrifugation at 4,500g for 20 minutes and the vector-containing supernatant was purified using a iodixanol gradient and ultracentrifugation (1.5 hours at 350,000g). The virus-containing iodixanol gradient fraction was further purified using an Acrodisc Mustang Q device (Pall Life Sciences, Port Washington, New York). For further concentration, desalting, and buffer exchange, the purified vector suspension was centrifuged in an Amicon Ultra device (Millipore). The AAV vectors were produced as serotype 5. The final number of AAV particles was determined using qPCR and was 7.4×10^{12} genomic particles/ml for AAV-CaMKII α -ChR2-mCherry and 1.4×10^{13} genomic particles/ml for AAV-DIO-Ef1 α -ChR2(H134R)-mCherry.

3.3 Electrode implantation and virus injection

Animals were anesthetized by inhalation of isofluorane (2.5%, Baxter Chemical AB) and fixed onto a stereotaxic frame (David Kopf Instruments, Tujunga, CA). A bipolar stainless steel stimulation/recording electrode (Plastics One, Roanoke, VA) was stereotaxically implanted in the ventral right hippocampus at the following coordinates (in mm): AP -2.9, ML 3.0, DV -3.0. A reference electrode was placed in the temporal muscle. Electrodes were placed into a pedestal (Plastics One Roanoke, VA) and fixed on the skull with dental cement (Kemdent).

AAV-CaMKII α -ChR2-mCherry (*paper II*) or AAV-DIO-Ef1 α -ChR2(H134R)-mCherry (*paper III*) viral vector suspensions were injected during the same surgery through a glass capillary in the left hippocampus

(contra-lateral to the electrode) at the following coordinates (in mm): AP -3.2, ML -3.1, DV -3.6 and -3.2. 0.5 μ l of viral suspension was injected at 0.1 μ l/minute in each location in the DV plane. The glass pipette was left in place for 5 minutes after each injection, to minimize back-flow of viral particles through the injection tract. Reference points for stereotaxic surgery were bregma for the AP axis, midline for the ML axis, and dura for the DV axis.

3.4 Rapid kindling and test stimulations

For inducing hyper-excitability (*papers II and III*), animals were subjected to rapid kindling 7 days after electrode implantation. Kindling is defined as a progressive increase in severity of EEG discharges and seizure behavior, in this case induced by electrical stimulation. As opposed to conventional kindling models, where stimulations are delivered once daily, the rapid kindling model is usually completed within one day, as the time between stimulations is much shorter, usually 5 minutes. The model is less laborious than conventional kindling, and allows the reliable induction of hyper-excitability states with minimal cell death and inflammatory response (Wood et al., 2011), although lacking the temporal resolution needed for studying epileptogenesis phenomena.

Before the induction of kindling, the individual threshold was determined by delivering stimulations (1 sec train consisting of 1 ms bipolar square wave pulses at 100 Hz) of increasing current in 10 μ A steps until a focal epileptiform afterdischarge (AD) of more than 5 sec duration was detected by electroencephalographic (EEG) recording. During rapid kindling induction, EEG activity was continuously recorded on a MacLab system (ADInstruments, Bella Vista, Australia) for 200 min except during stimulations, which consisted of 40 suprathreshold stimulation trains (10 s, 1 ms square wave pulses at 50 Hz, 400 μ A intensity) separated by 5 min interval between stimulations. Behavioral seizures were scored according to the Racine scale (Racine, 1972): grade 0, arrest, normal behavior; grade 1, facial twitches (nose, lips, eyes); grade 2, chewing, head nodding; grade 3, forelimb clonus; grade 4, rearing, falling on forelimbs; grade 5, imbalance and falling on side or back. Animals were used for electrophysiological recordings four to six weeks after stimulations (*papers II and III*).

3.4.1 Test stimulations

In a subset of animals (*paper II*), the individual threshold was measured again four weeks after the first kindling stimulations, to assess if animals achieved a hyper-excitability state at the time point of electrophysiology. Animals were then given 5 additional stimulations using the same parameters of the first 5 kindling stimulations. Seizure grades and AD duration were assessed as previously.

3.5 Slice preparation

Animals were briefly anesthetized with isofluorane and decapitated. The brain was quickly removed and immersed into a chilled sucrose-based cutting solution, containing (in mM): sucrose 195, KCl 2.5, CaCl₂ 0.5, MgCl₂ 7, NaHCO₃ 28, NaH₂PO₄ 12.5, glucose 7, ascorbate 1, pyruvate 3 (pH 7.2-7.4, 290-300 mOsm, *paper I*) or sucrose 75, NaCl 67, NaHCO₃ 26, glucose 25, KCl 2.5, NaH₂PO₄ 1.25, CaCl₂ 0.5, MgCl₂ 7 (pH 7.4, 305-310 mOsm, *papers II and III*). Solutions were constantly gassed with carbogen (95% O₂/5% CO₂). In *paper I*, the hippocampal formation was carefully dissected, transverse slices 250 μ m thick were produced with a vibratome and stored in sucrose-based solution at room temperature. In *papers II and III*, the entire left hemisphere was cut horizontally with a vibratome in 300 μ m slices containing the hippocampal formation and entorhinal cortex, and slices were stored in sucrose-based solution at 34 °C for 30 minutes before being transferred to room temperature. These modifications led to a generally improved slice quality and allowed greater survival of GABAergic interneurons, necessary for the experiments requiring recordings from adult tissue.

3.6 Electrophysiology

3.6.1 Principles of whole-cell electrophysiology

To investigate alterations in synaptic transmission and plasticity, a common electrophysiological technique known as whole-cell patch clamp was used. In principle, this method allows the recording of electrical activity from one single cell in the slice preparation, and although it can be technically challenging in some cases, it is extremely powerful and sensitive, permitting the investigation of single synaptic events in neurons.

First, the desired cell is selected in the slice according to pre-defined criteria. For this reason, the use of transgenic mice expressing fluorescent proteins in specific subsets of cells (e.g. GAD65-GFP or PV-tdTomato) is extremely useful. A glass pipette containing an electrode and a carefully prepared intracellular solution is then attached to the membrane of the selected cell. The small opening of the pipette (usually 1-2 μ m) is pressed against the membrane of the cell (Figure 8-1), and gentle suction is applied to assist the generation of a tight seal (gigaOhm seal) between the pipette tip and the cell membrane (Figure 8-2). Subsequently, more suction is applied until the membrane inside the pipette tip ruptures, while leaving the seal intact, granting access to the cell cytoplasm (Figure 8-3). The electrode contained in the pipette is now in contact with the interior of the cell, thus conducting electrical activity to an amplifier that converts the signals into recordable data.

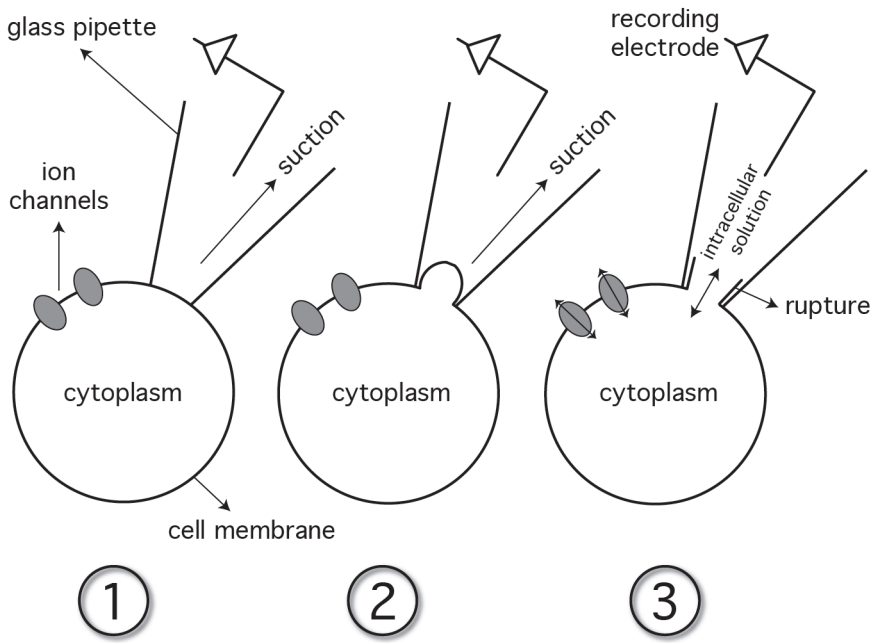


Figure 8: Principle of whole-cell patch clamp electrophysiology. **1**, the glass pipette is in contact with the cell membrane; **2**, a tight seal is formed by gentle suction; **3**, more suction causes the membrane to rupture, establishing the whole-cell configuration.

Two main configurations can be used to record different electrical signals from the neuron: voltage clamp and current clamp. In voltage clamp, the voltage is kept constant (i.e. at -70 mV) while observing the current (flow of ions) passing through the cell membrane. In current clamp, the current is kept constant while observing changes in the membrane potential. In this way, it is possible to measure intrinsic membrane properties of the recorded cells, response to current injections and incoming synaptic activity. Using different intracellular (in the pipette) and extracellular (in the bath) solutions it is possible to discriminate between different types of synaptic transmission (e.g. glutamatergic versus GABAergic) and manipulate the environment to study pharmacological profiles of determined cell populations.

3.6.2 Whole-cell electrophysiology

Individual slices were placed in a submerged recording chamber constantly perfused with gassed artificial cerebro-spinal fluid (aCSF) containing, in mM: NaCl 119, KCl 2.5, MgSO_4 1.3, CaCl_2 2.5, NaHCO_3 26.2, NaH_2PO_4 1 and glucose 11 (pH 7.2–7.4, 290–300 mOsm, *paper I*) or NaCl 119, NaHCO_3 26,

glucose 25, KCl 2.5, NaH_2PO_4 1.25, CaCl_2 2.5 and MgSO_4 1.3 (pH 7.4, 305–310 mOsm, *paper II* and *III*). GAD65-GFP (*paper I* and *II*) and PV-tdTomato (*paper III*) positive cells were visualized under fluorescent light and infrared differential interference contrast microscopy was used for visual approach of the recording pipette.

Recording pipettes were pulled from borosilicate glass with a Flaming-Brown pipette puller, had a tip resistance of 2.5–5 M Ω and contained (in mM):

- K-Gluconate 122.5, KCl 12.5, KOH-HEPES 10, KOH-EGTA 0.2, MgATP 2, Na_3GTP 0.3, NaCl 8, for measurement of intrinsic properties and firing patterns (*papers I–III*), acetylcholine-induced responses (*paper I*) and monitoring the response to light in Chr2-expressing cells (*paper II*);
- Cs-Gluconate 117.5, CsCl 17.5, NaCl 8, CsOH-HEPES 10, CsOH-EGTA 0.2, MgATP 2, Na_3GTP 0.3, QX-314 5, for measurement of spontaneous and miniature (*papers I–III*), stimulation-evoked (*paper I*), and light-evoked (*paper II*) excitatory post-synaptic currents (EPSCs);
- CsCl 135, CsOH 10, CsOH-EGTA 0.2, MgATP 2, Na_3GTP 0.3, NaCl 8, QX-314 5, for recording of spontaneous and miniature (*papers I* and *II*), stimulation-evoked (*papers I* and *II*) and light-evoked (*paper III*) inhibitory post-synaptic currents (IPSCs).

Biocytin (3–5 mg/ml) was routinely added to the pipette solution on the day of the recording. Recordings typically lasted 20–30 minutes, and biocytin was allowed to diffuse for additional 10 minutes at the end to assure complete diffusion in the axonal arbor. In *paper I*, biocytin was used at lower concentrations (0.5–1 mg/ml) and allowed to diffuse for 90 minutes in a subset of experiments. Series resistance (typically 8–30 M Ω) was constantly monitored via -5 mV voltage steps and recordings were discontinued after changes of $>20\%$ or if the resting membrane potential was more positive than -50 mV.

Firing pattern and accommodation were investigated by applying a single 1 sec, 500 pA depolarizing current step. Action potential threshold, amplitude, after-hyperpolarization and rheobase were measured by the first action potential of the train evoked with a 1 sec voltage ramp of 0–300 or 0–500 pA. Current-voltage relationship was analyzed by injecting consecutive incrementing 500 ms 10 pA current steps, from -200 to $+200$ pA.

EPSCs were recorded in the presence of 100 μM PTX to block GABAA receptors and isolate glutamate receptor mediated synaptic transmission. NBQX (5 μM , Tocris Bioscience) and D-AP5 (50 μM , Tocris Bioscience) were used during IPSCs recordings to block AMPA and NMDA glutamate receptors, respectively. TTX (1 μM , Tocris Bioscience) was added during miniature EPSCs and IPSCs recordings (*paper I* and *II*) to block voltage-gated sodium channels

and prevent generation of action potentials in the slice. The metabotropic group II receptor (mGluR II) agonist L-CCG-I (10 μ M, Tocris Bioscience) was used to selectively activate mGluR II, which are exclusively expressed on granule cell mossy fibers, and block mossy-fiber mediated synaptic transmission (*papers I and II*).

3.6.3 Stimulation protocols

Two different stimulation approaches were used for stimulating afferent fibers onto recorded cells: electrical and optogenetic. For stimulation-evoked EPSCs recordings (*paper I*), bipolar stainless steel stimulating electrodes were placed in the inner molecular layer and CA3 stratum lucidum. Stimulation-evoked IPSCs recordings were conducted with stimulation electrodes placed in the inner molecular layer (*paper I*), granule cell layer (*paper II*) and outer molecular layer (*paper II*). In all cases, stimulus duration was 100 μ s, and paired pulses were delivered with 50 (for EPSCs, *paper I*) and 100 ms (for IPSCs, *papers I and II*) inter stimulus interval (ISI) at 0.06 Hz.

Optogenetic stimulation of ChR2-expressing principal neurons (*paper II*) and PV-positive cells (*paper III*) was achieved by positioning a 400 μ m optical fiber above the tip of the dentate gyrus, connected to a 460 nm wavelength LED light source (Figure 9). Paired light pulses of 1-2 ms duration were delivered with 50 (for EPSCs, *paper II*) or 100, 250 and 500 ms (for IPSCs, *paper III*) ISI at 0.06 Hz. Additionally, trains of 10 light pulses at 10 and 20 Hz frequency were used

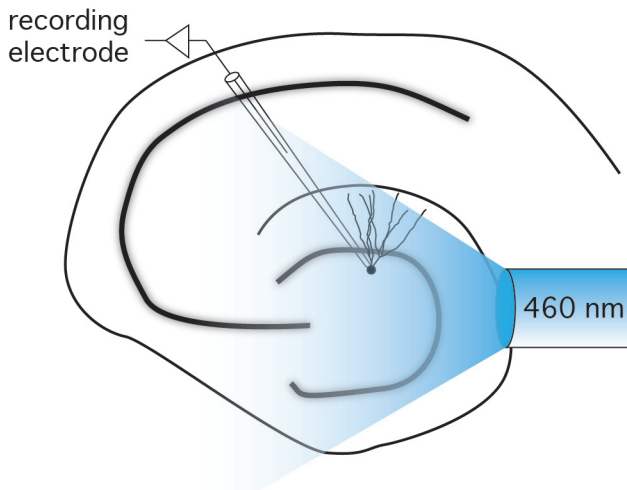


Figure 9: Experimental setup for optogenetic stimulations. An optical fiber connected to a 460 nm wavelength LED light source was placed above the tip of the dentate gyrus to stimulate ChR2 expressing neurons while recording from selected cells.

to study GABA release efficiency from PV-positive cells ensembles (*paper III*).

3.6.4 NPY application

NPY (synthetic, Schafer-N, Denmark, *papers I-III*) and free-acid NPY (Bachem AG, Switzerland, *paper I*) were dissolved in distilled water, stored in concentrated aliquots and diluted to 1 μM concentration in the perfusion solution immediately before use. Following a period of baseline recording, peptides were applied and allowed to diffuse in the recording chamber for 7 min before the continuation of the recordings. The choice of concentration of NPY is based on previously published work, where it has been shown to be the most effective in inhibiting Schaffer collateral-CA1 excitatory post-synaptic potentials in the hippocampus (Colmers et al., 1987). Care has been taken in using silicon-coated bottles and tubing for preventing the peptides from adhering to the tubing and container walls. The highly specific Y2 receptor blocker BIIE0246 (Boehringer Ingelheim Pharma, Germany) was initially dissolved in 70% ethanol and diluted 1:5000 to a final concentration of 0.6 μM in the perfusion solution. In experiments studying the contribution of Y2 receptors (*paper I*), BIIE0246 was present from the beginning of the recordings.

3.6.5 Data acquisition

Data from electrophysiology was acquired at 10 kHz and filtered at 2.9 kHz using HEKA amplifier and software (EPC 9 or 10 amplifier, PATCHMASTER, HEKA Elektronik, Germany) and off-line analysis was performed using FITMASTER (HEKA Elektronik), Igor Pro (Wavemetrics, Lake Oswego, OR), StatView (Abacus Concepts, Berkeley, CA), SPSS (IBM), GraphPad Prism (GraphPad software, San Diego, CA) or MiniAnalysis (Synaptosoft, Decatur, GA) software, whenever appropriate.

3.7 Immunohistochemical procedures

3.7.1 Immunostaining

For identifying cells recorded during electrophysiological measurements, at the end of the recording slices were immediately fixed in 4% Paraformaldehyde (PFA) in phosphate buffer (PB) for 12-24 hours and then stored in anti-freeze solution (ethyleneglycol and glycerol in PB buffer) at -20°C until processed.

To characterize the population of basket cells recorded in *paper I* and *II*, GAD65-GFP animals not used for electrophysiology received an overdose of pentobarbital (250 mg/kg i.p.) and were perfused transcardially with 50 ml of ice-cold saline (0.9% NaCl) and 50 ml of ice-cold 4% PFA in PB (pH 7.2-7.4),

or 25 ml of ice-cold 4% PFA, 0.025% glutaraldehyde in sodium acetate buffer (pH 6.5) and 25 ml of ice-cold 4% PFA in sodium borate buffer (pH 9.5). Brains were postfixed in 4% PFA in PB or in 4% PFA in sodium borate overnight, and then dehydrated/cryoprotected with 20% sucrose in PB. The brains were cut in 30 μ m sections and stored in anti-freeze solution at -20°C .

<i>Antigen</i>	<i>Raised in</i>	<i>Dilution</i>	<i>Provider</i>
GFP	rabbit	1:10000	Ab1218, abcam
mCherry, tdTomato	rat	1:1000	5F8, Chromotek
CCK	rabbit	1:5000	Ab43842, abcam
PV	mouse	1:2000	P3088, Sigma
Y2	rabbit	1:1000	RA14112, Neuromics

Table 1: Primary antibodies used for the different immunohistochemical stainings

For immunohistochemical staining against GFP (*paper I* and *II*), mCherry (*paper II* and *III*), tdTomato (*paper III*), CCK (*paper I*), PV (*paper I*), slices were rinsed three times with KPBS and pre-incubated for 1 hour in blocking solution (10% normal serum and 0.25% Triton X-100 in KPBS, T-KPBS). Sections were then incubated overnight at room temperature with the appropriate dilution of primary antibody (see Table 1) in blocking solution, rinsed three additional times in T-KPBS and incubated for 2 hours in the suitable secondary antibody (Jackson Immunoresearch, UK) in blocking solution. Slices were finally rinsed three times in KPBS, mounted on coated slides and cover-slipped with DABCO.

3.7.2 Axonal arbour reconstruction

An important step in all papers was the reconstruction of the axonal arbour of recorded interneurons, as it is the principal characteristic that allows to delineate the identity of different GABAergic cell subtypes. After recordings, slices were fixed as described above, and processed for immunohistochemistry against biocytin, which was included in the pipette solution.

In *paper I*, after a two-day incubation in 20% sucrose in PB, slices were additionally cut in 60 μ m sections using a microtome. The biocytin-filled neurons were visualized by incubating the sections in avidin–biotin conjugated horseradish peroxidase solution (ABC, Vector Laboratories, UK), and then reacting them with diaminobenzidine (DAB) and hydrogen peroxide solutions. The staining was then intensified by incubating slices in 0.5% OsO₄ (Sigma) solution. Serial microphotographs were taken throughout the whole thickness of the slices every 1 μ m, and groups of five consecutive images were merged using appropriate transparency filters with Canvas X software (ACD Systems, Victoria, Canada). Using the same software, drawings of the dendritic tree and axonal arborization

were made in each group of images and finally merged together.

In *paper II* and *III*, after permeabilization in T-KPBS, slices were incubated with Cy5- (Jackson Immunoresearch, UK) or Alexa 488- (Molecular Probes) conjugated streptavidin for 2 hours (1:200 dilution). Labeled neurons were examined with a confocal laser-scanning microscope (Leica). Confocal Z-stacks were obtained along the entire dendritic and axonal tree of the cells, which typically consisted of 40-50 planes.

3.7.3 Y2 immunohistochemistry and optical density measurements

In *paper II*, one particular objective was to analyse the differential distribution of Y2 immunopositive fibers in the dentate gyrus of normal and hyper-excitable animals. The immunohistochemical procedure differed slightly from what described above and should be reported separately. Briefly, slices from electrophysiological recordings and from non-kindled age-matched GAD65-GFP controls were cryoprotected in 20% sucrose in PB for two days and additionally cut in 50 μm sections using a microtome. Sections were then treated with 1% hydrogen peroxide for 30 minutes, pre-incubated for 1 hour in blocking solution containing normal goat serum (see above), incubated for 24 hours at 4°C with anti-Y2 receptor antibody (Table 1) and subsequently with 1:500 biotinylated goat anti-rabbit secondary antibody (Vector Laboratories, UK). Y2 immunoreactivity was visualized by incubating the sections in avidin-biotin conjugated horseradish peroxidase solution (ABC, Vector Laboratories, UK), and then reacting them with 0.5 mg/ml DAB, 0.025% cobalt chloride, 0.2% nickel ammonium sulfate and hydrogen peroxide solutions.

Microphotographs were taken from each section using the same exposure time and ambient light conditions, on the same day. To measure optical density of Y2-positive fibers, images were processed with ImageJ software (NIH, <http://rsbweb.nih.gov/ij/>). The density reading of the Y2-negative hippocampal fimbria structure was used as an internal reference for each section, and subtracted from the readings of the inner and outer molecular layers.

3.8 Statistics

Different statistical methods were used where appropriate to assess significant differences between groups, and included two-tailed paired *t*-tests (for analysing differences between certain pre- and post-NPY application parameters), two-tailed unpaired *t*-test (e.g. for testing significance of differences between kindled and control animals) and two-tailed Kolmogorov-Smirnov (*K-S*) test (e.g. for analysing differences in distribution of amplitudes and frequencies of

spontaneous and miniature EPSCs and IPSCs). Differences between the groups were considered significant with $P < 0.05$ for t -tests and $P < 0.01$ for K - S tests.

4 Results and comments

4.1 Effects of NPY on CCK-basket cells

The first part of the result section will focus on the effects of applied NPY on synaptic transmission onto CCK-basket cells in the dentate gyrus of normal (*paper I*) and hyper-excitable animals (*paper II*).

4.1.1 Identification of CCK-basket cells

In GAD65-GFP animals, several classes of inhibitory interneurons express GFP, including CCK-basket cells. In order to identify recorded cells as CCK-basket cells, several morphological and functional criteria had to be met (*paper I* and *II*). Cells had to be located in the border between the granule cell layer and the hilus, their soma had to be roughly pyramidal shaped, and their dendrites had to extend to the outer molecular layer on the apical side, and enter the hilus on the basal side. Moreover, cells had to fire low-frequency, non-accomodating action potentials upon depolarization induced by sustained current injection. Further supporting the CCK-basket cells identity of the recorded cells, we performed a series of experiments to show that cells selected with criteria described above express functional alpha7 nicotinic receptors, another characteristic property of CCK-basket cells. We show that putative CCK-basket cells respond to focal application of Acetylcholine (ACh) with an inward current that is readily blocked by the alpha7 nicotinic receptor antagonist MLA, but not by NBQX, D-AP5 or atropine (*paper I*). In addition, immunohistochemical evaluation of tissue from GAD65-GFP mice showed that a subpopulation of GFP cells in the border between the granule cell layer and the hilus express CCK, but not Parvalbumin (*paper I*). Lastly, the distribution of the axonal arbor had to be confined within the granule cell and inner molecular layers.

Taken together, the fulfilment of these criteria strongly suggests that recorded cells could be identified as CCK-basket cells, and allowed to positively discriminate between CCK-basket cells and other types of GFP-positive cells

present in the granule cell layer/hilus border of GAD65-GFP mice.

4.1.2 Intrinsic membrane properties

Since NPY has been previously shown to modulate passive membrane properties of a subtype of hippocampal interneurons (Paredes et al., 2003) through activation of post-synaptic Y1 receptors, we first wanted to evaluate whether application of exogenous NPY could influence the membrane properties of CCK-basket cells. We then recorded passive membrane properties of CCK-basket cells before and after application of NPY, in the normal (*paper I*) and hyper-excitable (from animals subjected to rapid kindling, *paper II*) hippocampus. Application of NPY did not alter the resting membrane potential, firing pattern, degree of frequency accommodation, action potential threshold, amplitude, duration, afterhyperpolarization or rheobase of recorded CCK-basket cells, suggesting that CCK-basket cells do not express post-synaptic NPY receptors.

4.1.3 Spontaneous excitatory synaptic transmission

Having established that passive membrane properties of CCK-basket cells are not affected by NPY, we wanted to determine whether incoming excitatory synaptic transmission onto CCK-basket cells could be modulated by NPY. We first recorded spontaneous excitatory post-synaptic currents (sEPSCs) by holding CCK-basket cells in voltage-clamp at -70 mV, in the presence of PTX to block GABA_A-mediated inhibitory transmission and isolate glutamate receptor mediated currents. sEPSCs are a mixture of currents that include those dependent on action potentials in pre-synaptic neurons, and action potential independent currents generated by the spontaneous fusion of glutamate-containing vesicles on the pre-synaptic side. Application of NPY reduced the frequency of sEPSCs recorded from CCK-basket cells in both normal and hyper-excitable conditions, but did not alter their amplitude, suggesting that NPY might act pre-synaptically and reduce glutamate release.

To determine if the suspected NPY-mediated reduction of glutamate release was dependent on pre-synaptic action potentials, we subsequently recorded miniature excitatory post-synaptic currents (mEPSCs) by applying TTX together with PTX in the perfusion solution to block voltage-gated sodium channels and prevent the formation of action potentials in the whole slice. Application of NPY significantly decreased the frequency of mEPSCs in both normal and kindled animals, without affecting their amplitude, suggesting that the effects of NPY are independent of action potentials.

4.1.4 Evoked excitatory synaptic transmission and short-term plasticity

A possible explanation underlying the reduction in sEPSCs and mEPSCs

frequency induced by NPY could be a decrease in release probability (Pr) of glutamate from pre-synaptic terminals. An indirect measure of glutamate Pr could be obtained by assessing alterations in the paired-pulse facilitation (PPF) of EPSCs, a form of short-term plasticity widely observed in central excitatory synapses. PPF is defined by the ability of synapses to increase neurotransmitter release in response to the second of two closely spaced afferent stimulations, and depends on residual Ca^{2+} concentration in the presynaptic terminals (Zucker and Regehr, 2002). The degree of PPF inversely relates to Pr , with large PPF values being associated with low Pr and low PPF indicating high Pr (Dobrunz and Stevens, 1997). Since NPY has been previously shown to decrease Pr of glutamate via modulation of Ca^{2+} influx in afferent pre-synaptic terminals of CA1 (Colmers et al., 1988; Qian et al., 1997), we wanted to evaluate whether PPF of EPSCs recorded from CCK-basket cells was also affected.

In normal animals (*paper I*), we used paired electrical stimulation of the inner molecular layer with 50 ms ISI to evoke EPSCs in CCK-basket cells that exhibited PPF. Application of NPY decreased the amplitude of both the first and the second response of the pair, but did not alter the PPF ratio, indicating that in these synapses NPY does not reduce glutamate Pr , and might decrease glutamate release by other mechanisms downstream to the attenuation of calcium entry. To determine if the effect of NPY was dependent on activation of Y2 receptors, we repeated the experiments but added the specific Y2 receptor blocker BIIE0246 to the perfusion solution before NPY application. In these conditions, NPY failed to cause a decrease in evoked EPSCs amplitudes, indicating an involvement of Y2 receptors. Moreover, to confirm that the observed effect was indeed mediated by NPY, in a separate set of experiments we applied a non-active form of NPY (*free-acid* NPY) instead of NPY and observed no effect.

To stimulate afferent excitatory fibers in hyper-excitabile animals (*paper II*), we used an optogenetic approach involving the expression of ChR2 in all the principal cell populations of the hippocampus, by injecting AAV vectors carrying the ChR2 transgene directed by the control of the CaMKII α promoter, which in the hippocampus is exclusively expressed in excitatory cells (Liu and Jones, 1996). Using this approach, we were able to stimulate all excitatory afferent fibers of CCK-basket cells at the same time, with millisecond precision. Two paired 1 ms blue light flashes with 50 ms ISI evoked EPSCs in CCK-basket cells (1eEPSCs) that exhibited PPF. Application of NPY caused a significant decrease in the amplitude of both responses of the pair, and a concomitant increase in the PPF ratio, indicating a reduction in the Pr of glutamate.

Seizures induce sprouting of mossy fibers (Tauck and Nadler, 1985; Cronin and Dudek, 1988), which have been shown to express Y2 receptors (Tu et al., 2006), and NPY *de novo* after seizures (Schwarzer et al., 1995). At the same time, mossy fibers are involved in the feedback loop of basket cells, controlling

network activity. Therefore, we were interested in evaluating the contribution of mossy fibers to the EPSCs induced by electrical and optogenetic stimulations. Therefore, we applied the specific mGluR II agonist L-CCG-I to selectively activate mGluR II receptors, which in the hippocampus are exclusively expressed by mossy fibers, and block mossy fiber-mediated synaptic transmission. In normal animals (*paper I*), L-CCG-I application caused a 30% decrease in the EPSCs evoked by stimulation of the inner molecular layer. In kindled animals (*paper II*), application of L-CCG-I decreased the amplitude of optogenetically evoked EPSCs by about 35%, indicating that both stimulation protocols were activating mossy fibers.

4.1.5 Spontaneous inhibitory synaptic transmission

Next we were interested in investigating whether inhibitory synaptic transmission onto CCK-basket cells was affected by NPY, as a direct modulation of inhibitory synapses onto interneurons would also alter their excitability and impact on the network. First we recorded spontaneous inhibitory post-synaptic currents (sIPSCs) from CCK-basket cells, in normal (*paper I*) and hyper-excitable (*paper II*) animals, pharmacologically isolated by blocking glutamate receptor-mediated synaptic transmission with NBQX and D-AP5. As for sEPSCs, sIPSCs are a mixture of action potential dependent and independent events. Application of NPY significantly decreased the frequency, but did not alter the amplitude, of sIPSCs in both conditions (*papers I and II*) indicating that NPY could act pre-synaptically to reduce GABA release.

The observed decrease in the frequency of sIPSCs recorded in CCK-basket cells could be partially explained by NPY-mediated inhibition of HIPP cells firing, as previously described (Paredes et al., 2003). To determine if this was the case, we added TTX in the perfusion solution, to block all action potentials in the slice, and recorded the effects of NPY application on action-potential independent mIPSCs. In both normal (*paper I*) and hyper-excitable (*paper II*) animals, NPY application significantly decreased the frequency of mIPSCs in CCK-basket cells, without affecting their amplitude, indicating that NPY does not only act through inhibition of HIPP cell firing.

4.1.6 Differential effects of NPY on perisomatic and dendritic inhibitory synapses

CCK-basket cells receive inhibitory afferents from different classes of GABAergic interneurons at synapses across the entire dendritic tree. The decrease in the frequency of sIPSCs and mIPSCs induced by NPY does not indicate whether perisomatic and dendritic inhibitory synapses are differentially modulated. It would be interesting to measure whether NPY differentially modulates perisomatic and dendritic synapses, as the consequences on CCK-

cell excitability would be different. Synaptic events at perisomatic or dendritic inhibitory synapses can be distinguished on the basis of their kinetics. IPSCs with fast rise and decay kinetics and relatively large amplitude are most likely to be generated by synapses in close proximity with the recording electrode (placed on the cell soma), while events with slow kinetics and smaller amplitudes are thought to be generated by synapses more distant to the cell soma (e.g. distal dendritic synapses) (Kobayashi and Buckmaster, 2003).

To address this question, we analysed the rise time values of sIPSCs and mIPSCs, before and after NPY application, in normal and hyper-excitable animals. In normal animals (*paper I*), application of NPY shifted the sIPSCs and mIPSCs rise time curves towards faster kinetics, indicating that dendritic inhibitory synapses were preferentially affected. Interestingly, in hyper-excitable animals (*paper II*) the effect was opposite, and application of NPY caused a shift in sIPSCs and mIPSCs rise times towards slower values, indicating a preferential action on perisomatic inhibitory synapses. These results indicate that the localization of NPY receptors responsible for the decrease in sIPSCs and mIPSCs frequency could be different between normal and hyper-excitable conditions.

4.1.7 Evoked inhibitory synaptic transmission

The data described above indicates that, in normal animals (*paper I*), NPY acts preferentially on dendritic inhibitory synapses. To determine whether perisomatic synapses were indeed not affected, we placed a stimulating electrode in the border between the granule cell and inner molecular layers and stimulated perisomatic inhibitory afferent fibers onto CCK-basket cells. Using NBQX and D-AP5 to isolate GABAergic transmission, paired stimulations with 100 ms ISI evoked IPSCs on CCK-basket cells that exhibited paired-pulse depression (PPD). Application of NPY caused a significant reduction in the amplitude of both the first and the second response of the pair, but did not alter the PPD ratio. Similarly to stimulation-induced EPSCs, application of the inactive form of NPY, *free acid* NPY, did not affect the amplitudes or the PPD of perisomatic IPSCs. Moreover, application of the Y2 receptor blocker BIIE0246, completely abolished NPY effect, indicating that Y2 receptor activation is necessary for the reduction of IPSCs induced by NPY. Taken together, these data indicate that perisomatic inhibitory synapses on CCK-basket cells are also affected by NPY, and the effect is dependent on Y2 receptor activation.

In hyper-excitable conditions, NPY had an opposite effect, and acted preferentially on perisomatic inhibitory synapses (*paper II*). To explore whether dendritic synapses were also affected, we placed a stimulating electrode in the outer third of the molecular layer, together with a control electrode in the granule cell layer, and separately stimulated dendritic and perisomatic inhibitory synapses

onto CCK-basket cells. Paired stimulations with 100 ms ISI at both pathways evoked IPSCs on CCK-basket cells expressing PPD. Application of NPY caused a significant decrease in the amplitude of both IPSCs pairs, without affecting the PPD ratio, indicating that both sets of inhibitory synapses are affected by NPY. In addition, the rise time analysis showed that IPSCs evoked by granule cell layer stimulation were significantly faster than IPSCs evoked by the electrode in the outer molecular layer, confirming that two different sets of synapses were activated by this stimulation paradigm.

4.1.8 Expression of Y2 receptors

One possible explanation for the preferential action of NPY on perisomatic inhibitory synapses in hyper-excitabile animals described in *paper II* could be a selective increase in NPY receptor expression in perisomatic regions compared to dendritic ones. To evaluate the differential distribution of NPY receptors, we performed immunocytochemistry experiments in slices from hyper-excitabile animals and age-matched controls. Between the three NPY receptors expressed in the hippocampus (Y1, Y2 and Y5), we chose to study the distribution of Y2 receptors, that we show mediate the effects of NPY on afferent inhibitory synapses onto CCK-basket cells in normal animals (*paper I*). Analysis of the Y2-immunoreactive fiber density revealed that expression of Y2 receptors was significantly increased in the inner molecular layer of hyper-excitabile animals compared to controls. Moreover, expression of Y2 receptors in the outer molecular layer (where dendritic inhibitory synapses onto CCK-basket cells are present) was overall lower, and the increase in expression induced by rapid kindling was slightly less pronounced. Although the immunohistochemical method used here does not distinguish between Y2 receptor expression in glutamatergic or GABAergic fibers, these data show that the observed preferential effect of NPY on perisomatic inhibitory synapses onto CCK-basket cells in hyper-excitabile animals is paralleled by an increase in Y2 receptor expression in perisomatic areas.

4.2 Effects of NPY on PV cells

The second part of the result section focuses on the effects of NPY and hyper-excitability on perisomatic inhibitory synapses from PV-positive cells onto dentate gyrus granule cells (*paper III*).

4.2.1 Expression of ChR2 in PV cells

The properties of Parvalbumin-to-granule cell (PV-GC) synapses have been extensively studied using paired recordings in both normal and epileptic animals (Kraushaar and Jonas, 2000; Hefft and Jonas, 2005; Zhang and Buckmaster, 2009). However, PV cells form ensembles interconnected via gap junctions that

function synergistically to control oscillatory activity of principal cell populations (Galarreta and Hestrin, 1999). Therefore, a more physiological approach for studying PV-GC synapses would be to explore post-synaptic responses in granule cells evoked by the stimulation of the multiple PV cells at the same time. To achieve this goal, we used an optogenetic approach involving the expression of a ChR2 variant (ChR2-H134R) selectively in PV-expressing cells in the hippocampus, by injecting a Cre-dependent AAV viral vector (AAV-DIO-Ef1 α -ChR2(H134R)-mCherry) in a mouse line that expresses Cre under the control of the PV promoter (PV-Cre). Using two injection sites in the ventral and medial hippocampus, we achieved strong and long-lasting expression of ChR2 in PV cells of all areas of the hippocampal formation, including dentate gyrus, CA1 and CA3.

4.2.2 NPY does not affect PV-GC synapses

The first goal was to evaluate whether NPY affects GABAergic synaptic transmission at PV-GC synapses in normal animals. We therefore recorded from dentate gyrus granule cells, in the presence of NBQX and D-AP5 to block glutamatergic synaptic transmission, and stimulated PV cells by blue light flashes delivered through an optical fiber (see Experimental procedures). Two paired 1 ms light pulses with 100 ms ISI elicited large amplitude post-synaptic currents (light-evoked inhibitory post-synaptic currents, leIPSCs) in granule cells that exhibited PPD. However, application of NPY did not alter the amplitude of either response of the pair, and did not affect the PPD ratio.

One possible explanation underlying the lack of effect of NPY on PV-GC synapses could be low biological activity of the applied peptide in our recording conditions. Since PV cells receive a major excitatory drive from granule cells mossy fibers, as part of their feedback inhibitory loop, and mossy fiber-mediated synaptic transmission has been previously shown to be sensitive to NPY (McQuiston and Colmers, 1996), we sought to investigate whether sEPSCs recorded from PV cells were affected by NPY. To prospectively identify PV cells for recordings, we used a transgenic mouse line created by crossing PV-Cre mice with the CAG-lox-STOP-lox-tdTomato reporter line. In the offspring, PV cells are labelled with tdTomato, allowing identification of PV cells in the slice. tdTomato positive cells in this mouse line showed high-frequency firing patterns upon sustained depolarization, and axonal arborizations strictly confined to the granule cell layer, confirming their identity as PV-positive cells. Application of NPY markedly reduced the frequency of sEPSCs recorded from PV cells, without affecting their amplitudes, confirming that the applied peptide is biologically active.

Because NPY did not alter PV-GC IPSCs in normal animals, and because the applied peptide is functional, we speculated that in normal conditions PV-GC synapses do not express pre-synaptic NPY receptors. However, the expression of

NPY and its receptors is highly regulated by seizures and hyper-excitability states, and therefore we hypothesized that PV-GC synapses might become sensitive to NPY in hyper-excitability conditions. We induced hyper-excitability by electrical rapid kindling, and recorded leIPSCs from granule cells four to six weeks later. Application of NPY did not alter the amplitude or the PPD ratio of leIPSCs, similarly to what observed in normal animals, suggesting that PV terminals onto granule cells do not express pre-synaptic NPY receptors.

4.2.3 Hyper-excitability alters GABA release at PV-GC synapses

The second objective of the study was to investigate whether hyper-excitability conditions could alter the properties of PV-GC synapses. First we wanted to analyse possible differences in GABA release probability (Pr) between normal and hyper-excitability animals, and therefore we recorded paired-pulses leIPSCs induced by 1 ms light flashes with 100, 250 and 500 ms ISI, from granule cells of both groups. However, the analysis of PPD ratios at all ISI did not reveal differences between the groups, indicating that GABA Pr of PV-GC synapses is not changed in hyper-excitability conditions.

To further analyse the properties of PV-GC synapses, and possibly reveal variations in GABA release due to altered release or changes in readily releasable pool of GABA, we challenged PV cells with repetitive stimulations by applying trains of 10 pulses, and analysed the ratios between each response and the first response of the train. With a stimulation frequency of 10 Hz (100 ms ISI), we found that the ratio at the 10th stimulation was significantly lower in controls compared to hyper-excitability animals. However, when the stimulation frequency was increased to 20 Hz (50 ms ISI), we found that the ratios were significantly smaller in control compared to kindled animals from the 5th stimulation onwards. Unfortunately, higher stimulation frequencies could not be achieved due to the speed limitations of the ChR2 variant used here, and further experiments using improved ChR2 variants (e.g. ChETA) are necessary to study the behaviour of PV-GC synapses at higher, more physiological frequencies (e.g. gamma-band frequencies, 50-100 Hz). Taken together, these data show that PV-GC synapses respond with increased GABA release in hyper-excitability animals, indicating that this type of perisomatic synapses might play an important role in hyper-excitability states.

5 General discussion

5.1 NPY and CCK-basket cells

In *paper I* and *II*, we show that afferent synapses onto CCK-basket cells are modulated by the endogenous excitability modulator NPY in both normal and hyper-excitable conditions. Excitatory and inhibitory drive onto CCK-basket cells is generally decreased by NPY, but a differential modulation of inhibitory synapses occurs between normal and hyper-excitable hippocampi.

5.1.1 Identification of CCK-basket cells

There are at least 16 subtypes of GABAergic interneurons described so far in all major areas of the hippocampus (Somogyi and Klausberger, 2005; Houser, 2007), and their classification is based on different anatomical, electrophysiological and biochemical features (Freund and Buzsaki, 1996). In *paper I* and *II*, we were interested in studying the effects of NPY on CCK-basket cells, a particular subpopulation of GABAergic interneurons proposed as major modulators of hippocampal network activity. To label CCK-basket cells for electrophysiological recordings, we used a mouse line expressing GFP under the control of the GAD65 promoter.

Several lines of evidence support the notion that recorded cells are CCK-basket cells. First, CCK-basket cells in GAD65-GFP mice express GFP. Second, the morphology resembles that of CCK-basket cells, with apical dendrites extending to the outer molecular layer, basal dendrites entering the hilus, and axonal arborisations confined to the granule cell and inner molecular layers (Hefft and Jonas, 2005). Third, cells fire low-frequency, accommodating action potential trains upon depolarization. Finally, cells respond to ACh with a fast inward current that is dependent on activation of $\alpha 7$ nicotinic receptors. Together, these data strongly indicate that recorded cells could be identified as CCK-basket cells, although the possibility that a minority of cells were of another subpopulation of GABAergic interneurons cannot be completely excluded.

5.1.2 Generation of hyper-excitability

In *paper II*, we explored whether hyper-excitability alters the responsiveness of CCK-basket cells afferent synapses to NPY. To induce hyper-excitability, we used a well-established rapid kindling stimulation protocol, and assessed the resulting hyper-excitability by stimulation-induced seizure susceptibility. At the time point for electrophysiological measurements, four weeks after the initial kindling, animals showed an increase in the duration of afterdischarges induced by threshold stimulation, and an increased number of stage 3-5 seizures. These data is consistent with previous results (Elmer et al., 1996), and demonstrates that animals have acquired a hyper-excitabile state at the time point of electrophysiological investigations.

5.1.3 Excitatory input onto CCK-basket cells

In *paper I* and *II*, we show that NPY decreases the frequency of sEPSCs and mEPSCs without affecting their amplitude. Such changes are usually indicative of a pre-synaptic site of action, and suggest that NPY might reduce *Pr* of glutamate. In support of this, similar alterations induced by NPY have been previously described in excitatory synapses onto CA3 pyramidal neurons (McQuiston and Colmers, 1996). Moreover, the decrease in sEPSC and mEPSC frequency was paralleled by an increase in the PPF ratio of optogenetically evoked EPSCs in hyper-excitabile animals (*paper II*), further supporting a decreased glutamate *Pr*. However, NPY did not alter the PPF of electrical stimulation evoked EPSCs in normal animals (*paper I*). Effects of NPY on glutamate release are thought to be mediated by activation of Y2 receptors, which induces a reduction in Ca^{2+} influx via pre-synaptic N- and P/Q-type voltage gated calcium channels (VGCC), as shown in Schaffer Collateral to CA1 excitatory synapses (Qian et al., 1997). However, little is known about the mechanisms of NPY action on glutamate release onto GABAergic cells, and we cannot exclude that in normal animals NPY might act through other mechanisms downstream to the attenuation of calcium entry, or have post-synaptic actions as well. These data suggest that hyper-excitability might alter the way specific glutamatergic synapses onto CCK-basket cells react to NPY, but further experiments are needed to define the exact mechanisms. The calcium dependent mechanisms of neurotransmitter release in pre-synaptic terminals rely on several vesicular proteins, and hyperexcitability might trigger changes in the expression or function of calcium sensors, such as synaptotagmin proteins, therefore altering the fusion of vesicles and possibly release properties. Alternatively, Y2 receptor signalling has been shown to reduce calcium influx through both N-type, P/Q-type and other undefined VGCC (Qian et al., 1997), and a differential preference for one or the other channel type might contribute differently to the decrease in neurotransmitter release, and changes in release probability, between normal and hyperexcitable animals. These

hypothesis could be tested by using VGCC blockers specific for N- or P/Q-type, in combination with electrical or optogenetic stimulations. However, one has to keep in mind that the two sets of experiments (*papers I and II*) were designed and performed separately, with some differences in animal age and slicing procedures, and conclusions drawn from direct comparisons have to be treated with caution. In addition, the methodology used for stimulating CCK-basket cell glutamatergic afferent fibers was also different (electrical vs. optogenetic), and could also contribute to the differences in NPY-induced effects on glutamate release.

CCK-basket cells receive excitatory inputs from perforant path and associational-commissural fibers on their apical dendrites in the molecular layer, and from mossy fiber collaterals on their basal dendrites in the hilus (Kneisler and Dingledine, 1995a; Scharfman, 1995; Freund and Buzsaki, 1996). Moreover, some evidence suggests that basket cells are also the target of CA3 axons back-projecting to the dentate gyrus (Kneisler and Dingledine, 1995b; Scharfman, 2007). Perforant path and associational-commissural fibers are thought to lack Y2 receptor, as indirectly concluded by the failure of NPY to alter stimulation-induced EPSPs and EPSCs recorded in the granule cell layer and from single granule cells (Klapstein and Colmers, 1993). However, the inner molecular layer, where associational-commissural fibers are present, does contain Y2-immunopositive fibers (*paper II*) (Tu et al., 2006), and it is not known whether associational fiber synapses on interneurons differ from those on granule cells. On the other hand, mossy fibers do express Y2 receptors, as previously shown by immunohistochemistry and electrophysiology (McQuiston and Colmers, 1996; Stanic et al., 2006), and contribute to 30–35% of the total excitatory input onto CCK-basket cells (*paper I and II*). Therefore, it cannot be excluded that both mossy fibers and associational-commissural fibers are affected by NPY, but our data and data from the literature might indicate that the effect on mossy fibers is somewhat more pronounced.

5.1.4 Inhibitory input onto CCK-basket cells

In both normal and hyper-excitable animals (*paper I and II*), NPY decreased the frequency of sIPSCs and mIPSCs recorded from CCK-basket cells. Such changes in the frequency and not in the amplitude of spontaneous currents are usually attributable to a pre-synaptic site of action (Behr et al., 2002), and might indicate that NPY acts pre-synaptically to decrease GABA release.

CCK-basket cells receive inhibitory input in the molecular layer from HIPP and HICAP cells, perisomatically from other basket cells (Nunzi et al., 1985), and from Calretinin-positive interneuron-specific-interneurons (CR-IS) in the inner molecular layer (Gulyas et al., 1996). At the moment, it is not clear which of these inputs, or whether all of them, are affected by NPY. In normal

animals (*paper I*), the shift towards faster rise time kinetics observed in sIPSCs and mIPSCs seems to indicate that dendritic inhibitory synapses are more likely to be affected by NPY. However, IPSCs induced by stimulation of the inner molecular layer were also decreased by NPY application, suggesting that NPY effect is not exclusive to dendritic inhibitory synapses onto CCK-basket cells and may also affect perisomatic synapses (from CR-IS cells or other CCK-basket cells).

In hyper-excitabile animals (*paper II*), NPY shifted the rise time of sIPSCs towards slower values, suggesting a preferential action on perisomatic inhibitory afferents onto CCK-basket cells. Such difference between normal and kindled animals could be explained by a differential modulation of Y2 receptor expression. In support, Y2 receptor fiber density was higher, and more up-regulated by kindling, in the inner compared to the outer molecular layer. However, immunohistochemical methods do not allow the investigation of the source of Y2 receptor expression, since Y2-positive glutamatergic and GABAergic fibers are equally stained. It is possible that in basal conditions, Y2-positive fibers in the inner molecular layer are mostly constituted by glutamatergic associational-commissural fibers, but the increase in Y2 receptor expression observed after kindling is selective for GABAergic fibers from CR-IS and CCK-basket cells, thus increasing the preference for NPY to act on perisomatic inhibitory synapses in these conditions.

5.1.5 Functional implications

CCK-basket cells are thought to act as fine-tuning devices of hippocampal network activity, due to the variety of modulatory receptors they selectively express. In particular, CCK-basket cells seem to regulate gamma-frequency oscillations, which are believed to be driven by PV-basket cells, and have been shown to convert into higher frequency epileptiform activity (Traub et al., 2005). The data presented in this thesis add NPY to the range of modulatory mechanisms that can alter the functionality of CCK-basket cells, which could be particularly important in those conditions where NPY and its receptors are up-regulated (e.g. epileptic or hyper-excitabile states).

In normal animals (*paper I*), the effect of NPY onto CCK-basket cells afferents seems to dampen the overall excitability of CCK-basket cells, as excitatory and inhibitory afferents were equally decreased by NPY application. In particular, NPY preferentially acted on dendritic inhibitory synapses onto CCK-basket cells, which are important for regulating plasticity of glutamatergic excitatory dendritic inputs from other principal cells and remote excitatory afferents. Perisomatic inhibitory synapses were less affected, suggesting that the functional output of CCK-basket cells could be somewhat reduced.

On the other hand, in hyper-excitabile animals (*paper II*), the preference of

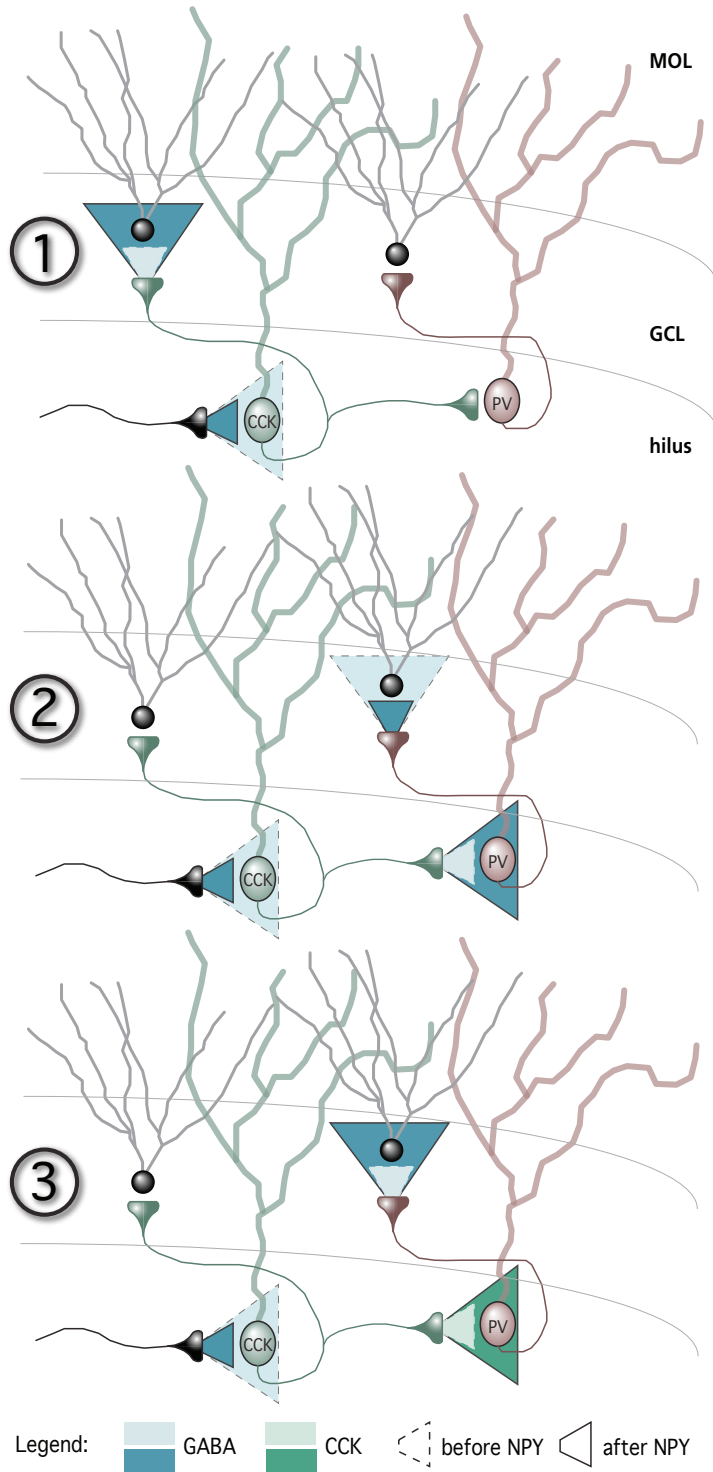


Figure 10: (page 63) Possible functional implications of NPY effects on CCK-basket cells afferents. Perisomatic inhibitory inputs to CCK-basket cells are decreased by NPY. This could result in: **1**, increased GABA release from CCK-basket cells; **2**, lowered granule cell inhibition by PV-basket cells; **3**, CCK-mediated depolarization of PV-basket cells, and consequent increased synchronization of granule cells.

NPY action was shifted towards perisomatic inhibitory synapses, indicating that in these conditions CCK-basket cells might be more prone to fire action potentials. Three possible scenarios below summarize the possible resulting impact on principal cell inhibition:

I. Perisomatic inhibitory synapses are strategically located to control the output of targeted neurons, thanks to their close spatial vicinity to the axon initial segment. The NPY-induced decrease of perisomatic inhibitory input might therefore counteract the paralleled decrease in glutamatergic excitatory input and possibly increase the probability of action potential generation from CCK-basket cells, increasing downstream inhibition of principal cells (Figure 10-1). Such action would represent an adaptive response to the increased excitability of the network.

II. It is becoming increasingly evident that the direct inhibition of principal cells by GABA release is not the only mechanism by which inhibitory interneurons might influence epileptiform activity and seizures (Avoli and de Curtis, 2011). In fact, excessive activity of certain classes of interneurons such as PV-basket cells could instead promote principal cell synchrony and generation of epileptiform discharges, due to their highly synchronized GABA release and extent of interconnectivity via gap junctions. Since CCK-basket cell axons also target PV-basket cells (Karson et al., 2009), an NPY-mediated increase in CCK-to-PV inhibition could potentially diminish the contribution of PV-basket cells to principal cell synchronization (Figure 10-2), counteracting the development of epileptiform activity and seizures.

III. During high-frequency activity in the hippocampus, CCK-basket cells also release CCK together with GABA (Ghijssen et al., 2001), and CCK has been previously shown to depolarize PV-basket cells in CA1 and in the dentate gyrus, increasing their synchronizing impact on principal cells (Deng and Lei, 2006; Foldy et al., 2007). Hypothetical NPY-mediated increase of CCK release would therefore depolarize PV-basket cells and in turn promote the generation of epileptiform activity (Figure 10-3).

Like most biological processes, the overall outcome of the effects of NPY on CCK-basket cells afferents cannot be classified as black or white, but is most likely a shade of grey. The three scenarios described above do not exclude each other,

and the global impact on principal cell excitability is probably determined by a mixture of all three. To delineate further which NPY mechanisms are operating, the use of cell-specific expression of optogenetic tools could provide several advantages. By expressing silencing opsins (e.g. NpHR-derived halorhodopsins) in CCK-basket cells, it would be possible to inhibit GABA release selectively from CCK-basket cells, and therefore quantify the NPY-induced changes in inhibitory drive from CCK-basket cells onto granule cells and PV-basket cells. In addition, such strategies could be used in combination with CCK receptor blockers, to receive further insight on the contribution of the NPY-induced alterations of CCK release. Moreover, afferent and efferent synapses of other subpopulations of interneurons could also be affected by NPY. The mechanisms by which NPY affects inhibitory cell populations could become targets for tailoring gene therapy approaches based on NPY, with the aim of reducing unwanted side effects by only targeting synapses that would contribute to seizure-suppressant actions.

5.2 NPY and PV cells

In *paper III*, we show that synchronous GABA release from Parvalbumin interneurons onto granule cells is not affected by NPY, in neither normal nor hyper-excitable conditions, suggesting that NPY does not regulate these inhibitory synapses. However, GABA release from PV synapses onto granule cell is strengthened during high frequency activity in the hyper-excitable hippocampus, and could possibly promote the synchronization of granule cells and the generation of seizures. Therefore, the possibility that NPY actions on CCK-basket cells might normalize the activity of PV cells (Figure 10-2) could represent an important alternative therapeutic approach for epilepsy.

5.2.1 Stimulation of PV cells

To selectively and synchronously stimulate the ensemble of PV cells in the hippocampus, we used an optogenetic approach involving the injection of a Cre-dependent AAV viral vector carrying ChR2(H134R) in PV-Cre mice. There are two main subclasses of GABAergic interneurons expressing PV in the hippocampus: basket cells and axo-axonic (or chandelier) cells. Despite the similar electrophysiological properties, basket cells and axo-axonic cells slightly differ with regards to the subcellular domain where they target principal cells. Basket cells innervate the cell soma and proximal dendrites, while axo-axonic cells are specialized in targeting the axon initial segment of principal cells. Data from paired electrophysiological recordings show that the large amplitude inhibitory post-synaptic currents evoked in pyramidal cells by the stimulation of these basket and axo-axonic cells are indistinguishable from each other (Buhl et al., 1994). Moreover, the two cell types seem to share the same firing pattern

during gamma-oscillations (Tukker et al., 2007) and theta activity (Klausberger et al., 2003) recorded in vivo. However, recent evidence suggests that GABAergic inputs from axo-axonic cells have a more depolarized reversal potential compared to those from basket cells (Szabadics et al., 2006), indicating that axo-axonic cells might fulfil a different function in the network. In our experiments, since the expression of Cre is driven by the PV promoter, both subclasses express ChR2 and are synchronously activated by blue light pulses.

5.2.2 NPY on PV-GC synapses

Inhibitory post-synaptic currents evoked in granule cells by optogenetic stimulation of PV cells were not affected by application of NPY. This finding could be explained by a low biological activity of the applied peptide, or by a lack of expression of pre-synaptic NPY receptors in PV-GC terminals. Low biological activity of the peptide does not seem to be a likely explanation, since NPY could significantly decrease the frequency of sEPSCs recorded from PV cells. Therefore, lack of NPY receptor expression in PV-GC terminals could account for the absence of NPY effect. Between all NPY receptors, three are mostly expressed in the hippocampal formation (Y1, Y2 and Y5) (Redrobe et al., 1999), and in the first part of this thesis (*paper I*) we showed that NPY action through activation of Y2 receptors could effectively decrease GABA release. In the granule cell layer, where most of the axons from PV positive basket and axo-axonic cells are present, there are moderate levels of Y2 receptor expression (Stanic et al., 2006), but our data suggests that cell types other than PV might be responsible for Y2 expression, e.g. CCK-basket cells.

Taken together, the lack of direct modulation of PV-GC synaptic transmission by NPY seems to imply that PV cells ensembles do not participate in the NPY-induced modulation of epileptiform activity and seizures. However, NPY did decrease glutamatergic transmission at excitatory afferents onto PV cells, and this modulation could potentially impact PV cell excitability and overall inhibition of granule cells.

5.2.3 Enhanced GABA release at PV-GC synapses

The second finding of the study was an increased endurance of GABA release during high frequency optogenetic stimulation in hyper-excitabile conditions. To compare the basic properties of GABA release at PV-GC synapses between normal and hyper-excitabile conditions, we recorded lIPSCs in granule cells evoked by paired light stimulations at different ISI and by trains of 10 stimulations at 10 and 20 Hz. The ratio between the two responses evoked by paired stimulations did not differ between the two groups, suggesting that basic *Pr* of GABA is not altered (Baldelli et al., 2005). When challenged by trains of stimulations, we found that PV cells responded with increased GABA release in

hyper-excitability conditions, indicating an enhanced readily releasable pool (RRP) of GABA at PV-GC synapses in hyper-excitability animals. However, the exact quantification of the GABA RRP is not possible in our recording conditions, since the amplitudes of *le*IPSCs are also dependent on the number of PV cells that are activated by the light stimulation.

The present findings seem to be in contrast with what has been previously published in the pilocarpine model of epilepsy, where the RRP of GABA has been found to be decreased at PV-GC synapses (Zhang and Buckmaster, 2009). However, fundamental differences in study design might explain this controversy. First, the optogenetic approach used here allows to investigate the effects of stimulation of the entire PV cell ensemble, in a more physiological manner than paired recordings, and might unveil more subtle differences that could be hidden by the lower resolution provided by other techniques. Second, systemic pilocarpine injection produces high levels of cell death and inflammation (Voutsinos-Porche et al., 2004), therefore differences in synaptic transmission observed in this model might not only be dependent on increased excitability. On the contrary, the rapid kindling model used here only produced hyper-excitability with minor cell death and inflammation (Wood et al., 2011).

5.2.4 Functional implications

The increased GABA release observed in PV-GC synapses in hyper-excitability conditions might result in two possible scenarios:

I. Overall inhibition of granule cells seems to be decreased in animal models of epilepsy, as measured by a lower frequency of spontaneous and miniature IPSCs (Kobayashi and Buckmaster, 2003), but perisomatic inhibitory input, and specifically that from PV cells, seems to be preserved (Wyeth et al., 2010). Therefore, an increase in GABA release from PV synapses might counteract the loss of inhibition and the increased excitability of the network, and be part of an adaptive response to hyper-excitability conditions.

II. Due to their ability to efficiently synchronize large numbers of principal cells, an increased GABA release from PV cells might promote the generation of epileptiform discharges and be a secondary cause underlying the development of hyper-excitability. In addition, sprouted mossy fibers that develop in hyper-excitability conditions form synaptic contacts with both granule cells and PV cells (Kotti et al., 1997; Sloviter et al., 2006), and might further increase the resonance of the oscillatory network.

6 Concluding remarks

NPY is an important neuropeptide involved in various brain functions, and a powerful endogenous excitability modulator tightly linked to epilepsy and seizures. The seizure-suppressant effects of NPY have largely been explained based on its actions on principal cells and glutamatergic synapses, but effects on inhibitory cell populations have not been explored in details. This thesis provides evidence that certain hippocampal inhibitory networks are largely regulated by NPY, in both normal and hyper-excitable conditions. These findings are relevant to the understanding of physiological processes, where NPY is endogenously expressed, highly modulated by seizures and hyper-excitable conditions, and released as a volume transmitter, but also for tailoring NPY-based gene therapy approaches for epilepsy.

In addition, the increased GABA release from Parvalbumin cells perisomatic inhibitory synapses on granule cells described here might be an important mechanism underlying the generation of high-frequency activity in the hyper-excitable hippocampus, and could become an alternative target for defining antiepileptic treatment strategies.

Acknowledgements

Writing the acknowledgement part of the thesis could sometimes be a more difficult process than writing the thesis itself, mostly because of the fear of forgetting somebody and getting the evil eye in the corridor the next day. Because of that, I prefer to skip many than forgetting few, but will try my best. And if you still feel like you should have been in this list but aren't, feel free to curse me, I probably deserved it.

First I have to thank my **family**, mom, dad, brother, grandmas, grandpas and other relatives, because they have been great at doing what a family should do, that is supporting me and driving me forward, although they always appeared to be more concerned for the fate and wealth of my mice than interested in the actual science. Thanks for not complaining too much when three years turned into four, then five and now six.

Thanks to **Merab**, my main supervisor, for giving me the opportunity to work in your team, having your office door always open, and in general for contributing enormously to my scientific growth. It took some courage to hire me after only a ten-minute Skype conversation, but I hope you did not regret it and I paid you back, at least partially. You have been a great inspiration, have showed me what science is really about, and have always welcomed my ideas and comments with a smile. It was a great pleasure working with you, and I hope we'll keep working together in the future. Thanks also to **Tamuna**, for opening up your house once a year and hosting those nice barbecue dinners.

Thanks to **Olle**, my second supervisor. There are few words that can correctly describe your passion for what you do and have been doing for many years. You are a contagious driving force for the whole department, and I always enjoyed the scientific discussions we had together as well as your speeches at Christmas parties and group dinners. Thanks for creating a great environment to work in, and keeping us all on our feet when we needed to, with a genuine kick in the rear.

Thanks to other members of the EEG. **Andreas**, you were the first person I met on my first day at BMC, and I've been always impressed by your attitude towards science. Although you scared me off for the first month or two, we then managed to accomplish many things together. It's always been a pleasure to be around you, both in the lab and out, enjoying happy hour beers in San Diego and Budapest. **Jan Spieznegl**, thanks for being a very genuine person, for sharing an office and countless days in the patch clamp room, assigning nicknames to our rigs (which can't be repeated here for obvious reasons) and for the great days we had roadtripping around Scandinavia, burning spacepoles and pleasure-cruising. I hope the tradition will keep going. **Irene**, your always-positive attitude has

taught me to chill out, relax and not to fight against things that are out of my control. Thanks for being a great friend over the years. I'll try to visit you, Marc and your two pups more often in the future. Thanks also to **Natalia** and **Fredrik**, my new office mates, good luck with your own theses (but don't always rely on luck, Fortuna is a bitch) and to **My** and **Marita**, for nerdy patch clamp discussions and for helping with my noise frustrations. **Nora**, thanks for helping out with everything else and for taking over my zillions of breedings. **Katarina**, thanks for all the work you do backstage. Thanks also to past EEG members, **Katie J** for introducing me to the patch clamp and homebrewing universes, **Angelica** for trying (even though remarkably unsuccessfully) to produce the Mango crazy mouse with me, and **Mikael** for the whisky bottle.

Thanks to **Carlo**, because in nearly ten years of science together you have taught me so many things that I don't even have space to mention them all here. You are an extremely hard working and highly talented scientist, and after all we've been through together you will always be one of my closest friends. I miss having you around. Thanks also to **James**, for sharing an apartment with me, for letting me beat you at the Playstation, for the many nights out in our early Lund days, and for the many days that I hope will come. **Jackie** and **Daniela**, take care of these two, they need to be looked after more than you might think.

On the other side of the corridor, thanks to the amazing :) **Katie C**, for always smiling and for proofreading the entire thesis, even though you might have had better things to do, you know, with the baby and stuff. **Pietro**, thanks for the concerts, the chats about music and Italian political madness. Thanks to **Karthik**, for your kindness and for feeding Mac vs. PC discussions (which I obviously won since you now have a Mac too). I wish you the best of luck with your married life. On the other building, thanks to **Emanuela** mini-Monny, for always being there when we had to share our frustrations about flu-related, respiratory-obstructing symptoms, and for sharing cells when I needed some. Sometimes you tend to take things a little bit too seriously, but that's what makes you who you are. **Daniel**, thanks for bringing some more Mediterranean character in the lab, and for the mojitos. **Stuart**, thanks for the many laughs, the crisis meetings, the festmetoden, poker nights and the general madness. **Jan B**, for the many golf rounds, and for accepting defeat with honour. **Ariane** and **Martina**, thanks for your friendship and for keeping those two guys where they should be. Thanks also to all the other past and present Restorative Neurologists, you know who you are.

Other people that should be mentioned here include, in random order: **Krzzstzzfs**, thanks for the DT/progressive discussions and the beers at Neurotrain meetings; **Ajoy** "Kumar", for your friendship and your awesome middle name; Pekka, for your remarkable and impenetrable finnishness; **Shane** and **Helene**, for the nights out and the fun; **Bengt**, thanks for the great cover; **Marcus**, **Markus** and **Christer** of the best contemporary prog rock band Soniq Circus, for giving

me the weekly three-hour distraction I sometimes really needed; compare **Marco**, because I know you'll always be a great friend, after coping with me for 25 years; **Pietro, Virgilio** and all the others, for great annual dinners, barbecues, and your continuous support and friendship; the Italian-Swedish crew, **Manolo, Alessandra, Franzetta** et al., for the Italian dinners and everything you've done for me; **Veronica**, thanks for helping out with the translation, good luck with your saline treatment significance; **Matteo**, for letting me visit in Munich and all the things we've been together in these ten years, I really appreciate your friendship.

Last but certainly not least, thanks to **Litsa**, my girlfriend, sambo and (much) better half. I literally could not have done this without you. Thanks for letting me wake up next to you every morning, and for your extreme support at all stages of this marathon. With you life seems a lot easier to tackle. Thanks also to **Betty Spaghetta**, **Parthena, Grigorios** and the other Nikitidis, for embracing me as part of your family.

References

- Andersen P, Bliss TV, Lomo T, Olsen LI, Skrede KK (1969) Lamellar organization of hippocampal excitatory pathways. *Acta physiologica Scandinavica* 76:4A-5A.
- Atasoy D, Aponte Y, Su HH, Sternson SM (2008) A FLEX switch targets Channelrhodopsin-2 to multiple cell types for imaging and long-range circuit mapping. *The Journal of neuroscience : the official journal of the Society for Neuroscience* 28:7025-7030.
- Avoli M (1983) Is epilepsy a disorder of inhibition or excitation? *Progress in clinical and biological research* 124:23-37.
- Avoli M, de Curtis M (2011) GABAergic synchronization in the limbic system and its role in the generation of epileptiform activity. *Progress in neurobiology* 95:104-132.
- Bacci A, Huguenard JR, Prince DA (2002) Differential modulation of synaptic transmission by neuropeptide Y in rat neocortical neurons. *Proceedings of the National Academy of Sciences of the United States of America* 99:17125-17130.
- Balasubramaniam AA (1997) Neuropeptide Y family of hormones: receptor subtypes and antagonists. *Peptides* 18:445-457.
- Baldelli P, Hernandez-Guijo JM, Carabelli V, Carbone E (2005) Brain-derived neurotrophic factor enhances GABA release probability and nonuniform distribution of N- and P/Q-type channels on release sites of hippocampal inhibitory synapses. *The Journal of neuroscience : the official journal of the Society for Neuroscience* 25:3358-3368.
- Baraban SC, Hollopeter G, Erickson JC, Schwartzkroin PA, Palmiter RD (1997) Knock-out mice reveal a critical antiepileptic role for neuropeptide Y. *The Journal of neuroscience : the official journal of the Society for Neuroscience* 17:8927-8936.
- Bausch SB, McNamara JO (2004) Contributions of mossy fiber and CA1 pyramidal cell sprouting to dentate granule cell hyperexcitability in kainic acid-treated hippocampal slice cultures. *Journal of neurophysiology* 92:3582-3595.
- Behr J, Gebhardt C, Heinemann U, Mody I (2002) Kindling enhances kainate receptor-mediated depression of GABAergic inhibition in rat granule cells. *The European journal of neuroscience* 16:861-867.
- Berndt A, Schoenenberger P, Mattis J, Tye KM, Deisseroth K, Hegemann P, Oertner TG (2011) High-efficiency channelrhodopsins for fast neuronal stimulation at low light levels. *Proceedings of the National Academy of Sciences of the United States of America* 108:7595-7600.
- Boyden ES, Zhang F, Bamberg E, Nagel G, Deisseroth K (2005) Millisecond-timescale, genetically targeted optical control of neural activity. *Nature neuroscience* 8:1263-1268.
- Brager DH, Luther PW, Erdelyi F, Szabo G, Alger BE (2003) Regulation of exocytosis from single visualized GABAergic boutons in hippocampal slices. *The Journal of neuroscience : the official journal of the Society for Neuroscience* 23:10475-10486.
- Buhl EH, Halasy K, Somogyi P (1994) Diverse sources of hippocampal unitary inhibitory postsynaptic potentials and the number of synaptic release sites. *Nature* 368:823-828.

- Cardin JA, Carlen M, Meletis K, Knoblich U, Zhang F, Deisseroth K, Tsai LH, Moore CI (2009) Driving fast-spiking cells induces gamma rhythm and controls sensory responses. *Nature* 459:663-667.
- Carnahan J, Nawa H (1995) Regulation of neuropeptide expression in the brain by neurotrophins. Potential role in vivo. *Molecular neurobiology* 10:135-149.
- Colmers WF, Lukowiak K, Pittman QJ (1987) Presynaptic action of neuropeptide Y in area CA1 of the rat hippocampal slice. *The Journal of physiology* 383:285-299.
- Colmers WF, Lukowiak K, Pittman QJ (1988) Neuropeptide Y action in the rat hippocampal slice: site and mechanism of presynaptic inhibition. *The Journal of neuroscience : the official journal of the Society for Neuroscience* 8:3827-3837.
- Cronin J, Dudek FE (1988) Chronic seizures and collateral sprouting of dentate mossy fibers after kainic acid treatment in rats. *Brain research* 474:181-184.
- Cronin J, Obenaus A, Houser CR, Dudek FE (1992) Electrophysiology of dentate granule cells after kainate-induced synaptic reorganization of the mossy fibers. *Brain research* 573:305-310.
- De Potter WP, Dillen L, Annaert W, Tombeur K, Berghmans R, Coen EP (1988) Evidence for the co-storage and co-release of neuropeptide Y and noradrenaline from large dense cored vesicles in sympathetic nerves of the bovine vas deferens. *Synapse* 2:157-162.
- Deng PY, Lei S (2006) Bidirectional modulation of GABAergic transmission by cholecystokinin in hippocampal dentate gyrus granule cells of juvenile rats. *The Journal of physiology* 572:425-442.
- Dobrunz LE, Stevens CF (1997) Heterogeneity of release probability, facilitation, and depletion at central synapses. *Neuron* 18:995-1008.
- Elmer E, Kokaia M, Kokaia Z, Ferencz I, Lindvall O (1996) Delayed kindling development after rapidly recurring seizures: relation to mossy fiber sprouting and neurotrophin, GAP-43 and dynorphin gene expression. *Brain research* 712:19-34.
- Engel J, Jr. (2001) Mesial temporal lobe epilepsy: what have we learned? *The Neuroscientist : a review journal bringing neurobiology, neurology and psychiatry* 7:340-352.
- Engel J, Jr., Wiebe S, French J, Sperling M, Williamson P, Spencer D, Gumnit R, Zahn C, Westbrook E, Enos B (2003) Practice parameter: temporal lobe and localized neocortical resections for epilepsy. *Epilepsia* 44:741-751.
- Eslamboli A, Georgievska B, Ridley RM, Baker HF, Muzyczka N, Burger C, Mandel RJ, Annett L, Kirik D (2005) Continuous low-level glial cell line-derived neurotrophic factor delivery using recombinant adeno-associated viral vectors provides neuroprotection and induces behavioral recovery in a primate model of Parkinson's disease. *The Journal of neuroscience : the official journal of the Society for Neuroscience* 25:769-777.
- Ferezou I, Cauli B, Hill EL, Rossier J, Hamel E, Lambolez B (2002) 5-HT₃ receptors mediate serotonergic fast synaptic excitation of neocortical vasoactive intestinal peptide/cholecystokinin interneurons. *The Journal of neuroscience : the official journal of the Society for Neuroscience* 22:7389-7397.
- Fisher RS, Webber WR, Lesser RP, Arroyo S, Uematsu S (1992) High-frequency EEG activity at the start of seizures. *Journal of clinical neurophysiology : official publication of the American Electroencephalographic Society* 9:441-448.
- Fisher RS, van Emde Boas W, Blume W, Elger C, Genton P, Lee P, Engel J, Jr. (2005) Epileptic seizures and epilepsy: definitions proposed by the International League Against Epilepsy (ILAE) and the International Bureau for Epilepsy (IBE). *Epilepsia* 46:470-472.
- Foldy C, Lee SY, Szabadics J, Neu A, Soltesz I (2007) Cell type-specific gating of perisomatic inhibition by cholecystokinin. *Nature neuroscience* 10:1128-1130.
- Freedman R, Wetmore C, Stromberg I, Leonard S, Olson L (1993) Alpha-bungarotoxin binding to hippocampal interneurons: immunocytochemical characterization and effects on growth factor expression. *The Journal of neuroscience : the official journal of the Society for*

- Neuroscience 13:1965-1975.
- Freund TF (2003) Interneuron Diversity series: Rhythm and mood in perisomatic inhibition. *Trends in neurosciences* 26:489-495.
- Freund TF, Buzsaki G (1996) Interneurons of the hippocampus. *Hippocampus* 6:347-470.
- Freund TF, Katona I (2007) Perisomatic inhibition. *Neuron* 56:33-42.
- Freund TF, Gulyas AI, Acsady L, Gorcs T, Toth K (1990) Serotonergic control of the hippocampus via local inhibitory interneurons. *Proceedings of the National Academy of Sciences of the United States of America* 87:8501-8505.
- Fries P, Reynolds JH, Rorie AE, Desimone R (2001) Modulation of oscillatory neuronal synchronization by selective visual attention. *Science* 291:1560-1563.
- Galarreta M, Hestrin S (1999) A network of fast-spiking cells in the neocortex connected by electrical synapses. *Nature* 402:72-75.
- Ghijssen WE, Leenders AG, Wiegant VM (2001) Regulation of cholecystokinin release from central nerve terminals. *Peptides* 22:1213-1221.
- Gotzsche CR, Nikitidou L, Sorensen AT, Olesen MV, Sorensen G, Christiansen SH, Angehagen M, Woldbye DP, Kokaia M (2012) Combined gene overexpression of neuropeptide Y and its receptor Y5 in the hippocampus suppresses seizures. *Neurobiology of disease* 45:288-296.
- Gruber B, Greber S, Sperk G (1993) Kainic acid seizures cause enhanced expression of cholecystokinin-octapeptide in the cortex and hippocampus of the rat. *Synapse* 15:221-228.
- Gruber B, Greber S, Rupp E, Sperk G (1994) Differential NPY mRNA expression in granule cells and interneurons of the rat dentate gyrus after kainic acid injection. *Hippocampus* 4:474-482.
- Gulyas AI, Hajos N, Freund TF (1996) Interneurons containing calretinin are specialized to control other interneurons in the rat hippocampus. *The Journal of neuroscience : the official journal of the Society for Neuroscience* 16:3397-3411.
- Gulyas AI, Megias M, Emri Z, Freund TF (1999) Total number and ratio of excitatory and inhibitory synapses converging onto single interneurons of different types in the CA1 area of the rat hippocampus. *The Journal of neuroscience : the official journal of the Society for Neuroscience* 19:10082-10097.
- Gunaydin LA, Yizhar O, Berndt A, Sohal VS, Deisseroth K, Hegemann P (2010) Ultrafast optogenetic control. *Nature neuroscience* 13:387-392.
- Hefft S, Jonas P (2005) Asynchronous GABA release generates long-lasting inhibition at a hippocampal interneuron-principal neuron synapse. *Nature neuroscience* 8:1319-1328.
- Hendry SH, Jones EG, DeFelipe J, Schmechel D, Brandon C, Emson PC (1984) Neuropeptide-containing neurons of the cerebral cortex are also GABAergic. *Proceedings of the National Academy of Sciences of the United States of America* 81:6526-6530.
- Hippenmeyer S, Vrieseling E, Sigrist M, Portmann T, Laengle C, Ladle DR, Arber S (2005) A developmental switch in the response of DRG neurons to ETS transcription factor signaling. *PLoS biology* 3:e159.
- Hoess R, Abremski K (1990) In: *Nucleic Acids and Molecular Biology* (Eckstein F, Lilley D, eds): Springer-Verlag, Berlin/Heidelberg.
- Hokfelt T (1991) Neuropeptides in perspective: the last ten years. *Neuron* 7:867-879.
- Hokfelt T, Bartfai T, Bloom F (2003) Neuropeptides: opportunities for drug discovery. *Lancet neurology* 2:463-472.
- Houser CR (2007) Interneurons of the dentate gyrus: an overview of cell types, terminal fields and neurochemical identity. *Progress in brain research* 163:217-232.
- Houser CR, Miyashiro JE, Swartz BE, Walsh GO, Rich JR, Delgado-Escueta AV (1990) Altered patterns of dynorphin immunoreactivity suggest mossy fiber reorganization in human hippocampal epilepsy. *The Journal of neuroscience : the official journal of the Society for*

- Neuroscience 10:267-282.
- Karson MA, Tang AH, Milner TA, Alger BE (2009) Synaptic cross talk between perisomatic-targeting interneuron classes expressing cholecystokinin and parvalbumin in hippocampus. *The Journal of neuroscience : the official journal of the Society for Neuroscience* 29:4140-4154.
- Katona I, Sperlagh B, Sik A, Kafalvi A, Vizi ES, Mackie K, Freund TF (1999) Presynaptically located CB1 cannabinoid receptors regulate GABA release from axon terminals of specific hippocampal interneurons. *The Journal of neuroscience : the official journal of the Society for Neuroscience* 19:4544-4558.
- Klapstein GJ, Colmers WF (1993) On the sites of presynaptic inhibition by neuropeptide Y in rat hippocampus in vitro. *Hippocampus* 3:103-111.
- Klapstein GJ, Colmers WF (1997) Neuropeptide Y suppresses epileptiform activity in rat hippocampus in vitro. *Journal of neurophysiology* 78:1651-1661.
- Klausberger T, Magill PJ, Marton LF, Roberts JD, Cobden PM, Buzsaki G, Somogyi P (2003) Brain-state- and cell-type-specific firing of hippocampal interneurons in vivo. *Nature* 421:844-848.
- Kneisler TB, Dingledine R (1995a) Spontaneous and synaptic input from granule cells and the perforant path to dentate basket cells in the rat hippocampus. *Hippocampus* 5:151-164.
- Kneisler TB, Dingledine R (1995b) Synaptic input from CA3 pyramidal cells to dentate basket cells in rat hippocampus. *The Journal of physiology* 487 (Pt 1):125-146.
- Kobayashi M, Buckmaster PS (2003) Reduced inhibition of dentate granule cells in a model of temporal lobe epilepsy. *The Journal of neuroscience : the official journal of the Society for Neuroscience* 23:2440-2452.
- Kofler N, Kirchmair E, Schwarzer C, Sperk G (1997) Altered expression of NPY-Y1 receptors in kainic acid induced epilepsy in rats. *Neurosci Lett* 230:129-132.
- Kokaia M, Sørensen AT (2011) The treatment of neurological diseases under a new light: the importance of optogenetics. *Drugs Today (Barc)*. 2011 Jan;47(1):53-62.
- Kotti T, Riekkinen PJ, Sr., Miettinen R (1997) Characterization of target cells for aberrant mossy fiber collaterals in the dentate gyrus of epileptic rat. *Experimental neurology* 146:323-330.
- Kraushaar U, Jonas P (2000) Efficacy and stability of quantal GABA release at a hippocampal interneuron-principal neuron synapse. *The Journal of neuroscience : the official journal of the Society for Neuroscience* 20:5594-5607.
- Lavenex P, Amaral DG (2000) Hippocampal-neocortical interaction: a hierarchy of associativity. *Hippocampus* 10:420-430.
- Lin JY, Lin MZ, Steinbach P, Tsien RY (2009) Characterization of engineered channelrhodopsin variants with improved properties and kinetics. *Biophysical journal* 96:1803-1814.
- Liu XB, Jones EG (1996) Localization of alpha type II calcium calmodulin-dependent protein kinase at glutamatergic but not gamma-aminobutyric acid (GABAergic) synapses in thalamus and cerebral cortex. *Proceedings of the National Academy of Sciences of the United States of America* 93:7332-7336.
- Llinas R, Ribary U (1993) Coherent 40-Hz oscillation characterizes dream state in humans. *Proceedings of the National Academy of Sciences of the United States of America* 90:2078-2081.
- Lutzenberger W, Ripper B, Busse L, Birbaumer N, Kaiser J (2002) Dynamics of gamma-band activity during an audiospatial working memory task in humans. *The Journal of neuroscience : the official journal of the Society for Neuroscience* 22:5630-5638.
- Mack A, Sauer B, Abremski K, Hoess R (1992) Stoichiometry of the Cre recombinase bound to the lox recombining site. *Nucleic acids research* 20:4451-4455.
- Madisen L, Zwingman TA, Sunkin SM, Oh SW, Zariwala HA, Gu H, Ng LL, Palmiter RD, Hawrylycz MJ, Jones AR, Lein ES, Zeng H (2010) A robust and high-throughput Cre reporting and characterization system for the whole mouse brain. *Nature neuroscience*

- 13:133-140.
- Magloczky Z, Freund TF (1993) Selective neuronal death in the contralateral hippocampus following unilateral kainate injections into the CA3 subfield. *Neuroscience* 56:317-335.
- Magloczky Z, Wittner L, Borhegyi Z, Halasz P, Vajda J, Czirjak S, Freund TF (2000) Changes in the distribution and connectivity of interneurons in the epileptic human dentate gyrus. *Neuroscience* 96:7-25.
- Marchionni I, Maccaferri G (2009) Quantitative dynamics and spatial profile of perisomatic GABAergic input during epileptiform synchronization in the CA1 hippocampus. *The Journal of physiology* 587:5691-5708.
- Marksteiner J, Ortler M, Bellmann R, Sperk G (1990) Neuropeptide Y biosynthesis is markedly induced in mossy fibers during temporal lobe epilepsy of the rat. *Neurosci Lett* 112:143-148.
- Mathern GW, Babb TL, Pretorius JK, Leite JP (1995) Reactive synaptogenesis and neuron densities for neuropeptide Y, somatostatin, and glutamate decarboxylase immunoreactivity in the epileptogenic human fascia dentata. *The Journal of neuroscience : the official journal of the Society for Neuroscience* 15:3990-4004.
- Matyas F, Freund TF, Gulyas AI (2004) Convergence of excitatory and inhibitory inputs onto CCK-containing basket cells in the CA1 area of the rat hippocampus. *The European journal of neuroscience* 19:1243-1256.
- McQuiston AR, Colmers WF (1996) Neuropeptide Y2 receptors inhibit the frequency of spontaneous but not miniature EPSCs in CA3 pyramidal cells of rat hippocampus. *Journal of neurophysiology* 76:3159-3168.
- Michel MC, Beck-Sickinger A, Cox H, Doods HN, Herzog H, Larhammar D, Quirion R, Schwartz T, Westfall T (1998) XVI. International Union of Pharmacology recommendations for the nomenclature of neuropeptide Y, peptide YY, and pancreatic polypeptide receptors. *Pharmacological reviews* 50:143-150.
- Miles R, Toth K, Gulyas AI, Hajos N, Freund TF (1996) Differences between somatic and dendritic inhibition in the hippocampus. *Neuron* 16:815-823.
- Mody I, Otis TS, Staley KJ, Kohr G (1992) The balance between excitation and inhibition in dentate granule cells and its role in epilepsy. *Epilepsy research Supplement* 9:331-339.
- Molnar P, Nadler JV (1999) Mossy fiber-granule cell synapses in the normal and epileptic rat dentate gyrus studied with minimal laser photostimulation. *Journal of neurophysiology* 82:1883-1894.
- Nagel G, Brauner M, Liewald JF, Adeishvili N, Bamberg E, Gottschalk A (2005) Light activation of channelrhodopsin-2 in excitable cells of *Caenorhabditis elegans* triggers rapid behavioral responses. *Current biology : CB* 15:2279-2284.
- Nagel G, Szellas T, Huhn W, Kateriya S, Adeishvili N, Berthold P, Ollig D, Hegemann P, Bamberg E (2003) Channelrhodopsin-2, a directly light-gated cation-selective membrane channel. *Proceedings of the National Academy of Sciences of the United States of America* 100:13940-13945.
- Noe F, Pool AH, Nissinen J, Gobbi M, Bland R, Rizzi M, Balducci C, Ferraguti F, Sperk G, During MJ, Pitkanen A, Vezzani A (2008) Neuropeptide Y gene therapy decreases chronic spontaneous seizures in a rat model of temporal lobe epilepsy. *Brain : a journal of neurology* 131:1506-1515.
- Nunzi MG, Gorio A, Milan F, Freund TF, Somogyi P, Smith AD (1985) Cholecystokinin-immunoreactive cells form symmetrical synaptic contacts with pyramidal and nonpyramidal neurons in the hippocampus. *The Journal of comparative neurology* 237:485-505.
- Papp EC, Hajos N, Acsady L, Freund TF (1999) Medial septal and median raphe innervation of vasoactive intestinal polypeptide-containing interneurons in the hippocampus. *Neuroscience* 90:369-382.
- Paredes MF, Greenwood J, Baraban SC (2003) Neuropeptide Y modulates a G protein-coupled

- inwardly rectifying potassium current in the mouse hippocampus. *Neurosci Lett* 340:9-12.
- Perez Y, Morin F, Beaulieu C, Lacaille JC (1996) Axonal sprouting of CA1 pyramidal cells in hyperexcitable hippocampal slices of kainate-treated rats. *The European journal of neuroscience* 8:736-748.
- Porter JT, Cauli B, Tsuzuki K, Lambolez B, Rossier J, Audinat E (1999) Selective excitation of subtypes of neocortical interneurons by nicotinic receptors. *The Journal of neuroscience : the official journal of the Society for Neuroscience* 19:5228-5235.
- Qian J, Colmers WF, Saggau P (1997) Inhibition of synaptic transmission by neuropeptide Y in rat hippocampal area CA1: modulation of presynaptic Ca²⁺ entry. *The Journal of neuroscience : the official journal of the Society for Neuroscience* 17:8169-8177.
- Racine RJ (1972) Modification of seizure activity by electrical stimulation. II. Motor seizure. *Electroencephalogr Clin Neurophysiol* 32:281-294.
- Redrobe JP, Dumont Y, St-Pierre JA, Quirion R (1999) Multiple receptors for neuropeptide Y in the hippocampus: putative roles in seizures and cognition. *Brain research* 848:153-166.
- Ribak CE, Peterson GM (1991) Intragranular mossy fibers in rats and gerbils form synapses with the somata and proximal dendrites of basket cells in the dentate gyrus. *Hippocampus* 1:355-364.
- Richichi C, Lin EJ, Stefanin D, Colella D, Ravizza T, Grignaschi G, Veglianesi P, Sperk G, During MJ, Vezzani A (2004) Anticonvulsant and antiepileptogenic effects mediated by adeno-associated virus vector neuropeptide Y expression in the rat hippocampus. *The Journal of neuroscience : the official journal of the Society for Neuroscience* 24:3051-3059.
- Robbins RJ, Brines ML, Kim JH, Adrian T, de Lanerolle N, Welsh S, Spencer DD (1991) A selective loss of somatostatin in the hippocampus of patients with temporal lobe epilepsy. *Annals of neurology* 29:325-332.
- Scharfman HE (1995) Electrophysiological evidence that dentate hilar mossy cells are excitatory and innervate both granule cells and interneurons. *Journal of neurophysiology* 74:179-194.
- Scharfman HE (2007) The CA3 "backprojection" to the dentate gyrus. *Progress in brain research* 163:627-637.
- Scharfman HE, Sollas AL, Berger RE, Goodman JH (2003) Electrophysiological evidence of monosynaptic excitatory transmission between granule cells after seizure-induced mossy fiber sprouting. *Journal of neurophysiology* 90:2536-2547.
- Schwarzer C, Kofler N, Sperk G (1998) Up-regulation of neuropeptide Y-Y2 receptors in an animal model of temporal lobe epilepsy. *Mol Pharmacol* 53:6-13.
- Schwarzer C, Williamson JM, Lothman EW, Vezzani A, Sperk G (1995) Somatostatin, neuropeptide Y, neurokinin B and cholecystokinin immunoreactivity in two chronic models of temporal lobe epilepsy. *Neuroscience* 69:831-845.
- Seino M (2006) Classification criteria of epileptic seizures and syndromes. *Epilepsy research* 70 Suppl 1:S27-33.
- Sloviter RS (1989) Calcium-binding protein (calbindin-D28k) and parvalbumin immunocytochemistry: localization in the rat hippocampus with specific reference to the selective vulnerability of hippocampal neurons to seizure activity. *The Journal of comparative neurology* 280:183-196.
- Sloviter RS, Zappone CA, Harvey BD, Frotscher M (2006) Kainic acid-induced recurrent mossy fiber innervation of dentate gyrus inhibitory interneurons: possible anatomical substrate of granule cell hyper-inhibition in chronically epileptic rats. *The Journal of comparative neurology* 494:944-960.
- Smith BN, Dudek FE (2001) Short- and long-term changes in CA1 network excitability after kainate treatment in rats. *Journal of neurophysiology* 85:1-9.
- Sohal VS, Zhang F, Yizhar O, Deisseroth K (2009) Parvalbumin neurons and gamma rhythms enhance cortical circuit performance. *Nature* 459:698-702.
- Somogyi P, Klausberger T (2005) Defined types of cortical interneurone structure space and spike

- timing in the hippocampus. *The Journal of physiology* 562:9-26.
- Sorensen AT, Kanter-Schlifke I, Lin EJ, During MJ, Kokaia M (2008a) Activity-dependent volume transmission by transgene NPY attenuates glutamate release and LTP in the subiculum. *Molecular and cellular neurosciences* 39:229-237.
- Sorensen AT, Kanter-Schlifke I, Carli M, Balducci C, Noe F, During MJ, Vezzani A, Kokaia M (2008b) NPY gene transfer in the hippocampus attenuates synaptic plasticity and learning. *Hippocampus* 18:564-574.
- Sperk G, Marksteiner J, Gruber B, Bellmann R, Mahata M, Ortler M (1992) Functional changes in neuropeptide Y- and somatostatin-containing neurons induced by limbic seizures in the rat. *Neuroscience* 50:831-846.
- Stanic D, Brumovsky P, Fetissov S, Shuster S, Herzog H, Hokfelt T (2006) Characterization of neuropeptide Y2 receptor protein expression in the mouse brain. I. Distribution in cell bodies and nerve terminals. *The Journal of comparative neurology* 499:357-390.
- Sutula T, Cascino G, Cavazos J, Parada I, Ramirez L (1989) Mossy fiber synaptic reorganization in the epileptic human temporal lobe. *Annals of neurology* 26:321-330.
- Szabadics J, Varga C, Molnar G, Olah S, Barzo P, Tamas G (2006) Excitatory effect of GABAergic axo-axonic cells in cortical microcircuits. *Science* 311:233-235.
- Tauck DL, Nadler JV (1985) Evidence of functional mossy fiber sprouting in hippocampal formation of kainic acid-treated rats. *The Journal of neuroscience : the official journal of the Society for Neuroscience* 5:1016-1022.
- Thureson-Klein A, Klein RL, Zhu PC (1986) Exocytosis from large dense cored vesicles as a mechanism for neuropeptide release in the peripheral and central nervous system. *Scanning electron microscopy*:179-187.
- Traub RD, Kopell N, Bibbig A, Buhl EH, LeBeau FE, Whittington MA (2001) Gap junctions between interneuron dendrites can enhance synchrony of gamma oscillations in distributed networks. *The Journal of neuroscience : the official journal of the Society for Neuroscience* 21:9478-9486.
- Traub RD, Pais I, Bibbig A, Lebeau FE, Buhl EH, Garner H, Monyer H, Whittington MA (2005) Transient depression of excitatory synapses on interneurons contributes to epileptiform bursts during gamma oscillations in the mouse hippocampal slice. *Journal of neurophysiology* 94:1225-1235.
- Tu B, Jiao Y, Herzog H, Nadler JV (2006) Neuropeptide Y regulates recurrent mossy fiber synaptic transmission less effectively in mice than in rats: Correlation with Y2 receptor plasticity. *Neuroscience* 143:1085-1094.
- Tukker JJ, Fuentealba P, Hartwich K, Somogyi P, Klausberger T (2007) Cell type-specific tuning of hippocampal interneuron firing during gamma oscillations in vivo. *The Journal of neuroscience : the official journal of the Society for Neuroscience* 27:8184-8189.
- Vezzani A, Sperk G, Colmers WF (1999) Neuropeptide Y: emerging evidence for a functional role in seizure modulation. *Trends in neurosciences* 22:25-30.
- Vezzani A, Michalkiewicz M, Michalkiewicz T, Moneta D, Ravizza T, Richichi C, Aliprandi M, Mule F, Pirona L, Gobbi M, Schwarzer C, Sperk G (2002) Seizure susceptibility and epileptogenesis are decreased in transgenic rats overexpressing neuropeptide Y. *Neuroscience* 110:237-243.
- Voutsinos-Porche B, Koning E, Kaplan H, Ferrandon A, Guenounou M, Nehlig A, Motte J (2004) Temporal patterns of the cerebral inflammatory response in the rat lithium-pilocarpine model of temporal lobe epilepsy. *Neurobiology of disease* 17:385-402.
- Wahlestedt C, Pich EM, Koob GF, Yee F, Heilig M (1993) Modulation of anxiety and neuropeptide Y-Y1 receptors by antisense oligodeoxynucleotides. *Science* 259:528-531.
- Witter MP, Amaral DG (2004) Hippocampal Formation. In: *The Rat Nervous System*, Third Edition (Paxinos G, ed): Elsevier.
- Wittner L, Eross L, Czirjak S, Halasz P, Freund TF, Maglóczy Z (2005) Surviving CA1 pyramidal

- cells receive intact perisomatic inhibitory input in the human epileptic hippocampus. *Brain : a journal of neurology* 128:138-152.
- Wittner L, Magloczky Z, Borhegyi Z, Halasz P, Toth S, Eross L, Szabo Z, Freund TF (2001) Preservation of perisomatic inhibitory input of granule cells in the epileptic human dentate gyrus. *Neuroscience* 108:587-600.
- Woldbye DP, Madsen TM, Larsen PJ, Mikkelsen JD, Bolwig TG (1996) Neuropeptide Y inhibits hippocampal seizures and wet dog shakes. *Brain research* 737:162-168.
- Woldbye DP, Larsen PJ, Mikkelsen JD, Klemp K, Madsen TM, Bolwig TG (1997) Powerful inhibition of kainic acid seizures by neuropeptide Y via Y5-like receptors. *Nat Med* 3:761-764.
- Woldbye DP, Angehagen M, Gotzsche CR, Elbrond-Bek H, Sorensen AT, Christiansen SH, Olesen MV, Nikitidou L, Hansen TV, Kanter-Schlifke I, Kokaia M (2010) Adeno-associated viral vector-induced overexpression of neuropeptide Y Y2 receptors in the hippocampus suppresses seizures. *Brain : a journal of neurology* 133:2778-2788.
- Wood JC, Jackson JS, Jakubs K, Chapman KZ, Ekdahl CT, Kokaia Z, Kokaia M, Lindvall O (2011) Functional integration of new hippocampal neurons following insults to the adult brain is determined by characteristics of pathological environment. *Experimental neurology* 229:484-493.
- Wyeth MS, Zhang N, Mody I, Houser CR (2010) Selective reduction of cholecystokinin-positive basket cell innervation in a model of temporal lobe epilepsy. *The Journal of neuroscience : the official journal of the Society for Neuroscience* 30:8993-9006.
- Zhang W, Buckmaster PS (2009) Dysfunction of the dentate basket cell circuit in a rat model of temporal lobe epilepsy. *The Journal of neuroscience : the official journal of the Society for Neuroscience* 29:7846-7856.
- Zucker RS, Regehr WG (2002) Short-term synaptic plasticity. *Annual review of physiology* 64:355-405.

Paper I

Tuning Afferent Synapses of Hippocampal Interneurons by Neuropeptide Y

Marco Ledri,¹ Andreas Toft Sørensen,¹ Ferenc Erdelyi,² Gabor Szabo,² and Merab Kokaia^{1*}

ABSTRACT: Cholecystokinin (CCK)-expressing basket cells encompass a subclass of inhibitory GABAergic interneurons that regulate memory-forming oscillatory network activity of the hippocampal formation in accordance to the emotional and motivational state of the animal, conveyed onto these cells by respective extrahippocampal afferents. Various excitatory and inhibitory afferent and efferent synapses of the hippocampal CCK basket cells express serotonergic, cholinergic, cannabinoid, and benzodiazepine sensitive receptors, all contributing to their functional plasticity. We explored whether CCK basket cells are modulated by neuropeptide Y (NPY), one of the major local neuropeptides that strongly inhibits hippocampal excitability and has significant effect on its memory function. Here, using GAD65-GFP transgenic mice for prospective identification of CCK basket cells and whole-cell patch-clamp recordings, we show for the first time that excitatory and inhibitory inputs onto CCK basket cells in the dentate gyrus of the hippocampus are modulated by NPY through activation of NPY Y2 receptors. The frequency of spontaneous and miniature EPSCs, as well as the amplitudes of stimulation-evoked EPSCs were decreased. Similarly, the frequency of both spontaneous and miniature IPSCs, and the amplitudes of stimulation-evoked IPSCs were decreased after NPY application. Most of the effects of NPY could be attributed to a presynaptic site of action. Our data provide the first evidence that the excitatory and inhibitory inputs onto the CCK basket cells could be modulated by local levels of NPY, and may change the way these cells process extrahippocampal afferent information, influencing hippocampal function and its network excitability during normal and pathological oscillatory activities. © 2009 Wiley-Liss, Inc.

KEY WORDS: basket cell; synaptic transmission; Y2 receptor; EPSCs; IPSCs

INTRODUCTION

Because of wide network connections to principal cells, heterogeneous population of inhibitory interneurons in the cortex and hippocampal formation define timely and spatially precise phases of action potential generation in principal cell ensembles (Buzsáki and Chrobak, 1995),

thus participating in information processing, memory function, and synaptic plasticity (Gray, 1994; Buzsáki and Chrobak, 1995). In the hippocampal formation, parvalbumin (PV)-positive basket cells inhibit principal cells in a feed-forward and feed-back manner, and are involved in generation of network γ -frequency oscillations (30–90 Hz), which determine action potential timing of the principal cells and may play a role in memory formation (Buzsáki et al., 1983; Lisman and Idiart, 1995; Lisman, 1999). Modulation and fine-tuning of γ -frequency oscillations, particularly by emotional, motivational and general neurophysiological state of the animal, is proposed to be achieved by another subclass of basket cells that express cholecystokinin (CCK) (Freund, 2003). These cells receive serotonergic afferents from the raphe nucleus (Freund et al., 1990; Papp et al., 1999; Ferezou et al., 2002), express $\alpha 7$ nicotinic receptors (Freedman et al., 1993; Frazier et al., 1998; Morales et al., 2008), their inhibitory synapses on principal cells express CB1 cannabinoid receptors presynaptically (Katona et al., 1999) and benzodiazepine-responsive (Low et al., 2000) $\alpha 2$ GABA_A receptor subunit postsynaptically (Nyiri et al., 2001). The γ -frequency oscillations can also be transformed into higher frequency oscillatory bursting or epileptiform activity (Traub et al., 2005), which may promote epileptogenesis in experimental animals.

Neuropeptide Y (NPY) is a 36-amino acid peptide abundantly expressed and widely distributed in the central nervous system, and has been shown to be involved in regulation of feeding, blood pressure, anxiety, and memory (Wahlestedt et al., 1993; Balasubramaniam, 1997). NPY has also been shown to inhibit hippocampal excitability and seizure activity in the brain (Smialowska et al., 1996; Bijak, 1999; Vezzani et al., 1999; Richichi et al., 2004). NPY-knock out (KO) mice display more severe kainate seizures (Baraban et al., 1997), while transgenic rats overexpressing NPY (Vezzani et al., 2002), or those transduced with recombinant AAV-NPY virus (Richichi et al., 2004) are more resistant to chemically and/or electrically induced seizures, respectively. The mechanisms underlying the NPY effect on seizures are not completely understood, but are thought to be due to reduced glutamate release because of attenuation of G-protein dependent calcium influx into the presynapses of

¹ Experimental Epilepsy Group, Wallenberg Neuroscience Center, Lund University Hospital, Sweden; ² Department of Gene Technology and Developmental Neurobiology, Institute for Experimental Medicine, Budapest, Hungary

Grant sponsor: EU Commission grant EPICURE; Grant number: LSH-037315; Grant sponsors: EU Commission grant NEUROTRAIN, Segerfalk Foundation, Crafoord Foundation, Kock Foundation, Swedish Research Council

*Correspondence to: Merab Kokaia, Experimental Epilepsy Group, Wallenberg Neuroscience Center, Lund University Hospital, Sweden. E-mail: Merab.Kokaia@med.lu.se

Accepted for publication 13 October 2009

DOI 10.1002/hipo.20740

Published online 30 December 2009 in Wiley Online Library (wileyonlinelibrary.com).

principal cells (Qian et al., 1997; Colmers et al., 1988). NPY also decreases the amplitude of stimulation-evoked IPSCs in cortical inhibitory interneurons (Bacci et al., 2002). Until now, no data has been available on the effects of NPY on the synaptic transmission onto inhibitory interneurons in the hippocampal formation.

The objectives of this study were to explore whether and how NPY modulates excitatory and/or inhibitory synaptic afferent inputs to the CCK basket cells in the dentate gyrus, and identify NPY receptor subtypes involved in such effects. In the central nervous system, three NPY receptor subtypes (Y1, Y2, Y5) are more abundant and expressed in different areas, including the hippocampal formation and the neocortex (Dumont et al., 1993; Dumont et al., 1998).

MATERIALS AND METHODS

Animals

Glutamic Acid Decarboxylase 65 (GAD65)-GFP mice, 14–28 days old, were used for these experiments. In this transgenic line, GFP is expressed under the control of the GAD65 promoter (Lopez-Bendito et al., 2004). All experiments were conducted according to international guidelines on the use of animals, as well as Swedish Animal Welfare Agency guidelines and approved by the local Ethical Committee for Experimental Animals.

Slice Preparation For Electrophysiology

For hippocampal slice preparation, animals were decapitated, the brains were rapidly removed and placed in ice-cold sucrose solution (pH 7.2–7.4, mOsm 290–300) containing (in mM): sucrose 195, KCl 2.5, CaCl₂ 0.5, MgCl₂ 7, NaHCO₃ 28, NaH₂PO₄ 12.5, glucose 7, ascorbate 1, pyruvate 3. Hippocampi were dissected, transverse slices (250 µm) were cut with a vibratome (3,000 Deluxe, Ted Pella Inc., CA) and placed in sucrose solution at room temperature and constantly oxygenated with carbogen (95% O₂/5% CO₂).

Slices were then transferred to artificial cerebro-spinal fluid (aCSF, pH 7.2–7.4, mOsm 290–300) containing (in mM): NaCl 119, KCl 2.5, MgSO₄ 1.3, CaCl₂ 2.5, NaHCO₃ 26.2, NaH₂PO₄ 1, and glucose 11, held at room temperature and oxygenated with carbogen. Slices were allowed to rest in aCSF for a minimum of 1 h before the start of the recordings.

Whole-Cell Patch-Clamp Electrophysiology

Individual slices were placed in a submerged recording chamber constantly perfused with gassed aCSF at room temperature, unless otherwise noted. GAD65-GFP positive cells in the dentate gyrus were visualized by fluorescent light, and infrared light was used for visual approach of the recording pipette. Recording pipettes (3–6 MΩ resistance) were pulled from borosilicate glass with a Flaming-Brown horizontal puller (P-97, Sut-

ter Instruments, CA), and contained (in mM): K-Gluconate 122.5, KCl 12.5, KOH-HEPES 10, KOH-EGTA 0.2, MgATP 2, Na₃GTP 0.3, NaCl 8 (pH 7.2–7.4, mOsm 290–300) for measurements of intrinsic properties and acetylcholine (ACh)-induced responses; Cs-Gluconate 117.5, CsCl 17.5, NaCl 8, CsOH-HEPES 10, CsOH-EGTA 0.2, MgATP 2, Na₃GTP 0.3, QX-314 5 (pH 7.2–7.4, mOsm 290–300) for spontaneous, miniature and stimulation-evoked excitatory postsynaptic currents recordings (sEPSCs, mEPSCs and EPSCs, respectively); CsCl 135, CsOH 10, CsOH-EGTA 0.2, MgATP 2, Na₃GTP 0.3, NaCl 8, QX-314 5 (pH 7.2–7.4, mOsm 290–300) for spontaneous, miniature and stimulation-evoked inhibitory postsynaptic currents recordings (sIPSCs, mIPSCs, and IPSCs, respectively).

EPSCs were recorded in the presence of 100-µM picrotoxin (PTX, Tocris Bioscience, Ellisville, MI) to block γ-aminobutyric acid A (GABA_A) receptors. 50 µM DL-2-amino-5-phosphonovaleric acid (D-AP5, Tocris) and 5 µM 2,3-dihydroxy-6-nitro-7-sulfamoyl-benzo[f]quinoxaline-2,3-dione (NBQX, Tocris) were used during IPSC recordings to block *N*-Methyl-D-Aspartate (NMDA) and α-amino-3-hydroxy-5-methylisoxazole-4-propionic acid (AMPA) receptors, respectively. For mEPSC and mIPSC recordings, 1 µM Tetrodotoxin (TTX, Tocris) was used to block voltage-gated sodium channels and prevent generation of action potentials.

For stimulation-evoked recordings (i.e., EPSCs and IPSCs), stainless steel bipolar microelectrodes were used for stimulating the border between the inner third of the molecular layer and the granule cell layer of the dentate gyrus or the *stratum lucidum* of CA3. Paired-pulse stimulations at 0.1 Hz were used with 50 ms or 100 ms interstimulus interval (ISI) to elicit paired-pulse EPSCs or IPSCs.

NPY (Schafer-N, Copenhagen, Denmark) and “free-acid NPY” (Bachem AG, Switzerland) were dissolved in distilled water, stored in concentrated aliquots and diluted to 1-µM concentration in the perfusion solution immediately before use. Peptides were allowed to diffuse in the recording chamber for 7 min before the continuation of the recordings, and were present until the end of the experiment. Silicon-coated tubings and bottles were used to prevent the peptides from adhering to the tubing and container walls. The highly specific Y2 receptor blocker (S)-N2-[[1-[2-[4-[(R,S)-5,11-dihydro-6(6h)-oxodibenz[b,e]azepin-11-yl]-1-π peraziny]-2-oxoethyl] cyclopentyl] acetyl]-N-[2-[1,2-dihydro-3,5(4H)-dioxo-1,2-diphenyl-3H-1,2,4-triazol-4-yl]e thyl]-argininamid (BIIE0246, Boehringer Ingelheim Pharma, Germany) was initially dissolved in ethanol (70%) and then diluted 1:5,000 in the perfusion solution to reach a final concentration of 0.6 µM. The specific metabotropic group II receptor (mGluR II) agonist (2S,1's,2's)-2-(Carboxycyclopropyl)-glycine (L-CCG-I, 10 µM, Tocris) was used to activate mGluR II, which are exclusively expressed presynaptically on mossy fibers, to selectively block glutamate release from mossy fibers and respective mossy fiber-specific EPSCs in postsynaptic neurons (Castillo et al., 1997; Kokaia et al., 1998). PTX or D-AP5 and NBQX were applied at the end of the experiments to verify that synaptic currents were generated by respective receptor acti-

vation. Biocytin (0.5 mg/ml, Sigma) was routinely dissolved in the pipette solution and used for retrospective identification of the recorded cells.

Data were sampled at 10 kHz with an EPC-10 amplifier (HEKA Elektronik, Lambrecht, Germany) and stored on a G4 Macintosh computer using PatchMaster software (HEKA) for offline analysis.

Focal Application of Acetylcholine

For focal application, ACh-containing pipette (similar to the recording pipette) was placed in the hilus 5–10 μ m away from the cell soma of the recorded cell, and brief microinjections were made by applying pressure pulses (10–20 ms) of 2–4 PSI to the pipette using a Picospritzer II (General Valve, Fairfield, NJ). Whole-cell currents were recorded in putative GFP+/CCK+ cells, voltage clamped at -70 mV. To confirm that ACh-induced currents were generated by activation of nicotinic $\alpha 7$ receptors, we first applied atropine (a selective muscarinic receptor antagonist, 5 μ M, Sigma) to the perfusion solution, followed by a combination of TTX, NBQX and D-AP5 to block action potentials and glutamate receptors. Finally, the selective $\alpha 7$ nicotinic acetylcholine receptor (nAChR) antagonist methyllycaconitine (MLA, 50 μ M, Sigma) was added.

Immunohistochemical Procedures

For identification of the recorded cells, slices from electrophysiological recordings were first fixed in 4% paraformaldehyde (PFA) in phosphate buffer (PB) for 12–24 h and then stored in Walter's antifreeze solution (ethylenglycol and glycerol in PB buffer) at -20°C . To characterize the population of basket cells recorded in this study, GAD65-GFP animals not used for electrophysiology received an overdose of pentobarbital (250 mg/kg i.p.) and were perfused transcardially with 50 ml of ice-cold saline (0.9% NaCl) and 50 ml of ice-cold 4% PFA in PB (pH 7.2–7.4) (for PV immunohistochemistry) or 25 ml of ice-cold 4% PFA, 0.025% glutaraldehyde in sodium acetate buffer (pH 6.5) and 25 ml of ice-cold 4% PFA in sodium borate buffer (pH 9.5) (for CCK immunohistochemistry). Brains were postfixed in 4% PFA in PB or in 4% PFA in sodium borate overnight, and then dehydrated/cryoprotected with 20% sucrose in PB. The brains were cut in 30 μ m sections and stored in antifreeze solution at -20°C .

For staining, slices were rinsed three times with KPBS and preincubated for 1 h in blocking solution (5% normal serum and 0.25% Triton X-100 in KPBS). For GFP/PV and GFP/CCK double staining, sections were incubated overnight at room temperature with either 1:10,000 rabbit anti-GFP (ab290, Abcam, Cambridge, UK) and 1:2,000 mouse anti-PV (P 3,088, Sigma), or 1:10,000 mouse anti-GFP (ab1218, Abcam) and 1:5,000 rabbit anti-CCK (ab43842, Abcam). For GFP/biocytin double staining, sections from electrophysiological recordings were incubated overnight at room temperature with 1:10,000 rabbit anti-GFP (Abcam). Sections were then incubated for 2 h at room temperature with either FITC-conjugated goat antirabbit and Cy3-conjugated donkey antimouse,

or FITC-conjugated donkey antimouse and Cy3-conjugated goat antirabbit, or FITC-conjugated goat antirabbit and Cy3-conjugated streptavidin. Slices were rinsed with KPBS or 0.25% Triton X-100 in KPBS between incubations, and finally mounted on coated slides and coverslipped with DABCO. All secondary antibodies and Cy3-streptavidin were purchased from Jackson ImmunoResearch (Suffolk, UK) and were used at 1:400 dilution.

Morphological Identification of Basket Cells

For morphological identification, biocytin was allowed to diffuse from the recording pipette into the recorded cells for 90 min. After fixation in 4% paraformaldehyde overnight, slices were cryoprotected in 20% sucrose in PB for two days and additionally cut in 60- μ m sections using a microtome. The biocytin-filled neurons were visualized by incubating the sections in avidin-biotin conjugated horseradish peroxidase solution (ABC, Vector Laboratories, UK), and then reacting them with diaminobenzidine and hydrogen peroxide solutions. The staining was then intensified by incubating slices in 0.5% OsO_4 (Sigma) solution, dehydrated, mounted on coated slides and coverslipped with Pertex (Histolab Products AB, Sweden). Serial microphotographs were taken throughout the whole thickness of the slices every 1 μ m, and groups of five consecutive images were merged using appropriate transparency filters with Canvas X software (ACD Systems, Victoria, Canada). Using the same software, drawings of the dendritic tree and axonal arborization were made in each group of images and finally merged together.

Data Analysis and Statistics

Only recordings from cells resembling basket cell morphology and showing colocalization of GFP and biocytin were accepted for analysis. Input and series resistance were constantly monitored during recordings, and calculated from the current response of the cells upon a constant 50 μ s duration -5 mV test pulses. Only recordings during which the whole-cell series resistance varied less than 20% were included in the analysis. Off-line analysis was performed using FitMaster (HEKA Elektronik), IgorPro (Wavemetrics, Lake Oswego, OR) and MiniAnalysis (Synaptosoft Inc., Decatur, GA) software.

Action potential (AP) threshold was defined as the point where the fastest rising phase started. AP amplitude and AP half-duration were defined as the difference between the threshold and the peak, in mV and ms, respectively. Paired-pulse facilitation and depression (PPF and PPD, respectively) were expressed as the ratio between the amplitude of the second and the first response of the pair, in percentage. Before and after NPY application differences in resting membrane potential (RMP), AP threshold, AP amplitude, AP half-duration, AP afterhyperpolarization (AHP), spontaneous and miniature currents inter event interval (IEI) and amplitude mean values, evoked EPSCs and IPSCs amplitudes, PPF and PPD were assessed with Student's paired *t*-test using StatView software (Abacus Concepts, Berkeley, CA). Frequency and amplitude of

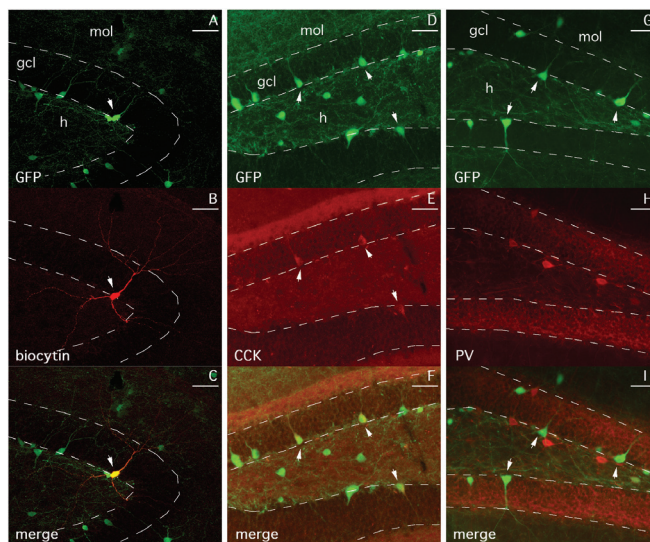


FIGURE 1. GFP-labeled basket cells in GAD65-GFP mice express CCK. A–C, Representative basket cell recorded in this study shows colocalization of GFP (A) and biocytin (B). Merged image is shown on (C). D–F, GFP-labeled putative basket cells

(arrows) show colocalization (F) of GFP (D) and CCK (E). G–I, GFP-labeled cells (G) are negative for PV immunostaining (H); note no double-staining on the merged image (I). Scale bars 50 μ m. gcl, granule cell layer, mol, molecular layer, h, hilus.

spontaneous and miniature postsynaptic currents, and sIPSC rise times (10–90%) were analyzed using MiniAnalysis software and differences between the groups were calculated with cumulative fraction curves combined with Kolmogorov-Smirnov (K-S) test. Events were automatically recognized by the software and included in the statistic analysis if their magnitude was at least 5 times bigger than the calculated average root mean square (RMS) noise. For each recording, only the last 65 events before start of NPY application and the first 65 events after equilibration of NPY (7 min after start of NPY application) were included in the analysis. For sIPSCs and mIPSCs, 100 events were included. Values are presented as means \pm SEM. Differences are considered significant with $P < 0.05$ for paired t -test and $P < 0.01$ for K-S test.

RESULTS

Identification of CCK Basket Cells and Effects of NPY on Intrinsic Membrane Properties

Putative GAD65/GFP positive basket cells for electrophysiological recordings were selected by the following morphological

criteria: (1) the cell soma had to be located on the border between the granule cell layer and the hilus of the dentate gyrus, (2) the cell soma had to be roughly pyramidal shaped, (3) the main apical dendrite had to cross the granule cell layer and reach the molecular layer, and (4) the basal dendrites had to extend into the hilus (an example is shown in Figs. 1A–C). These cells were positive for CCK immunoreactivity (Figs. 1D–F), negative for PV immunoreactivity (Figs. 1G–I), and displayed extensive axonal arborization confined mostly to the granule cell and inner molecular layers, consistent to the CCK-positive basket cell morphology (Freund and Buzsaki, 1996; Hefft and Jonas, 2005) (Fig. 2A).

Moreover, all the cells in which membrane properties were evaluated generated typical low-frequency regular action potentials with significant frequency accommodation, another typical characteristic of the CCK-positive basket cell subpopulation (Scharfman, 1995; Cauli et al., 1997; Pawelzik et al., 2002). To further confirm the CCK basket cell identity, we focally applied ACh to the soma of the recorded neurons and analyzed ACh-evoked currents. Experiments were conducted at $32 \pm 1^\circ\text{C}$. In 8 out of 11 cells, ACh induced fast inward currents with average amplitude of 109.1 ± 38.6 pA. Neither atropine, nor the combination of NBQX, D-AP5 and TTX affected the ACh-induced currents (Fig. 2B; middle and bottom traces,

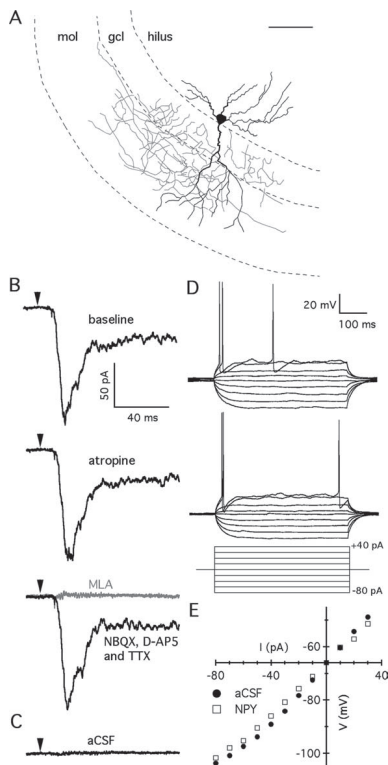


FIGURE 2. CCK basket cells exhibit characteristic morphological and electrophysiological phenotype and express functional $\alpha 7$ nAChR. **A**, Neuronal reconstruction of a recorded cell shows typical CCK-positive basket cell morphology. Dendrites (black) branch into the outer molecular layer and the hilus, while the axonal arborization (gray) is mostly confined to the granule cell and inner molecular layers. Scale bar 50 μ m. **B**, Focal application of ACh to the cell soma evokes an inward current (top) that is not affected by atropine (middle), or by the combination of NBQX, D-AP5 and TTX (bottom), but it is readily blocked by MLA (bottom, gray trace). Arrowhead indicates the start-time of ACh application. Traces are averages of six consecutive responses. **C**, Control experiment showing that application of aCSF does not evoke any detectable whole-cell current. **D**, Voltage responses of a CCK basket cell to current pulses injected via the patch pipette before (top) and after (middle) application of 1 μ M NPY. Bottom traces show superimposed respective current pulses applied through the patch pipette. Positive steps are 10 pA consecutive pulses whereas negative steps are 20 pA consecutive pulses. The cell shows regular-spiking behavior upon depolarization, generating action potentials with considerable accommodation, typical of CCK-expressing basket cells. **E**, The current-voltage (I–V) curve from the experiment shown in **D** is not affected by NPY application.

respectively). Subsequent application of the specific $\alpha 7$ nicotinic receptor antagonist MLA completely blocked the ACh-induced currents (Fig. 2B bottom, gray trace), indicating that the recorded basket cells expressed postsynaptic $\alpha 7$ nAChR. As an additional control we applied aCSF (vehicle) instead of ACh through the application pipette using exactly the same experimental paradigm, and could not detect any whole-cell currents in the recorded basket cells (Fig. 2C). Taken together, these data suggest that around 70% of the recorded GFP+ cells selected by our criteria express $\alpha 7$ nAChR. This finding is consistent with the previously published observations on the coexpression of CCK and $\alpha 7$ nAChR in the dentate gyrus (Morales et al., 2008), and further supports the CCK basket cell identity of the recorded neurons in this study.

Application of NPY did not change the membrane and intrinsic properties of the recorded CCK basket cells. The mean resting membrane potential (-67.4 ± 1.5 mV before and -63.6 ± 3.2 mV after NPY application, respectively), as well as input resistance, action potential threshold, amplitude and half duration, amplitude of afterhyperpolarization (Table 1) and voltage responses to square 500 ms current pulses were not affected (Figs. 2D,E). Thus, NPY does not seem to alter any of the intrinsic properties of the CCK basket cells in the dentate gyrus.

NPY Decreases the Frequency of Spontaneous and Miniature EPSCs Onto CCK Basket Cells

Next we asked whether NPY application affects excitatory synaptic transmission onto the CCK basket cells. First we recorded sEPSCs in whole-cell voltage-clamp configuration at -70 mV, and with the presence of PTX in the perfusion solution to block GABA_A receptors and to pharmacologically isolate glutamate receptor mediated currents. In the same conditions, but with the addition of TTX in the perfusion solution to block action potentials, mEPSCs were recorded. Both experiments were performed at $32 \pm 1^\circ\text{C}$. Figure 3 shows representative traces of sEPSCs (3A) and mEPSCs (3B), blocked by D-AP5 and NBQX (3C), confirming that they are generated

TABLE 1. Intrinsic Properties and Action Potential Measures of Dentate Gyrus CCK Basket Cells, Before (aCSF) and After (NPY) Application of NPY

	aCSF (n = 5)	NPY (n = 5)	P-value
RMP	-67.4 ± 1.5	63.6 ± 3.2	0.132
R input (M Ω)	481.4 ± 71	373 ± 54	0.284
AP threshold (mV)	-41.8 ± 2.2	-42.1 ± 1.6	0.652
AP amplitude (mV)	84.3 ± 2.5	83.4 ± 2.4	0.303
AP half-duration (ms)	1.14 ± 0.02	1.18 ± 0.04	0.374
AHP (mV)	18.5 ± 2.8	19.6 ± 2.4	0.495

The right column shows the Student's paired *t*-test *P*-value. NPY does not affect any of the properties evaluated. RMP, resting membrane potential; R, resistance; AP, action potential; AHP, afterhyperpolarization.

by glutamate receptor activation. The mean frequency of sEPSCs was significantly decreased after application of NPY (2.7 ± 0.3 Hz before and 1.3 ± 0.3 Hz after NPY, respectively, $P < 0.05$, paired t -test, Fig. 3D left) while their mean amplitude was not different (15.0 ± 3.3 pA before and 13.5 ± 1.8 pA after NPY, respectively, $P > 0.05$, paired t -test, Fig. 3D right). Similarly, the mean frequency of mEPSCs was reduced significantly after NPY application (1.0 ± 0.2 Hz before and 0.5 ± 0.1 Hz after NPY, respectively, $P < 0.05$, paired t -test, Fig. 3E left) and the mean amplitude was not affected (12.5 ± 1.0 pA before and 13.3 ± 1.1 pA after NPY, respectively, $P > 0.05$, paired t -test, Fig. 3E right). The following K-S analysis of cumulative fraction confirmed that there was a significant decrease in the frequency of sEPSCs (Fig. 3F) and mEPSCs (Fig. 3H) after the application of NPY, as shown by the increase in IELs. However, the amplitudes of neither sEPSCs (Fig. 3G) nor mEPSCs (Fig. 3I) were significantly dif-

ferent after NPY was added to the perfusion solution. Taken together, these data indicate that NPY decreases the frequency of both action potential dependent and independent excitatory postsynaptic currents onto CCK basket cells, possibly by inhibiting presynaptic glutamate release.

NPY Decreases the Amplitude of Evoked EPSCs Via Y2 Receptors, Without Changing Short-Term Synaptic Plasticity

One possible explanation of decreased frequency of sEPSCs and mEPSCs after NPY application could be decreased release probability (P_r) of glutamate at presynaptic terminals (Colmers et al., 1987; Tu et al., 2005). Some insight of glutamate P_r may be obtained by measuring alterations in paired-pulse facilitation of EPSCs, a presynaptic form of short-term plasticity observed in central excitatory synapses (Zucker and Regehr, 2002). The ratio of paired EPSC amplitudes seems to be in an inverse relation with glutamate P_r . Large paired-pulse facilitation (PPF) is normally associated with relatively low glutamate P_r , while low PPF or paired-pulse depression (PPD) is normally indicative of relatively high glutamate P_r in synapses (Zucker and Stockbridge, 1983; Debanne et al., 1996; Murthy et al., 1997; Jakubs et al., 2006). Therefore, we evaluated NPY's effect on PPF of EPSCs recorded in CCK basket cells. To stimulate both mossy and possible associational-commissural fiber inputs to the CCK basket cells, we placed the stimulating electrode in the border between the granule cell and molecular layers of the dentate gyrus. With PTX present in the perfusion solution to block GABA_A receptors and isolate glutamate-mediated synaptic transmission to the CCK basket cells, paired stimulations (with 50 ms ISI) elicited monosynaptic EPSCs

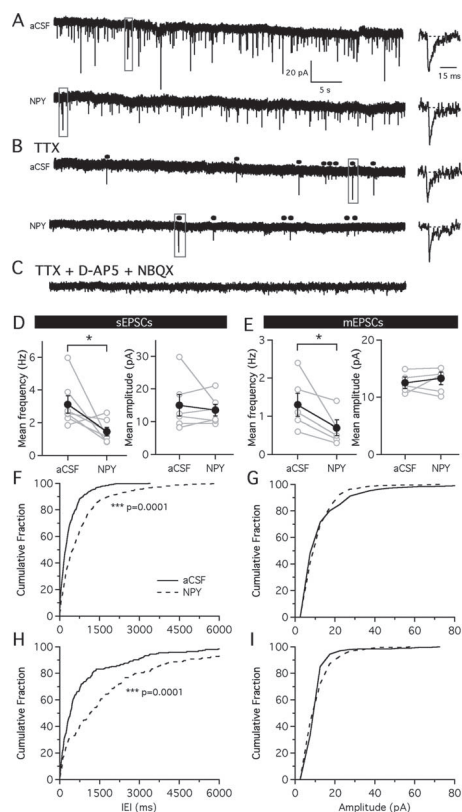


FIGURE 3. The frequency of sEPSCs and mEPSCs is decreased after NPY application. **A**, Representative traces showing sEPSCs before (top), and after NPY application (bottom). **B**, Representative traces showing mEPSCs before (top), and after NPY application (bottom) recorded in the presence of TTX. Insets on the right show individual sEPSCs in different time resolution extracted from the respective traces on the left. **C**, Miniature EPSCs are blocked by NBQX and D-AP5 application, confirming their generation by activation of the glutamatergic receptors. **D**, Mean frequency (left) and amplitude (right) of sEPSCs before and after NPY application. A significant decrease in the frequency was found when NPY was applied to the bath ($P < 0.05$, $n = 6$), but the amplitude of sEPSCs was not changed ($P > 0.05$). **E**, The mean frequency of mEPSCs recorded after the application of NPY is decreased (left, $P < 0.05$, $n = 5$), while the amplitude is unchanged (right, $P > 0.05$). Gray lines and open circles represent individual recordings, black lines and closed circles represent mean values. **F–G**, Cumulative fraction curves of the inter event intervals (IEIs) and amplitudes of sEPSCs before (solid line) and after (dashed line) NPY application. The IEIs of sEPSCs recorded after NPY application are significantly increased ($***P < 0.01$), but amplitudes are not affected ($P > 0.01$). **H–I**, Cumulative fraction curves of IEIs and amplitudes of mEPSCs recorded in presence of 1 μM TTX before (solid line) and after (dashed line) NPY application. IEIs are significantly increased after application of NPY ($***P < 0.01$). Amplitudes are not affected ($P > 0.01$).

that displayed paired-pulse facilitation (representative traces are shown in Figs. 4A,B).

Application of NPY caused a significant decrease in the amplitude of both the first and the second evoked EPSCs induced by granule cell-molecular layer border stimulation (by about 30% from 28.9 ± 2.7 to 20.8 ± 1.9 pA for the first EPSC, and from 45.3 ± 4.6 to 31.3 ± 2.1 pA for the second EPSC, respectively, $P < 0.05$, paired t -test, Fig. 4C). However, the PPF ratio of EPSCs was not altered by NPY application (163.1 ± 17.7 before, and $163.4 \pm 15.1\%$ after NPY application, respectively, $P > 0.05$, paired t -test, Fig. 4C). To confirm that decreased amplitude for stimulation-evoked EPSCs was indeed due to NPY, instead of NPY we added "free-acid NPY," which is a nonactive form of the peptide, and observed no changes neither in EPSC amplitudes nor in PPF ratios (39.0 ± 1.7 before and 35.2 ± 4.6 pA after "free-acid NPY" application for the first pulse; 66.5 ± 9.2 before and 64.6 ± 19.8 pA after "free-acid NPY" for the second pulse; 170.0 ± 15.4 before and $183.4 \pm 20.4\%$ after "free-acid NPY" for the PPF ratio; $P > 0.05$ in all cases, paired t -test, Fig. 4D). Moreover, we performed the same experiment, but in addition to NPY we applied the highly specific Y2 receptor blocker BIIE0246 into the perfusion solution. In this situation, NPY had no effect on the amplitude of neither first (33.8 ± 4.7 and 33.0 ± 8.1 pA, before and after NPY application, respectively, $P > 0.05$, paired t -test, Fig. 4E) nor the second stimulation-induced EPSC (45.5 ± 6.8 and 41.4 ± 12.5 pA, before and after NPY application, respectively, $P > 0.05$, paired t -test, Fig. 4C), or on the PPF ratio (134.7 ± 8.0 and $123.5 \pm 11.8\%$, before and after NPY application, respectively, $P > 0.05$, paired t -test, Fig. 4E).

To confirm that we have targeted both mossy fiber and associational fibers with our stimulation electrode in the granule cell-molecular layer border, in a separate set of experiments, we additionally stimulated mossy fibers antidromically in the *stratum lucidum* of CA3 (see experimental setup, Fig. 5A), which would effectively induce only mossy fiber EPSCs in CCK basket cells. The EPSCs generated by antidromic stimulation of mossy fibers were completely abolished by L-CCG-I (Fig. 5B, p1), a specific agonist of mGluR II that are expressed exclusively on the mossy fiber terminals and block glutamate release when activated (Castillo et al., 1997; Kokaia et al., 1998). In contrast, L-CCG-I only partially (by 30%) blocked EPSCs induced in the same basket cells by stimulation of granule cell-molecular layer border (from 28.5 ± 5.3 to 20.8 ± 7.2 pA for the first EPSC; and from 42.0 ± 7.8 to 29.5 ± 10.2 pA for the second EPSC, $P < 0.05$; no change in PPF, 147.0 ± 8.3 and $135.9 \pm 8.9\%$, $P > 0.05$, paired t -test, Fig. 5C), indicating that these EPSCs were partially induced by associational-commissural fiber activation (Fig. 5B, p2). Moreover, to evaluate if the stimulation of the granule cell-molecular layer border induced monosynaptic EPSCs, we recorded the pharmacologically isolated NMDA component of the responses, holding the cells at +40 mV in the presence of PTX and NBQX (Fig. 5D, black trace), to block GABA_A and AMPA receptors, respectively. The stimulation induced positive synaptic currents in CCK basket cells that were readily blocked by the application of D-AP5, confirming that

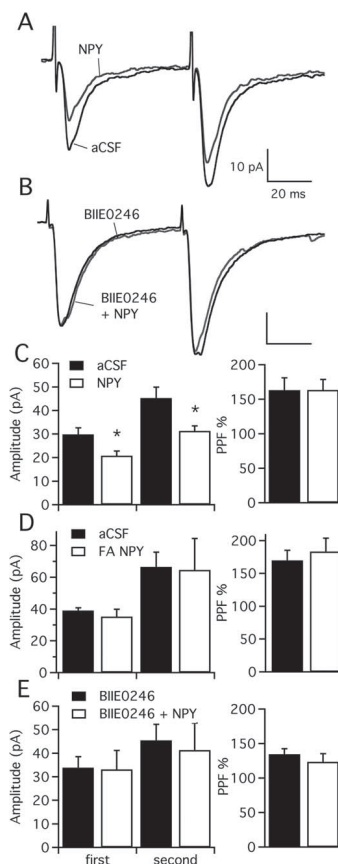


FIGURE 4. NPY decreases the amplitude of evoked EPSCs recorded in CCK basket cells. **A**, Superimposed representative traces of evoked EPSCs before (aCSF) and after (NPY) NPY application. **B**, Superimposed representative traces of evoked EPSCs before (BIIE0246) and after (BIIE0246+NPY) application of NPY in the presence of the Y2 receptor blocker BIIE0246 (scale bars as in **A**). **C**, Mean amplitudes of stimulation-evoked EPSCs. Both first and second pulse are significantly decreased after application of NPY ($P < 0.05$, $n = 14$), but the PPF ratio is unchanged ($P > 0.05$). **D**, "free-acid NPY" (FA NPY) does not influence evoked EPSCs. The amplitude of the first and the second pulse was not affected by the application of FA NPY, neither was the PPF ratio ($P > 0.05$ in all cases, $n = 4$), confirming that the effect seen in **C** is NPY-specific. **E**, Application of the Y2 specific receptor blocker BIIE0246 throughout the experiment completely blocked the effect of NPY on the EPSC amplitudes ($P > 0.05$, $n = 6$), indicating that Y2 receptors are involved. Values are means ± SEM. Traces are averages of 12 consecutive responses.

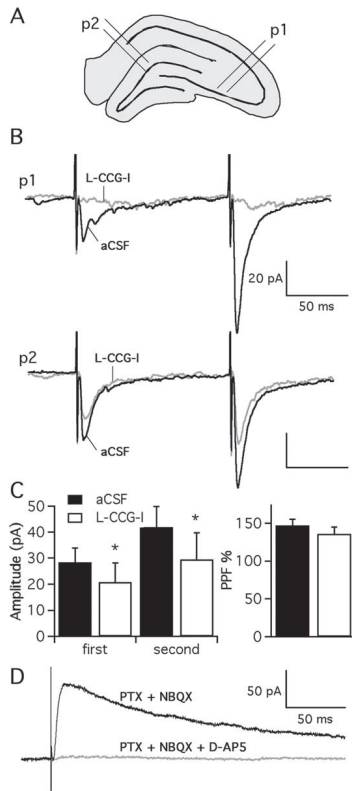


FIGURE 5. Stimulation of the dentate granule cell-molecular layer border activates mossy fibers. (A) Schematic illustration of the experimental setup. One stimulating electrode was placed in the stratum lucidum of CA3 (p1) and a second was placed in the granule cell-inner molecular layer border (p2). Recordings were made from CCK basket cells in the granule cell layer/hilus border. (B) Representative traces (averages of 12 consecutive responses) showing that the application of L-CCG-I in the perfusion solution totally blocks p1 stimulation-induced responses (top), while only partially blocks p2-induced responses (bottom). (C) Bars representing the mean amplitude of p2 stimulation-induced responses before and after application of L-CCG-I. The amplitude of the first and the second EPSCs were significantly decreased after L-CCG-I application (left, $*P < 0.05$, $n = 6$), while the PPF ratio remained unchanged (right, $P > 0.05$). (D) Representative trace (average of six consecutive responses) showing the NMDA receptor generated synaptic current evoked by stimulation of the granule cell-molecular layer border, recorded at +40 mV in the presence of PTX and NBQX (black trace). The response was readily blocked by application of D-AP5 (gray trace).

they were generated by NMDA receptor activation and thus were monosynaptic (Fig. 5D, gray trace).

Taken together, these results confirm that the observed decrease of stimulation-evoked monosynaptic EPSC amplitudes was due to NPY application, and that NPY acts via activation of the Y2 receptor subtype. The unchanged PPF of EPSCs, however, indicates that the effect of NPY may not be due to decreased overall glutamate P_r in these synapses, and together with the data of L-CCG-I application (both NPY and L-CCG-I induced similar decrease in amplitude of EPSCs without altering PPF), may support the notion that NPY effect on stimulation induced EPSCs is predominantly mediated by effects on mossy fibers.

NPY Decreases the Frequency of Spontaneous and Miniature Inhibitory Postsynaptic Currents Onto CCK Basket Cells

Next we hypothesized that NPY could also influence inhibitory afferent synapses on the CCK basket cells. We first recorded sIPSCs in whole-cell voltage-clamp configuration at -70 mV in the presence of D-AP5 and NBQX in the perfusion medium to block NMDA and AMPA receptors and pharmacologically isolate GABA_A receptor-mediated postsynaptic currents. Miniature IPSCs were recorded in similar conditions as above but with the addition of TTX in the perfusion solution to block action potentials. Figure 6 shows representative traces of sIPSCs (Fig. 6A) and mIPSCs (Fig. 6B) recorded in aCSF and after NPY addition. Both sIPSCs and mIPSCs were blocked by adding PTX to the perfusion solution (Fig. 6C), confirming their generation by activation of GABA_A receptors. The mean frequency of sIPSCs was significantly decreased after NPY was added to the perfusion solution (from 3.7 ± 1.1 to 2.3 ± 0.6 Hz, $P < 0.05$, paired t -test, Fig. 6D left), but the mean amplitude was not changed by application of NPY (29.1 ± 1.8 before and 30.3 ± 2.5 pA after NPY, $P > 0.05$, paired t -test, Fig. 6D right). Cumulative fraction analysis confirmed that the sIPSCs generated by inhibitory synapses onto the CCK basket cells were less frequent after NPY was added to the perfusion solution ($P < 0.01$, K-S test, Fig. 6F), but that their amplitude was not changed ($P > 0.01$, K-S test, Fig. 6G). We then tested if the NPY-mediated decrease in the frequency of sIPSCs was dependent on action potentials, and added TTX to the perfusion solution to block action potentials. In these conditions, the mean frequency of mIPSCs was significantly decreased after application of NPY (2.8 ± 0.5 before and 2.1 ± 0.3 Hz after NPY, respectively, $P < 0.05$, paired t -test, Fig. 6E left), and the mean amplitude was unchanged (31.2 ± 1.7 before and 32.0 ± 1.8 pA after NPY, respectively, $P > 0.05$, paired t -test, Fig. 6E right). Cumulative fraction analysis confirmed a significant increase of IELs when NPY was added to the solution ($P < 0.01$, K-S test, Fig. 6H) and confirmed that the amplitude of mIPSCs was not affected ($P > 0.01$, K-S test, Fig. 6I). Taken together, these data indicate that the frequency of both action potential dependent and independent sIPSCs and mIPSCs in CCK basket cells are decreased by NPY application.

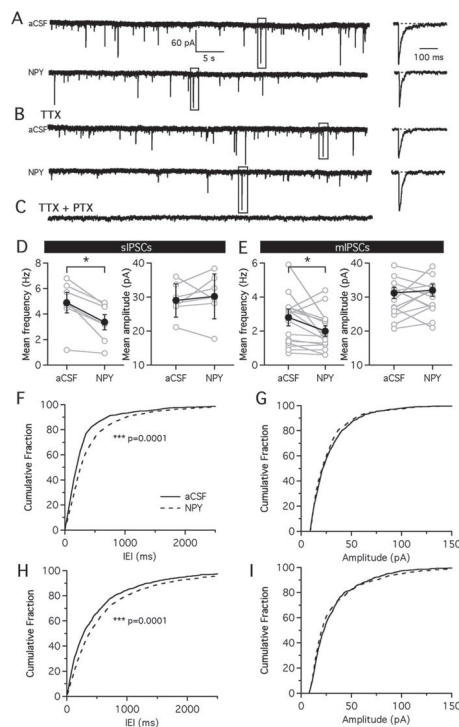


FIGURE 6. NPY decreases the frequency of sIPSCs and mIPSCs recorded in CCK basket cells. **A**, Representative traces of sIPSCs recorded in aCSF (top) and after the addition of NPY (bottom). **B**, Miniature IPSCs recorded in the presence of TTX before (top), and after application of NPY (bottom). Insets on the right show individual sIPSCs and mIPSCs at different time resolution extracted from the respective boxes on the left. **C**, mIPSCs are blocked by PTX, confirming their generation by activation of GABA_A receptors. **D**, The mean frequency of sIPSCs is decreased after NPY application (left, **P* < 0.05, *n* = 7), but the mean amplitude is not affected (right, *P* > 0.05). **E**, Similarly, the mean frequency of mIPSCs was decreased after NPY application (left, **P* < 0.05, *n* = 16) and the mean amplitude was not altered (right, *P* > 0.05). Gray lines and open circles represent individual recordings, black lines and closed circles represent mean values. **F**, IEIs of sIPSCs are significantly increased by NPY (****P* < 0.001). **G**, sIPSC amplitudes are not affected by NPY (*P* > 0.01). **H**, IEIs of mIPSCs are significantly increased by NPY (****P* < 0.001). **I**, mIPSC amplitudes are not affected by NPY (*P* > 0.01).

Spontaneous IPSCs in granule cells generated by synapses close to the cell soma (peri-somatic) can be distinguished from those generated by synapses on apical dendrites (dendritic) by their different kinetics (Kobayashi and Buckmaster, 2003). The

IPSCs with relatively high amplitude, and fast rise and decay times are thought to be generated by peri-somatic inhibitory synapses in proximity of the recording electrode (cell soma), while those with lower amplitude, and slow rise and decay times are most likely generated by synapses located distal to the cell soma, e.g., in apical dendrites of the neurons. To evaluate whether the decrease in IPSCs frequency after application of NPY was due to changes in perisomatic or distal dendritic synapses, we analyzed the rise time (10–90%) of sIPSCs and mIPSCs before and after NPY application. Representative traces are shown in Figure 7 (sIPSCs Fig. 7A top, mIPSCs Fig. 7B top). Mean values of rise times did not differ before and after NPY application (3.71 ± 0.2 before and 3.52 ± 0.2 ms after NPY for sIPSCs, *P* > 0.05, paired *t*-test; 3.24 ± 0.1 before and 3.21 ± 0.1 ms after NPY for mIPSCs, *P* > 0.05, paired *t*-test, data not shown). However, the cumulative fraction analysis showed that the rise time of sIPSCs and mIPSCs recorded after NPY application were significantly faster as compared with those before NPY application (*P* < 0.01, K-S test, Fig. 7A middle and 7B middle). Frequency distribution histograms further strengthened these findings. Before NPY application, the frequency distribution of sIPSCs (Fig. 7A bottom, black trace) exhibited a plateau at its highest level, indicating a continuum of events with variable rise times. Application of NPY abolished this plateau, and shifted the curve to the left (Fig. 7B bottom, red trace), now represented as a peak (not plateau) at its highest level, indicating that a higher percentage of events had fast rise times. The frequency distribution of mIPSCs rise times, before application of NPY (Fig. 7B bottom, black trace), showed a higher peak as compared to sIPSCs, suggesting that in presence of TTX a higher percentage of events had peri-somatic origin. This could be due to lower overall amplitude of mIPSCs as compared with sIPSCs, thus dendritic mIPSCs falling under detection threshold due to their relatively low amplitude (K-S test revealed that mIPSCs had significantly lower amplitudes than sIPSCs; *P* < 0.01, data not shown). Similar to sIPSCs, the application of NPY further sharpened and increased the main peak of frequency distribution for mIPSCs (Fig. 7B bottom), indicating a higher percentage of events with fast rise times.

These data indicate that NPY application decreased the frequency of sIPSCs and mIPSCs that are generated by synapses located remotely from the cell soma, i.e., dendritic inhibitory synapses, in relatively higher degree as compared to peri-somatic synapses.

Taken together, these data show that NPY attenuates spontaneous inhibitory synaptic drive onto the CCK basket cells, particularly decreasing the frequency of dendritic IPSCs. The observed overall decrease in the frequency of mIPSCs suggests that NPY can affect action potential-independent release of GABA in these synapses.

NPY Decreases Evoked IPSC Amplitude Via Activation of Y2 Receptors

Since the analysis of sIPSCs revealed that NPY affected mostly dendritic inhibitory synapses on the CCK basket cells,

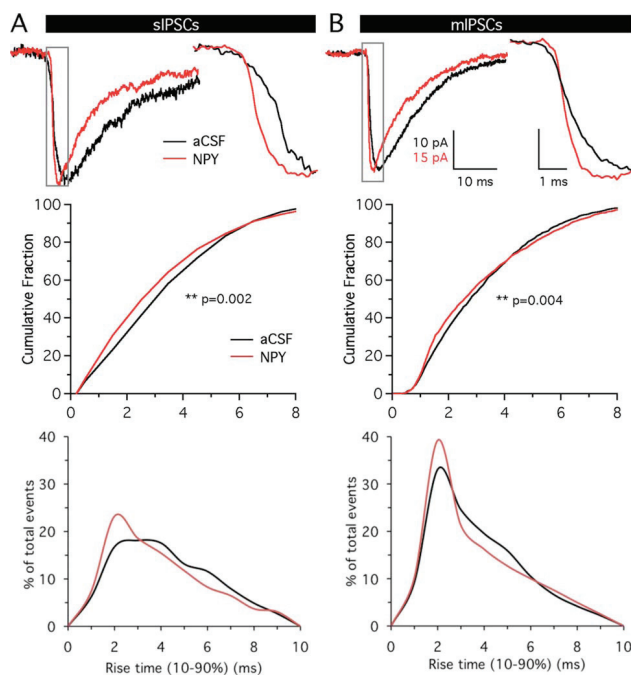


FIGURE 7. The rise time of sIPSCs and mIPSCs is decreased by NPY application. Representative traces of sIPSCs (A, top) and mIPSCs (B, top) before and after NPY application, showing the decrease in rise time. The initial rising slopes of the traces (box) is magnified on the right. Traces are averages of 10 consecutive sIPSCs, and normalized to peak current amplitude. Cumulative fraction curve of sIPSC (A, middle) and mIPSCs (B, middle) rise

times. The application of NPY (red traces) shifted the curve towards faster rise times (** $P < 0.01$, $n = 7$ for sIPSCs, $n = 16$ for mIPSCs). Frequency distribution histogram of sIPSCs (A, bottom) and mIPSCs (B, bottom) rise times. Application of NPY (red traces) shifted the curve to the left, indicating that a higher percentage of the events had faster rise times.

we were interested to selectively activate peri-somatic inhibitory synapses and explore more closely whether they indeed were not affected by NPY application. Therefore, a stimulating electrode was placed close to the granule cell layer in the inner molecular layer of the dentate gyrus and perisomatic inhibitory afferent fibers of the CCK basket cells were stimulated with paired-pulses (100 ms ISI), which induced paired-pulse depression (PPD) of monosynaptic IPSCs (representative traces are shown in Figs. 8A,B). D-AP5 and NBQX were used to block glutamate receptors and isolate GABA_A-mediated GABAergic synaptic transmission. When NPY was added in the perfusion solution, the mean amplitude of both first and second paired pulse-induced sIPSCs was decreased by approximately 40% (from 150.8 ± 28.9 to 93.8 ± 19.7 pA for the first response, and from 126.3 ± 39.4 to 74.3 ± 22.3 pA for the second

response, $P < 0.05$, paired t -test, Fig. 8C). The PPD ratio after NPY addition remained unchanged (76.8 ± 8.4 before and $74.6 \pm 6.6\%$, after NPY application, respectively; $P > 0.05$, paired t -test, Fig. 8C). To confirm that the decrease in IPSC amplitudes was specific to NPY, we applied “free-acid NPY” to the perfusion solution instead of NPY. In this case, IPSC amplitudes recorded in CCK basket cells were not altered and PPD ratio also remained unchanged (97.1 ± 5.5 before and 96.2 ± 20.7 pA after “free-acid NPY” application for the first pulse; 87.7 ± 16.6 before and 75.2 ± 19.1 pA after “free-acid NPY” for the second pulse; 89.2 ± 13.4 before and $89.4 \pm 18.3\%$ after “free-acid NPY” for the PPD ratio; $P > 0.05$ in all cases, paired t -test, Fig. 8D). To further confirm the specificity of NPY effect, we repeated the experiment in presence of NPY Y2 receptor antagonist BIIIE0246. In these conditions,

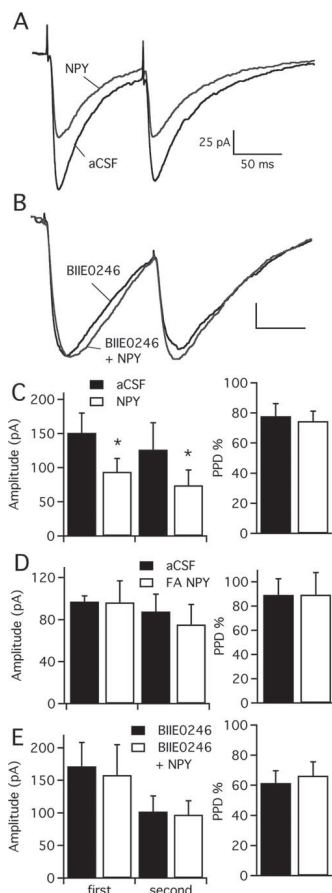


FIGURE 8. NPY decreases the amplitudes of evoked IPSCs recorded in CCK basket cells. **A**, Superimposed representative traces of evoked IPSCs before and after NPY application. **B**, Superimposed representative traces of evoked IPSCs in the presence of Y2 receptor blocker BIIE0246, before (BIIE0246), and after (BIIE0246+NPY) NPY application (scale bars as in **A**). **C**, The mean amplitude of the first and the second stimulation-evoked IPSCs is significantly decreased by NPY ($P < 0.05$, $n = 14$), while the paired-pulse depression ratio is unchanged ($P > 0.05$). **D**, The application of "free-acid NPY" (FA NPY) had no effect on the amplitude of evoked IPSCs, nor on the paired-pulse depression ratio ($P > 0.05$, $n = 4$), confirming the specificity of the effect seen in **C**. **E**, The presence of BIIE0246 in the perfusion solution completely prevented the effect of NPY ($P > 0.05$, $n = 5$), indicating the involvement of Y2 receptors. Values are means \pm SEM. Traces are averages of 12 consecutive responses.

NPY was no longer able to decrease IPSC amplitudes. The mean amplitude of the first pulse was 171.5 ± 36.7 pA before and 158.1 ± 46.8 pA after NPY application ($P > 0.05$, paired t -test, Fig. 8C); the mean amplitude of the second pulse was 102.1 ± 23.9 pA before and 97.1 ± 21.3 pA after NPY ($P > 0.05$, paired t -test, Fig. 8E). The PPD ratio also remained unchanged by NPY application when the Y2 blocker was present in the perfusion medium ($61.5 \pm 8.1\%$ before and $66.3 \pm 9.3\%$ after NPY application, $P > 0.05$, paired t -test, Fig. 8E). Taken together, these data show that NPY is able to decrease stimulation-evoked peri-somatic IPSCs in CCK basket cells via activation of Y2 receptors, without modifying PPD of IPSCs in these synapses.

DISCUSSION

Here we demonstrate for the first time that NPY modulates excitatory and inhibitory synaptic inputs to a subclass of GABAergic interneurons in the dentate gyrus of the hippocampal formation. The CCK basket cells are proposed as major modulators of hippocampal γ -frequency oscillations that occur during exploratory and memory consolidation activities of the animals, and are generated by another subtype of basket cells that lack CCK but express PV. The CCK basket cells receive inputs from outside the hippocampal formation, e.g., serotonin containing fibers from raphe nuclei, and express nicotinic $\alpha 7$, cannabinoid CB1, and benzodiazepine-sensitive $\alpha 2$ subunits of GABA_A receptors (Freund et al., 1990; Katona et al., 1999; Low et al., 2000; Nyiri et al., 2001; Ferezou et al., 2002; Klausberger et al., 2002). Our present data add NPY-induced Y2 receptor activation to the repertoire of neuromodulatory mechanisms that can locally alter the functionality of CCK basket cells by changing excitatory and inhibitory synaptic transmission onto these cells.

The CCK Basket Cells

There are at least 16 different subtypes of cortical interneurons (including hippocampal formation) identified so far (Freund and Buzsaki, 1996; Somogyi and Klausberger, 2005). This classification of cortical interneuron subtypes is based on anatomical, biochemical, and electrophysiological features of the different interneuron subpopulations (Buhl et al., 1994; Freund and Buzsaki, 1996; Somogyi and Klausberger, 2005). The subpopulation of dentate gyrus interneurons studied here are the CCK-positive basket cells. Several lines of evidence support this notion. First, these cells in GAD65-GFP mice express GFP (Lopez-Bendito et al., 2004), and their morphological features and location appears to resemble that of the CCK-positive basket cell population (Figs. 1A–C and 2A) (Freund and Buzsaki, 1996; Hefft and Jonas, 2005). Second, these cells are positive for CCK immunoreactivity (Figs. 1D–F), and negative for PV (Figs. 1G–I). It has been shown previously that in GAD65-GFP transgenic mice, a subpopulation of basket cells

situated on the granule cell layer-hilus border are labeled by GFP, and are also positive to CCK immunostaining (G. Szabo, unpublished observations). Third, these cells respond to ACh with a fast inward current generated by activation of postsynaptic $\alpha 7$ nicotinic receptors (Fig. 2B). Finally, these cells express electrophysiological properties characteristic of CCK basket cells, i.e., generating low-frequency and strongly accommodating action potentials when depolarized (Fig. 2D) (Scharfman, 1995; Cauli et al., 1997; Pawelzik et al., 2002).

Taken together, we can conclude that the vast majority of the cells recorded in this study are CCK-positive basket cells. We cannot completely rule out a possibility that some recorded cells might have been of yet another subpopulation type of interneurons, although clearly not PV-positive basket cells.

Excitatory Input Onto CCK Basket Cells

Our present data show for the first time that NPY application leads to decreased excitatory transmission onto CCK basket cells. Here we describe that the frequency of sEPSCs and mEPSCs is markedly decreased after NPY application.

Changes in the frequency of sEPSCs and mEPSCs and no change in their amplitude are indicative of a presynaptic site of action. In support, similar changes induced by NPY have been reported in excitatory synapses on CA3 pyramidal neurons of the hippocampal formation (McQuiston and Colmers, 1996). In line with these observations, it has been shown that NPY failed to alter the magnitude of AMPA/kainate receptor-generated postsynaptic responses induced by exogenously applied glutamate in CA1-CA3 pyramidal neurons (Colmers et al., 1987; McQuiston and Colmers, 1992). Possible mechanisms underlying these NPY effects are thought to be mediated by activation of presynaptic Y2 receptors that decrease glutamate release by attenuation of calcium entry into the presynaptic terminals via N- and P/Q-type voltage-dependent calcium channels, as shown for Schaffer collateral-CA1 synapses (Qian et al., 1997). However, in the CCK basket cells, the decrease in the amplitude of EPSCs induced by stimulation of the granule cell-molecular layer border was not accompanied by a change in the PPF, suggesting that NPY does not alter the overall Pr of glutamate in these synapses (Zucker and Stockbridge, 1983; Debanne et al., 1996; Murthy et al., 1997; Jakubs et al., 2006). Thus we cannot rule out that NPY may also have a postsynaptic site of action. Alternatively, NPY-induced reduction of glutamate release is mediated by other mechanisms downstream to the attenuation of calcium entry. Taken together, these data indicate that NPY may have both pre- and postsynaptic effects on the excitatory inputs to the CCK basket cells in an afferent specific manner.

The CCK basket cells receive at least two major excitatory afferent inputs: (i) perforant path (from entorhinal cortex) and associational-commissural fibers in the molecular layer of the dentate gyrus where basket cells have their apical dendrites (part of the feed-forward inhibitory circuits), and (ii) collaterals of mossy fibers (from granule cells) in the hilus, where basket cells have their basal dendrites (Kneisler and Dingledine, 1995;

Freund and Buzsaki, 1996). Perforant path and associational-commissural fibers are thought to lack Y2 receptors, as concluded indirectly by the failure of NPY to affect molecular layer fEPSPs or granule cell EPSCs induced by stimulation of afferent fibers in the molecular layer of the DG (Klapstein and Colmers, 1993). Currently, there is no evidence whether perforant path or associational-commissural fiber afferents on interneurons express Y2 receptors, although the inner molecular layer, where associational fibers are present, has been shown to be positive for Y2 receptor immunoreactivity (Tu et al., 2006). On the other hand, mossy fibers do express Y2 receptors, as demonstrated by electrophysiology and immunohistochemistry (McQuiston and Colmers, 1996; Stanic et al., 2006). In our experiments, stimulation of the inner molecular layer activates both mossy fiber and associational-commissural fiber synapses (Fig. 5B). Therefore, it cannot be excluded that both these excitatory synapses are affected by NPY. The fact that L-CCG-I and NPY had similar partial inhibitory effect on granule cell-molecular border stimulation-induced EPSCs in CCK basket cells, together with the data from the literature, may indicate that NPY predominantly acts on mossy fiber efferent synapses. Results of our study may have relevance also for endogenous NPY function, particularly in pathological situations, e.g., epilepsy, since mossy fibers sprout and start to express NPY *de novo* in response to seizures (Schwarzer et al., 1995; Lurton and Cavalheiro, 1997).

Inhibitory Input Onto CCK Basket Cells

The present data show for the first time that NPY application decreases spontaneous and miniature IPSC frequency in CCK basket cells. Such changes in synaptic drive are normally attributable to a presynaptic site of action (Behr et al., 2002; Yang et al., 2007). CCK basket cells receive inhibitory inputs in the molecular layer of the dentate gyrus at their dendrites, which can arise from HIPP or HICAP cells, and perisomatically from other basket cells (Nunzi et al., 1985). In addition, CCK basket cells receive inhibitory inputs from calretinin-expressing interneuron-specific cells (CR-IS) (i.e., inhibitory interneurons innervating specifically other inhibitory interneurons) (Gulyas et al., 1996). At the moment, it is not clear which of these inputs, or whether all of them, are affected by NPY application. Shift to faster sIPSC kinetics after NPY application shown here indicates that dendritic synapses are likely to be affected by NPY. It is not likely that this effect is due to NPY-induced inhibition of HIPP cell firing (Paredes et al., 2003), since it persisted even when TTX was added to the perfusion solution. NPY application also decreased the amplitude of IPSCs induced by stimulation of the molecular-granule cell layer border. Since axons from both CR-IS and basket cells seem to be predominantly located in the inner molecular layer (Nunzi et al., 1985; Gulyas et al., 1992; Freund and Buzsaki, 1996), our data suggest that the inhibitory afferent fibers from CR-IS and basket cells that innervate perisomatic and proximal dendritic regions of CCK basket cells are also affected by NPY and do express NPY Y2 receptors presynaptically. Decrease in

stimulation-evoked IPSCs has also been observed previously in cortical interneurons (Bacci et al., 2002). Whether the CCK basket cells themselves express Y2 receptors presynaptically on their axons innervating other CCK basket cells, or it is a separate class of interneurons that express Y2 receptors presynaptically (e.g., CR-1S cells), remains to be determined.

General Considerations

What are the possible physiological implications of the NPY-induced modulation of CCK basket cell afferents? It has been proposed that CCK basket cell networks are superimposed on the PV basket cell syncytium, and are involved in fine-tuning of γ -frequency oscillations generated by PV basket cells during exploratory and memory-forming activities in the hippocampal formation (Freund, 2003). Moreover, γ -frequency oscillations may be transformed into epileptiform discharges (Traub et al., 2005). One could speculate that NPY-induced alterations of excitatory and inhibitory synaptic inputs to CCK basket cells may modulate their extrahippocampal serotonergic and cholinergic afferents, as well as the release of CCK onto the PV basket cells. Altogether, these may secondarily influence gamma oscillations generated by PV basket cells (Foldy et al., 2007). Such scenario is most likely to take place during epileptiform discharges in the hippocampal formation, when NPY and Y2 receptors are upregulated (Gruber et al., 1994; Gobbi et al., 1998; Schwarzer et al., 1998), and NPY is released acting as a volume transmitter (Sørensen et al., 2008). Such action could also be part of the seizure-suppressant mechanisms exerted by AAV vector-transduced NPY in the hippocampus, shown recently (Sørensen et al., 2009; Noe et al., 2008).

REFERENCES

- Bacci A, Huguenard JR, Prince DA. 2002. Differential modulation of synaptic transmission by neuropeptide Y in rat neocortical neurons. *Proc Natl Acad Sci USA* 99:17125–17130.
- Balasubramaniam AA. 1997. Neuropeptide Y family of hormones: Receptor subtypes and antagonists. *Peptides* 18:445–457.
- Baraban SC, Hollopeter G, Erickson JC, Schwartzkroin PA, Palmiter RD. 1997. Knock-out mice reveal a critical antiepileptic role for neuropeptide Y. *J Neurosci* 17:8927–8936.
- Behr J, Gebhardt C, Heinemann U, Mody I. 2002. Kindling enhances kainate receptor-mediated depression of GABAergic inhibition in rat granule cells. *Eur J Neurosci* 16:861–867.
- Bijak M. 1999. Neuropeptide Y suppresses epileptiform activity in rat frontal cortex and hippocampus in vitro via different NPY receptor subtypes. *Neurosci Lett* 268:115–118.
- Buhl EH, Halasy K, Somogyi P. 1994. Diverse sources of hippocampal unitary inhibitory postsynaptic potentials and the number of synaptic release sites. *Nature* 368:823–828.
- Buzsaki G, Chrobak JJ. 1995. Temporal structure in spatially organized neuronal ensembles: A role for interneuronal networks. *Curr Opin Neurobiol* 5:504–510.
- Buzsaki G, Leung LW, Vanderwolf CH. 1983. Cellular bases of hippocampal EEG in the behaving rat. *Brain Res* 287:139–171.
- Castillo PE, Janz R, Sudhof TC, Tzounopoulos T, Malenka RC, Nicoll RA. 1997. Rab3A is essential for mossy fibre long-term potentiation in the hippocampus. *Nature* 388:590–593.
- Cauli B, Audinat E, Lambolez B, Angulo MC, Ropert N, Tsuzuki K, Hestrin S, Rossier J. 1997. Molecular and physiological diversity of cortical nonpyramidal cells. *J Neurosci* 17:3894–3906.
- Colmers WF, Lukowiak K, Pittman QJ. 1987. Presynaptic action of neuropeptide Y in area CA1 of the rat hippocampal slice. *J Physiol* 383:285–299.
- Colmers WF, Lukowiak K, Pittman QJ. 1988. Neuropeptide Y action in the rat hippocampal slice: Site and mechanism of presynaptic inhibition. *J Neurosci* 8:3827–3837.
- Debanne D, Guerin NC, Gahwiler BH, Thompson SM. 1996. Paired-pulse facilitation and depression at unitary synapses in rat hippocampus: Quantal fluctuation affects subsequent release. *J Physiol* 491(Part 1):163–176.
- Dumont Y, Fournier A, Quirion R. 1998. Expression and characterization of the neuropeptide Y Y5 receptor subtype in the rat brain. *J Neurosci* 18:5565–5574.
- Dumont Y, Fournier A, St-Pierre S, Quirion R. 1993. Comparative characterization and autoradiographic distribution of neuropeptide Y receptor subtypes in the rat brain. *J Neurosci* 13:73–86.
- Ferezou I, Cauli B, Hill EL, Rossier J, Hamel E, Lambolez B. 2002. 5-HT₃ receptors mediate serotonergic fast synaptic excitation of neocortical vasoactive intestinal peptide/cholecystokinin interneurons. *J Neurosci* 22:7389–7397.
- Foldy C, Lee SY, Szabadics J, Neu A, Soltesz I. 2007. Cell type-specific gating of perisomatic inhibition by cholecystokinin. *Nat Neurosci* 10:1128–1130.
- Frazier CJ, Rollins YD, Breese CR, Leonard S, Freedman R, Dunwiddie TV. 1998. Acetylcholine activates an alpha-bungarotoxin-sensitive nicotinic current in rat hippocampal interneurons, but not pyramidal cells. *J Neurosci* 18:1187–1195.
- Freedman R, Wetmore C, Stromberg I, Leonard S, Olson L. 1993. Alpha-bungarotoxin binding to hippocampal interneurons: Immunocytochemical characterization and effects on growth factor expression. *J Neurosci* 13:1965–1975.
- Freund TF. 2003. Interneuron diversity series: Rhythm and mood in perisomatic inhibition. *Trends Neurosci* 26:489–495.
- Freund TF, Buzsaki G. 1996. Interneurons of the hippocampus. *Hippocampus* 6:347–470.
- Freund TF, Gulyas AI, ACSády L, Gorcs T, Toth K. 1990. Serotonergic control of the hippocampus via local inhibitory interneurons. *Proc Natl Acad Sci USA* 87:8501–8505.
- Gobbi M, Gariboldi M, Piwko C, Hoyer D, Sperk G, Vezzani A. 1998. Distinct changes in peptide YY binding to, and mRNA levels of, Y1 and Y2 receptors in the rat hippocampus associated with kindling epileptogenesis. *J Neurochem* 70:1615–1622.
- Gray CM. 1994. Synchronous oscillations in neuronal systems: mechanisms and functions. *J Comput Neurosci* 1:11–38.
- Gruber B, Greber S, Rupp E, Sperk G. 1994. Differential NPY mRNA expression in granule cells and interneurons of the rat dentate gyrus after kainic acid injection. *Hippocampus* 4:474–482.
- Gulyas AI, Hajos N, Freund TF. 1996. Interneurons containing calretinin are specialized to control other interneurons in the rat hippocampus. *J Neurosci* 16:3397–3411.
- Gulyas AI, Miettinen R, Jacobowitz DM, Freund TF. 1992. Calretinin is present in non-pyramidal cells of the rat hippocampus—I. A new type of neuron specifically associated with the mossy fibre system. *Neuroscience* 48:1–27.
- Hefft S, Jonas P. 2005. Asynchronous GABA release generates long-lasting inhibition at a hippocampal interneuron-principal neuron synapse. *Nat Neurosci* 8:1319–1328.
- Jakubs K, Nanobashvili A, Bonde S, Ekdahl CT, Kokaia Z, Kokaia M, Lindvall O. 2006. Environment matters: synaptic properties of neurons born in the epileptic adult brain develop to reduce excitability. *Neuron* 52:1047–1059.
- Katona I, Sperlagh B, Sik A, Kalvay A, Vizi ES, Mackie K, Freund TF. 1999. Presynaptically located CB1 cannabinoid receptors

- regulate GABA release from axon terminals of specific hippocampal interneurons. *J Neurosci* 19:4544–4558.
- Klapstein GJ, Colmers WF. 1993. On the sites of presynaptic inhibition by neuropeptide Y in rat hippocampus in vitro. *Hippocampus* 3:103–111.
- Klausberger T, Roberts JD, Somogyi P. 2002. Cell type- and input-specific differences in the number and subtypes of synaptic GABA(A) receptors in the hippocampus. *J Neurosci* 22:2513–2521.
- Kneisler TB, Dingledine R. 1995. Spontaneous and synaptic input from granule cells and the perforant path to dentate basket cells in the rat hippocampus. *Hippocampus* 5:151–164.
- Kobayashi M, Buckmaster PS. 2003. Reduced inhibition of dentate granule cells in a model of temporal lobe epilepsy. *J Neurosci* 23:2440–2452.
- Kokaia M, Asztely F, Olofsson K, Sindreu CB, Kullmann DM, Lindvall O. 1998. Endogenous neurotrophin-3 regulates short-term plasticity at lateral perforant path-granule cell synapses. *J Neurosci* 18:8730–8739.
- Lisman JE. 1999. Relating hippocampal circuitry to function: Recall of memory sequences by reciprocal dentate-CA3 interactions. *Neuron* 22:233–242.
- Lisman JE, Idiart MA. 1995. Storage of 7 +/- 2 short-term memories in oscillatory subcycles. *Science* 267:1512–1515.
- Lopez-Bendito G, Sturgess K, Erdelyi F, Szabo G, Molnar Z, Paulsen O. 2004. Preferential origin and layer destination of GAD65-GFP cortical interneurons. *Cereb Cortex* 14:1122–1133.
- Low K, Crestani F, Keist R, Benke D, Brunig I, Benson JA, Fritschy JM, Rulicke T, Bluethmann H, Mohler H, Rudolph U. 2000. Molecular and neuronal substrate for the selective attenuation of anxiety. *Science* 290:131–134.
- Lurton D, Cavalheiro EA. 1997. Neuropeptide-Y immunoreactivity in the pilocarpine model of temporal lobe epilepsy. *Exp Brain Res* 116:186–190.
- McQuiston AR, Colmers WF. 1992. Neuropeptide Y does not alter NMDA conductances in CA3 pyramidal neurons: A slice-patch study. *Neurosci Lett* 138:261–264.
- McQuiston AR, Colmers WF. 1996. Neuropeptide Y2 receptors inhibit the frequency of spontaneous but not miniature EPSCs in CA3 pyramidal cells of rat hippocampus. *J Neurophysiol* 76:3159–3168.
- Morales M, Hein K, Vogel Z. 2008. Hippocampal interneurons co-express transcripts encoding the alpha7 nicotinic receptor subunit and the cannabinoid receptor 1. *Neuroscience* 152:70–81.
- Murthy VN, Sejnowski TJ, Stevens CF. 1997. Heterogeneous release properties of visualized individual hippocampal synapses. *Neuron* 18:599–612.
- Noe F, Pool AH, Nissinen J, Gobbi M, Bland R, Rizzi M, Balducci C, Ferraguti F, Sperk G, During MJ, Pitkanen A, Vezzani A. 2008. Neuropeptide Y gene therapy decreases chronic spontaneous seizures in a rat model of temporal lobe epilepsy. *Brain* 131(Part 6):1506–1515.
- Nunzi MG, Gorio A, Milan F, Freund TF, Somogyi P, Smith AD. 1985. Cholecystokinin-immunoreactive cells form symmetrical synaptic contacts with pyramidal and nonpyramidal neurons in the hippocampus. *J Comp Neurol* 237:485–505.
- Nyiri G, Freund TF, Somogyi P. 2001. Input-dependent synaptic targeting of alpha(2)-subunit-containing GABA(A) receptors in synapses of hippocampal pyramidal cells of the rat. *Eur J Neurosci* 13:428–442.
- Papp EC, Hajos N, Acsády L, Freund TF. 1999. Medial septal and median raphe innervation of vasopressin-intestinal polypeptide-containing interneurons in the hippocampus. *Neuroscience* 90:369–382.
- Paredes MF, Greenwood J, Baraban SC. 2003. Neuropeptide Y modulates a G protein-coupled inwardly rectifying potassium current in the mouse hippocampus. *Neurosci Lett* 340:9–12.
- Pawelzik H, Hughes DI, Thomson AM. 2002. Physiological and morphological diversity of immunocytochemically defined parvalbumin- and cholecystokinin-positive interneurons in CA1 of the adult rat hippocampus. *J Comp Neurol* 443:346–367.
- Qian J, Colmers WF, Saggau P. 1997. Inhibition of synaptic transmission by neuropeptide Y in rat hippocampal area CA1: Modulation of presynaptic Ca²⁺ entry. *J Neurosci* 17:8169–8177.
- Richichi C, Lin EJ, Stefanin D, Colella D, Ravizza T, Grignaschi G, Veglianesi P, Sperk G, During MJ, Vezzani A. 2004. Anticonvulsant and antiepileptogenic effects mediated by adeno-associated virus vector neuropeptide Y expression in the rat hippocampus. *J Neurosci* 24:3051–3059.
- Scharfman HE. 1995. Electrophysiological diversity of pyramidal-shaped neurons at the granule cell layer/hilus border of the rat dentate gyrus recorded in vitro. *Hippocampus* 5:287–305.
- Schwarzer C, Williamson JM, Lothman EW, Vezzani A, Sperk G. 1995. Somatostatin, neuropeptide Y, neurokinin B, cholecystokinin immunoreactivity in two chronic models of temporal lobe epilepsy. *Neuroscience* 69:831–845.
- Schwarzer C, Kofler N, Sperk G. 1998. Up-regulation of neuropeptide Y-Y2 receptors in an animal model of temporal lobe epilepsy. *Mol Pharmacol* 53:6–13.
- Smialowska M, Bijak M, Sopala M, Tokarski K. 1996. Inhibitory effect of NPY on the picrotoxin-induced activity in the hippocampus: A behavioural and electrophysiological study. *Neuropeptides* 30:7–12.
- Somogyi P, Klausberger T. 2005. Defined types of cortical interneurone structure space and spike timing in the hippocampus. *J Physiol* 562(Part 1):9–26.
- Sørensen AT, Kanter-Schlifke I, Lin EJ, During MJ, Kokaia M. 2008. Activity-dependent volume transmission by transgene NPY attenuates glutamate release and LTP in the subiculum. *Mol Cell Neurosci* 39:229–237.
- Sørensen AT, Nikitidou L, Ledri M, Lin EJ, During MJ, Kanter-Schlifke I, Kokaia M. 2009. Hippocampal NPY gene transfer attenuates seizures without affecting epilepsy-induced impairment of LTP. *Exp Neurol* 215:328–333.
- Stanic D, Brumovsky P, Fetisov S, Shuster S, Herzog H, Hokfelt T. 2006. Characterization of neuropeptide Y2 receptor protein expression in the mouse brain. I. Distribution in cell bodies and nerve terminals. *J Comp Neurol* 499:357–390.
- Traub RD, Pais I, Bibbig A, Lebeau FE, Buhl EH, Garner H, Monyer H, Whittington MA. 2005. Transient depression of excitatory synapses on interneurons contributes to epileptiform bursts during gamma oscillations in the mouse hippocampal slice. *J Neurophysiol* 94:1225–1235.
- Tu B, Jiao Y, Herzog H, Nadler JV. 2006. Neuropeptide Y regulates recurrent mossy fiber synaptic transmission less effectively in mice than in rats: Correlation with Y2 receptor plasticity. *Neuroscience* 143:1085–1094.
- Vezzani A, Sperk G, Colmers WF. 1999. Neuropeptide Y: Emerging evidence for a functional role in seizure modulation. *Trends Neurosci* 22:25–30.
- Vezzani A, Michalkiewicz M, Michalkiewicz T, Moneta D, Ravizza T, Richichi C, Aliprandi M, Mule F, Pirona L, Gobbi M, Schwarzer C, Sperk G. 2002. Seizure susceptibility and epileptogenesis are decreased in transgenic rats overexpressing neuropeptide Y. *Neuroscience* 110:237–243.
- Wahlestedt C, Pich EM, Koob GF, Yee F, Heilig M. 1993. Modulation of anxiety and neuropeptide Y-Y1 receptors by antisense oligodeoxynucleotides. *Science* 259:528–531.
- Yang L, Benardo LS, Valsamis H, Ling DS. 2007. Acute injury to superficial cortex leads to a decrease in synaptic inhibition and increase in excitation in neocortical layer V pyramidal cells. *J Neurophysiol* 97:178–187.
- Zucker RS, Stockbridge N. 1983. Presynaptic calcium diffusion and the time courses of transmitter release and synaptic facilitation at the squid giant synapse. *J Neurosci* 3:1263–1269.
- Zucker RS, Regehr WG. 2002. Short-term synaptic plasticity. *Annu Rev Physiol* 64:355–405.

Paper II

Altered profile of basket cell afferent synapses in hyperexcitable dentate gyrus revealed by optogenetic and two-pathway stimulations

Marco Ledri¹, Litsa Nikitidou¹, Ferenc Erdelyi², Gabor Szabo², Deniz Kirik³, Karl Deisseroth⁴ and Merab Kokaia¹

¹Experimental Epilepsy Group, Division of Neurology, Wallenberg Neuroscience Centre, Lund University Hospital, Sweden; ²Department of Gene Technology and Developmental Neurobiology, Institute for Experimental Medicine, Budapest, Hungary; ³Brain Repair and Imaging in Neural Systems (BRAINS) Unit, Department of Experimental Medical Sciences, Lund University Hospital, Sweden; ⁴Department of Bioengineering, Department of Psychiatry and Behavioral Sciences, Stanford University, Stanford, USA

Abstract

Cholecystokinin (CCK-) positive basket cells form a distinct class of inhibitory GABAergic interneurons, proposed to act as fine-tuning devices of hippocampal gamma-frequency (30-90 Hz) oscillations, which can convert into higher frequency seizure activity. Therefore, CCK-basket cells may play an important role in regulation of hyperexcitability and seizures in the hippocampus. In normal conditions, the endogenous excitability regulator Neuropeptide Y (NPY) has been shown to modulate afferent inputs onto dentate gyrus CCK-basket cells, providing a possible novel mechanism for excitability control in the hippocampus. Using GAD65-EGFP mice for CCK-basket cell identification, and whole-cell patch-clamp recordings, we explored whether effect of NPY on afferent synapses to CCK-basket cells is modified in the hyper-excitable dentate gyrus. To induce hyper-excitable state, recurrent seizures were evoked by electrical stimulation of the hippocampus using the well-characterized rapid kindling protocol. We found that the frequency of spontaneous and miniature excitatory and inhibitory postsynaptic currents recorded in CCK-basket cells were decreased by NPY. The EPSCs evoked in CCK-basket cells by optogenetic activation of principal neurons were also decreased in amplitude. Interestingly, we observed an increased proportion of sIPSCs with slower rise times, indicating that NPY may inhibit GABA release preferentially in peri-somatic synapses. These findings indicate that increased levels and release of NPY observed after seizures can modulate afferent inputs to CCK-basket cells, and therefore alter their impact on the oscillatory network activity and excitability in the hippocampus.

Introduction

Hippocampal basket cells form a distinct class of interneurons that provide inhibition to the cell bodies and proximal dendrites of principal cells. The spatial segregation and strategic location of their efferents enables efficient control of the output of principal neurons and consequently regulate oscillation rate, spike timing and activity synchronization of their targets (Cobb *et al.*, 1995; Ylinen *et al.*, 1995; Miles *et al.*, 1996). Two main populations of basket cells have been described in all

major areas of the hippocampus (Somogyi & Klausberger, 2005). These two populations have similar morphological appearance but express diverse protein markers and differ in functional characteristics. They can be distinguished by the expression of either the calcium binding protein Parvalbumin (PV) or the neuropeptide Cholecystokinin (CCK) (Freund & Katona, 2007). The PV-positive basket cells are proposed to act as clockwork devices for the induction of learning-related gamma-frequency (30-90 Hz) oscillations due to their ability to generate high-frequency action potentials and to release GABA in synchronous

manner (Freund, 2003). In contrast, action potentials of CCK basket cells are characterized by strong accommodation, the cells express a variety of receptors for modulatory neurotransmitters (e. g., 5-hydroxytryptamine 3, nicotinic $\alpha 4$ and $\alpha 7$, and Cannabinoid 1 receptors) (Freedman *et al.*, 1993; Katona *et al.*, 1999; Porter *et al.*, 1999; Ferezou *et al.*, 2002), and are thought to act as fine-tuning devices that modulate high-frequency network activity (Freund, 2003). Since gamma-frequency oscillations can convert into higher frequency epileptiform activity (Traub *et al.*, 2005) in hyper-excitabile states, CCK basket cells could play an important role in this conversion. In line with this notion, the endogenous factors that regulate hippocampal excitability, e.g., neuropeptide Y (NPY), also can modulate synaptic drive onto the CCK basket cells (Ledri *et al.*, 2011). During the hyper-excitabile state in animals (animal models of epilepsy) and in patients with temporal lobe epilepsy, numerous alterations of the synaptic efficacy, network connectivity and other structural reorganizations occur (cell death, axonal sprouting, synaptogenesis, neurogenesis, inflammation, etc.). Various subtypes of interneurons undergo cell death and their network connectivity is altered (Bausch, 2005). Of particular interest is that expression of NPY and its receptors also undergo considerable changes. After induction of seizures, NPY and Y2 receptor expression have been found to be up-regulated in hilar interneurons, dentate granule cells and mossy fibers (Marksteiner *et al.*, 1990; Gruber *et al.*, 1994; Schwarzer *et al.*, 1998; Vezzani *et al.*, 1999), while Y1 receptor expression in the dentate granule cell dendrites is down-regulated (Kofler *et al.*, 1997). Therefore, we hypothesized that afferent synaptic inputs onto CCK basket cells are likely to be modulated by endogenous excitability regulators such as NPY, and may play a role in normalizing hyper-excitability and high frequency activity during seizures.

Materials and methods

Animals

Young adult Glutamic Acid Decarboxylase 65-Enhanced Green Fluorescent Protein (GAD65-EGFP) mice were used (Brager *et al.*, 2003), at the age of seven to eight weeks at the time of the beginning of the experimental procedures. In this transgenic line, GFP is expressed under the control of the GAD65 promoter, allowing visual identification of several populations of inhibitory

European Journal of Neuroscience (2012), *in press*

interneurons, including CCK basket cells. All experiments were conducted according to international guidelines on the use of experimental animals, as well as the Swedish Animal Welfare Agency guidelines, and were approved by the local Ethical Committee for Experimental Animals.

Production of recombinant Adeno-Associated Viral vectors

An AAV-CamKIIa-ChR2-mCherry expression vector was constructed by excising (XbaI, EcoRI) the CamKIIa-ChR2-mCherry portion of a Lentiviral construct and cloning it in an AAV backbone vector containing the Woodchuck Post-transcriptional Regulatory Element (WPRE) and the human growth hormone polyadenylation (hGH-polyA) sequences flanked by inverted terminal repeats (ITR). Virus production was essentially performed as previously described (Eslamboli *et al.*, 2005), with minor modifications. Briefly, the transfer vector and the packaging plasmid, pDG5, were transfected into 293 cells. Seventy hours after transfection the cells were harvested and lysed using one freeze-thaw cycle. The crude lysate was clarified by centrifugation at 4,500g for 20 minutes and the vector-containing supernatant was purified using a iodixanol gradient and ultracentrifugation (1.5 hours at 350,000g). The virus-containing iodixanol gradient fraction was further purified using an Acrodisc Mustang Q device (Pall Life Sciences, Port Washington, New York). For further concentration, desalting, and buffer exchange, the purified vector suspension was centrifuged in an Amicon Ultra device (Millipore). The AAV vector was produced as serotype 5. The final number of AAV particles was determined using qPCR and was 7.4×10^{12} genomic particles/ml.

Electrode implantation and virus injection

Animals were anesthetized by inhalation of isoflurane (2.5%, Baxter Chemical AB) and fixed onto a stereotaxic frame (David Kopf Instruments, Tujunga, CA). A bipolar stainless steel stimulation/recording electrode (Plastics One, Roanoke, VA) was stereotaxically implanted in the ventral right hippocampus at the following coordinates (in mm): AP -2.9, ML 3.0, DV -3.0. A reference electrode was placed in the temporal muscle. Electrodes were placed into a pedestal (Plastics One Roanoke, VA) and fixed on the skull with dental cement (Kemdent).

In a subset of animals, during the same surgery, AAV-CamKIIa-ChR2-mCherry viral vector

suspension was injected through a glass capillary in the left hippocampus (contra-lateral to the electrode) at the following coordinates (in mm): AP -3.2, ML -3.1, DV -3.6 and -3.2. 0.5 μ l of viral suspension were injected at 0.1 μ l/minute in each location in the DV plane. The glass pipette was left in place for 5 minutes after each injection, to avoid back-flow of viral particles through the injection tract. Reference points for stereotaxic surgery were bregma for the AP axis, midline for the ML axis, and dura for the DV axis.

Electrical rapid kindling and test stimulations

At 7 days after electrode implantation and virus injection, the animals were subjected to electrical rapid kindling in the hippocampus, as previously described (Elmer *et al.*, 1996; Sorensen *et al.*, 2009). The individual threshold was determined by delivering stimulations (1 sec train consisting of 1 ms bipolar square wave pulses at 100 Hz) of increasing current in 10 μ A steps until a focal epileptiform afterdischarge (AD) of more than 5 sec duration was detected by electroencephalographic (EEG) recording. During rapid kindling induction, EEG activity was continuously recorded on a MacLab system (ADInstruments, Bella Vista, Australia) for 200 min except during stimulations, which consisted of 40 suprathreshold stimulation trains (10 s, 1 ms square wave pulses at 50 Hz, 400

A intensity) separated by 5 min interval between stimulations. Behavioral seizures were scored according to the Racine scale (Racine, 1972): grade 0, arrest, normal behavior; grade 1, facial twitches (nose, lips, eyes); grade 2, chewing, head nodding; grade 3, forelimb clonus; grade 4, rearing, falling on forelimbs; grade 5, imbalance and falling on side or back. Only animals that developed at least 6 stage 3–5 seizures were subsequently used for electrophysiology.

To assess if animals achieved a hyper-excitability state at the time point of electrophysiology, four weeks after the first kindling the individual threshold was re-measured in a subset of animals ($n=5$). Animals were then given 5 additional stimulations using the same parameters of the first 5 kindling stimulations. Seizure grades and AD duration were assessed as previously.

Slice preparation

Four to six weeks after stimulations, animals were briefly anesthetized with isoflurane and decapitated. The head was quickly immersed in chilled sucrose-based cutting solution, containing

(in mM): sucrose 75, NaCl 67, NaHCO₃ 26, glucose 25, KCl 2.5, NaH₂PO₄ 1.25, CaCl₂ 0.5, MgCl₂ 7 (pH 7.4, osmolarity 305–310 mOsm). The brain was removed and placed in a Sylgard-coated petri dish containing chilled sucrose-based solution, the cerebellum was discarded and the two hemispheres divided using a razor blade. The left hemisphere, contra-lateral to the stimulating electrode, was then positioned lying on the medial side and a “magic-cut” was performed on the dorsal cortex (Bischofberger *et al.*, 2006). The tissue was subsequently glued “magic-cut” side down on a pedestal and transferred to a cutting chamber containing sucrose-based solution maintained at 2–4 °C and constantly oxygenated with carbogen (95% O₂/5% CO₂). Transverse slices of 300 μ m thickness, comprising the hippocampus and entorhinal cortex, were cut on a vibrating microtome (VT1200S, Leica Microsystems, advancing speed was set at 0.05 mm/sec and amplitude at 1.7 mm), and immediately transferred to an incubation chamber containing sucrose-based solution constantly oxygenated with carbogen (95% O₂/5% CO₂) and maintained at 34 °C in a water bath. Slices were allowed to rest for 30 minutes before being transferred to room temperature and processed for electrophysiology.

Whole-cell patch-clamp electrophysiology

Individual slices were placed in a submerged recording chamber constantly perfused with gassed artificial cerebro-spinal fluid (aCSF) containing, in mM: NaCl 119, NaHCO₃ 26, glucose 25, KCl 2.5, NaH₂PO₄ 1.25, CaCl₂ 2.5 and MgSO₄ 1.3 (pH 7.4, osmolarity 305–310 mOsm). The temperature in the recording chamber was maintained at 32–34 °C, unless otherwise noted. GAD65-GFP positive cells were visualized under fluorescent light and infrared differential interference contrast microscopy was used for visual approach of the recording pipette. Recording pipettes (2.5–5 M Ω resistance) were pulled from thick-walled (1.5 mm outer diameter, 0.86 mm inner diameter) borosilicate glass with a Flaming-Brown horizontal puller (P-97, Sutter Instruments, CA), and contained (in mM): K-Gluconate 122.5, KCl 12.5, KOH-HEPES 10, KOH-EGTA 0.2, MgATP 2, Na₂GTP 0.3, NaCl 8 (pH 7.2–7.4, mOsm 300–310) for measurements of intrinsic properties and for monitoring the response to light in ChR2-expressing cells; Cs-Gluconate 117.5, CsCl 17.5, NaCl 8, CsOH-HEPES 10, CsOH-EGTA 0.2, MgATP 2, Na₂GTP 0.3, QX-314 5 (pH 7.2–7.4, mOsm 300–

310) for spontaneous, miniature and light-evoked excitatory post-synaptic currents recordings (sEPSCs, mEPSCs and lEPSCs, respectively); CsCl 135, CsOH 10, CsOH-EGTA 0.2, MgATP 2, Na₂GTP 0.3, NaCl 8, QX-314 5 (pH 7.2-7.4, mOsm 300-310) for spontaneous, miniature and dual stimulation-evoked inhibitory post-synaptic currents recordings (sIPSCs, mIPSCs and dsIPSCs, respectively). Biocytin (3-5 mg/ml) was routinely added to the pipette solution on the day of the recording. Recordings typically lasted 20-30 minutes, and biocytin was allowed to diffuse for additional 10 minutes at the end to assure complete diffusion in the axonal arbor. Uncompensated series resistance (typically 8-30 MΩ) was constantly monitored via -5 mV voltage steps and recordings were discontinued after changes of >20% or if the resting membrane potential was more positive than -50 mV.

Cells were held at -70 mV in voltage clamp and at 0 pA in current clamp recordings. Firing pattern and accommodation were investigated by applying a single 1 sec, 500 pA depolarizing current step. Action potential threshold, amplitude and rheobase were measured by the first action potential of the train evoked with a 1 sec voltage ramp of 0-300 or 0-500 pA. Current-voltage relationship was analyzed by injecting consecutive incrementing 500 ms 10 pA current steps, from -200 to +200 pA.

EPSCs were recorded in the presence of 100 μM Picrotoxin (PTX, Tocris Bioscience, Ellisville, MI) to block Gamma-aminobutyric acid A (GABA_A) receptors. 50 μM DL-2-amino-5-phosphonopivalic acid (D-AP5, Tocris) and 5 μM 2,3-dihydroxy-6-nitro-7-sulfamoyl-benzo[f]quinolaxaline-2,3-dione (NBQX, Tocris) were used during IPSC recordings to block N-Methyl-D-Aspartate (NMDA) and α-amino-3-hydroxy-5-methylisoxazole-4-propionic acid (AMPA) receptors, respectively. For mEPSC and mIPSC recordings, 1 μM Tetrodotoxin (TTX, Tocris) was used to block voltage-gated sodium channels and prevent generation of action potentials. The specific metabotropic group II receptor (mGluR II) agonist (2S,1'S,2'S)-2-(Carboxycyclopropyl)glycine (L-CCG-I, 10 μM, Tocris) was used to activate mGluR II, which are exclusively expressed presynaptically on mossy fibers, to selectively block glutamate release from mossy fibers and respective mossy fiber-specific EPSCs in postsynaptic neurons (Kokaia *et al.*, 1998).

For light-evoked EPSC recordings, a 400 μm thick optical fiber was positioned above the apex of the dentate gyrus. Light was generated by a 460 nm

European Journal of Neuroscience (2012), *in press*

wavelength LED light source (WT&T Technology, Quebec, Canada) and stimulation of pre-synaptic ChR2-expressing cells was achieved via paired 1-2 ms light pulses with 50 ms inter-stimulation-interval (ISI) at 0.06 Hz.

For dual stimulation-evoked IPSCs, two bipolar stainless steel stimulating electrodes were placed in the outer molecular layer and in the granule cell layer of the dentate gyrus, respectively. Paired-pulse stimulations were used at 0.06 Hz with 100 ms ISI.

NPY (Schafer-N, Copenhagen, Denmark) was dissolved in distilled water, stored in concentrated aliquots, diluted to 1 μM concentration in the perfusion solution immediately before use and allowed to diffuse in the recording chamber for 7 min before the continuation of the recordings. The concentration of NPY used here has been previously shown to be the most effective in inhibiting Schaffer collateral-CA1 excitatory post-synaptic potentials in the hippocampus (Colmers *et al.*, 1987). Silicon-coated tubing and bottles were used to prevent the peptide from adhering to the tubing and container walls. PTX or D-AP5 and NBQX were applied at the end of the experiments to verify that the synaptic currents were generated by respective receptor activation.

Data were sampled at 20 kHz with an EPC-10 amplifier (HEKA Elektronik, Lambrecht, Germany) and stored on a G4 Macintosh computer using PatchMaster software (HEKA) for offline analysis.

Immunohistochemistry and axonal arbor reconstruction

For identifying the cells recorded in this study, slices after electrophysiology were fixed in 4% Paraformaldehyde (PFA) in phosphate buffer (PB) for 12-24 hours and then stored in anti-freeze solution (ethylenglycol and glycerol in PB buffer) at -20°C until processed. For immunohistochemical staining against GFP and biocytin, slices were rinsed three times with KPBS and pre-incubated for 1 hour in blocking solution (10% normal goat serum and 0.25% Triton X-100 in KPBS, T-KPBS). Sections were then incubated overnight with 1:10,000 rabbit anti-GFP polyclonal antibody (ab1218, Abcam) in blocking solution, rinsed three additional times in T-KPBS and incubated for 2 hours in FITC-conjugated goat anti rabbit secondary antibody (1:400, Jackson Immunoresearch, Suffolk, UK) and Cy5-conjugated streptavidin (1:200, Jackson Immunoresearch, Suffolk, UK) in blocking solution. Slices were finally rinsed three times in KPBS,

mounted on coated slides and cover-slipped with DABCO. For evaluating the expression of AAV-CamKIIa-ChR2-mCherry, 1:1000 rat anti-mCherry (5F8, Chromotek, Germany) was added to the primary antibody incubation, and 1:400 Cy3-conjugated donkey anti-rat was added to the secondary antibodies.

For reconstruction of the axonal arborisation, labeled neurons were examined with a confocal laser-scanning microscope (Leica). Confocal Z-stacks were obtained along the entire dendritic and axonal tree of the cells, and typically consisted of 40–50 planes.

Y2 immunohistochemistry and optical density measurements

To analyze the distribution of Y2 receptors, after fixation in 4% PFA overnight, slices from electrophysiological measurements and from non-kindled GAD65-GFP age-matched controls were cryoprotected in 20% sucrose in PB for two days and additionally cut in 50- μ m sections using a microtome. Sections were processed for Y2 immunohistochemistry essentially as previously described (Tu *et al.*, 2006). Briefly, slices were treated with 1% hydrogen peroxide for 30 minutes, pre-incubated for 1 hour in blocking solution containing normal goat serum (see above), incubated for 24 hours at 4°C with 1:1000 rabbit anti-Y2 receptor antibody (RA14112, Neuromics, Edina, MN, USA) and subsequently with 1:500 biotinylated goat anti-rabbit secondary antibody (Vector Laboratories, UK). Y2 immunoreactivity was visualized by incubating the sections in avidin-biotin conjugated horseradish peroxidase solution (ABC, Vector Laboratories, UK), and then reacting them with 0.5 mg/ml diaminobenzidine (DAB), 0.025% cobalt chloride, 0.2% nickel ammonium sulfate and hydrogen peroxide solutions. Sections were finally dehydrated, mounted on coated slides and cover-slipped with Pertex (Histolab Products AB, Sweden).

Microphotographs were taken from each section using the same exposure time and ambient light conditions, on the same day. To measure optical density of Y2-positive fibers, images were processed with ImageJ software (NIH, <http://rsbweb.nih.gov/ij/>). The density reading of the Y2-negative hippocampal fimbria structure was used as an internal reference for each section, and subtracted from the readings of the inner and outer molecular layers. Values for optical density are presented as Arbitrary Units.

Data analysis and statistics

Only cells resembling CCK basket cells morphology, with axonal arborization confined to the inner molecular and granule cell layers, and showing co-localisation of GFP and biocytin were accepted for analysis. Off-line analysis was performed using FitMaster (HEKA Elektronik), IgorPro (Wavemetrics, Lake Oswego, OR) and MiniAnalysis (Synaptosoft Inc., Decatur, GA) software.

Action potential (AP) threshold was defined as the point where the fastest rising phase of the first action potential in the ramp started. Rheobase was defined as the current needed in the ramp to reach AP threshold. AP amplitude and AP half-duration were defined as the difference between the threshold and the peak, in mV and ms respectively. Paired-pulse facilitation and depression (PPF and PPD, respectively) were expressed as the ratio between the amplitude of the second and the first response of the pair, in percentage. Before and after NPY application differences in resting membrane potential (RMP), AP threshold, AP amplitude, spontaneous and miniature currents frequency and amplitude mean values, *le*EPSCs and *ds*IPSCs amplitudes, PPF and PPD were assessed with two-tailed Student's *t*-test using SPSS software (IBM). Optical density Arbitrary Unit measurements and stimulation-evoked IPSCs rise time comparisons were assessed with two-tailed Student's *t*-test. Inter-event-intervals (IEIs) and amplitude of spontaneous and miniature post-synaptic currents, and *s*IPSC rise times (10–90%) were analysed using MiniAnalysis software and differences between the groups were calculated with cumulative fraction curves combined with Kolmogorov-Smirnov (*K-S*) test. Events were automatically recognized by the software and included in the analysis if their magnitude was at least 5 times bigger than the calculated average root mean square (RMS) noise. For *s*EPSCs and *m*EPSCs recordings, only the last 150 events before start of NPY application and the first 150 events after equilibration of NPY (7 min after start of NPY application) were included in the analysis. For *s*IPSCs and *m*IPSCs recordings, 200 events were included. Values are presented as means \pm SEM. Differences are considered significant with $P < 0.05$ for Student's paired and un-paired *t*-test and $P < 0.01$ for *K-S* test.

Results

Electrical rapid kindling and assessment of hyper-excitability

To induce hyper-excitability in the hippocampus, animals were subjected to rapid kindling stimulations (Elmer *et al.*, 1996; Sorensen *et al.*, 2009). During the 40 rapid kindling stimulations, animals developed seizures ranging from stage 0 to 5. The average number of stage 3-5 seizures was 12.7 ± 0.3 per animal. Four weeks later, at the time point for electrophysiological recordings, hyper-excitability was assessed in a subset of animals by delivering five additional rapid re-kindling stimulations. During re-kindling, the duration of afterdischarges at threshold stimulations was increased more than 2 times (68.0 ± 10.5 s for the re-kindling stimulations compared to 32.2 ± 5.0 s for the initial kindling, $n=5$, $P=0.036$, two-tailed Student's *t*-test), and the average number of stage 3-5 seizures was significantly higher (3.0 ± 0.2 for the re-kindling stimulations compared to 2.4 ± 0.4 for the initial five stimulations, $n=5$, $P=0.031$, two-tailed Student's *t*-test). These data show that, at the time point of electrophysiological recordings, the animals have developed a hyper-excitabile state.

Identification of CCK basket cells and effects of NPY on intrinsic membrane properties

In GAD65-GFP animals, several different subpopulations of GABAergic interneurons express GFP. To identify CCK-positive basket cells, the following morphological criteria were used, as previously described (Ledri *et al.*, 2011): (1) the cell soma had to be located on the border between the granule cell layer and the hilus, and (2) it had to be roughly pyramidal shaped; (3) the main apical dendrite had to reach the molecular layer and (4) the basal dendrites had to extend into the hilus (an example is shown in Figure 1E-G). The cells displayed typical low-frequency, accommodating action potential firing pattern upon depolarization (Figures 1A and 1B), and their axonal arborization was mostly confined to the granule cell and inner molecular layers (Figure 1D). These characteristics are consistent with the CCK-basket cell identity of the recorded cells.

We first asked whether application of exogenous NPY could affect intrinsic membrane properties of CCK-basket cells in animals that have experienced recurrent seizures. The frequency of action potential firing (Figure 1A) and the degree of action potential

frequency accommodation (Figure 1C) were not affected by NPY application, as well as the mean rheobase (Figure 1B), resting membrane potential, action potential threshold, amplitude and duration ($n=6$, $P>0.05$, two-tailed Student's paired *t*-test, Table 1). Thus, NPY does not seem to alter intrinsic membrane properties of CCK-basket cells in kindled animals.

The frequency of spontaneous and miniature EPSCs onto the CCK-basket cells is decreased by NPY

Next we asked whether NPY could modulate afferent excitatory synapses of the CCK-basket cells. We first recorded sEPSCs in voltage-clamp mode at -70 mV (with PTX in the perfusion solution to block GABA_A receptors and pharmacologically isolate glutamate receptor-mediated currents) before and after application of 1 μ M NPY. Figure 2A shows representative traces of sEPSCs recorded from CCK-basket cells. The mean frequency of sEPSCs was significantly decreased by application of NPY (5.1 ± 0.6 Hz before and 3.9 ± 0.7 Hz after NPY application, $n=6$, $P=0.008$, two-tailed Student's paired *t*-test, Figure 2B left) while the mean amplitude was not affected (17.9 ± 1.2 pA before and 19.4 ± 3.6 after NPY application, $n=6$, $P=0.69$, two-tailed Student's paired *t*-test, Figure 2B right). The subsequent *K-S* analysis of cumulative fraction of sEPSCs confirmed that the frequency was decreased (increase of IELs, $n=6$, $P<0.001$, *K-S* test, Figure 2C) and that the amplitude was not affected ($n=6$, $P>0.01$, *K-S* test, Figure 2D). We then asked whether the observed effect of NPY was due to decrease in action potential generation, and applied NPY while recording action potential-independent mEPSCs by adding TTX in the perfusion solution to block voltage-gated sodium channels, and thereby action potentials, in all neurons. Figure 2E shows representative mEPSCs recordings. Similar

Table 1: NPY does not affect the intrinsic membrane properties of CCK-basket cells in the dentate gyrus of kindled animals. RMP, Resting Membrane Potential; AP, Action Potential.

	Baseline (n=6)	NPY (n=6)
RMP	-57.5 ± 2.7 mV	-56.2 ± 2.7 mV
Input Resistance	256.5 ± 51.8 M Ω	244.5 ± 51.6 M Ω
AP threshold	-35.0 ± 1.6 mV	-36.2 ± 1.6 mV
AP amplitude	72.9 ± 1.5 mV	71.3 ± 2.2 mV
AP half-duration	1.4 ± 0.1 ms	1.6 ± 0.1 ms
Rheobase	106.7 ± 25.5 pA	93.3 ± 22.1 pA

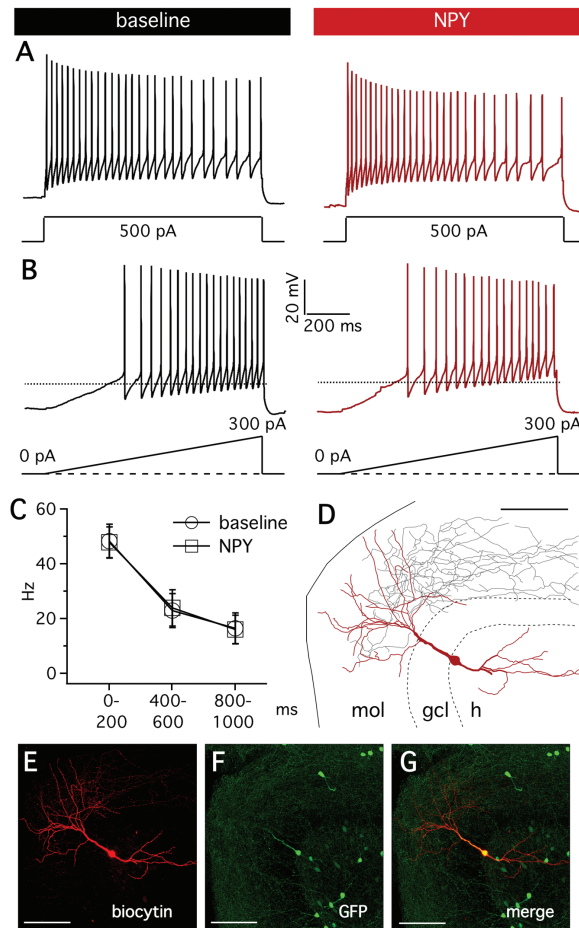


Figure 1. NPY does not affect intrinsic membrane properties of CCK-basket cells in the dentate gyrus.

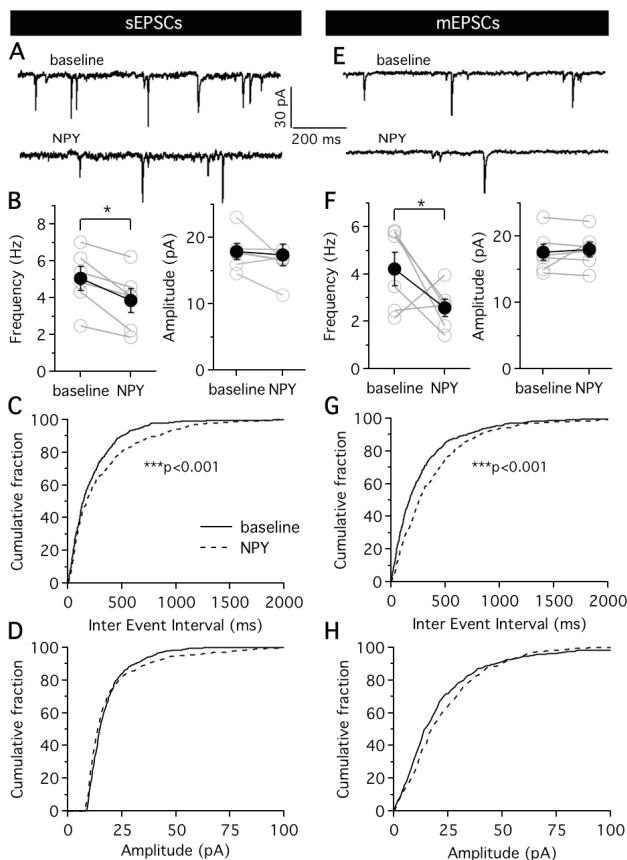
A, The typical regular-spiking accommodating response of a representative CCK-basket cell to a single 1 s, 500 pA depolarizing pulse injected through the patch pipette was not different between baseline (*left*, black trace) and after NPY application (*right*, red trace). **B,** Representative traces showing the response of a CCK-basket cell to a current ramp consisting of 300 pA over 1 s. Action potential threshold (*dashed line*) and rheobase of CCK-basket cells did not differ before (*left*, black trace) and after (*right*, red trace) NPY application. **C,** Action potential firing frequency and degree of frequency accommodation were not changed by NPY application. Action potential frequency was measured at three time points during the 1 s depolarization pulse as in **A**. **D,** Neuronal reconstruction of a CCK-basket cell included in the study showing the typical distribution of dendritic (*red*) and axonal (*black*) arborizations. **E,** The same cell as in **D** shows immunostaining for biocytin and GFP (**F**). Merge is shown in **G**. Scale bars in **D-G** are 100 μ m.

to sEPSCs, the mean frequency of mEPSCs was decreased by application of NPY (4.2 ± 0.7 Hz before and 2.6 ± 0.4 Hz after NPY application, $n=5$, $P=0.031$, two-tailed Student's paired t -test, Figure 2F left) but the mean amplitude was unaffected (17.6 ± 1.3 pA before and 18.0 ± 1.1 pA after NPY

application, $n=5$, $P=0.48$, two-tailed Student's paired t -test, Figure 2F right). The subsequent $K-S$ analysis of cumulative fraction for mEPSCs confirmed these results (Figures 2G and 2H). Taken together, these data demonstrate that NPY decreases the frequency of both action potential-

Figure 2. NPY decreases the frequency of spontaneous and miniature EPSCs on CCK-basket cells but does not alter their amplitude.

A, Representative traces of sEPSCs recorded from CCK-basket cells during baseline (*top*) and after NPY application (*bottom*). **B**, The mean frequency of sEPSCs was decreased by NPY application (*left*, $*P < 0.05$), but the amplitude was not changed (*right*, $P > 0.05$). Grey lines and open circles represent individual recordings, black lines and solid circles represent mean values. **C–D**, Cumulative fraction analysis of Inter Event Intervals (IEIs) and amplitudes of sEPSCs during baseline (*solid line*) and after NPY application (*dashed line*). IEIs were significantly increased by NPY application ($***P < 0.001$) while amplitudes were not affected ($P > 0.01$). **E**, Representative traces of mEPSCs recorded from CCK-basket cells in the presence of 1 μ M TTX before (*top*) and after (*bottom*) NPY application. Note the reduced frequency of events compared to sEPSCs (**A**). **F**, NPY decreased the mean frequency of mEPSCs (*left*, $*P < 0.05$), but did not affect their amplitudes (*right*, $P > 0.05$). **G**, Cumulative fraction curves showing that IEIs of mEPSCs were increased after NPY application ($***P < 0.001$), and **H**, amplitudes were not affected ($P > 0.01$).



dependent and independent excitatory postsynaptic currents and suggest that NPY might act pre-synaptically by decreasing glutamate release.

Effects of NPY on short-term synaptic plasticity of EPSCs onto CCK-basket cells

The observed NPY-induced decrease in the frequency of both sEPSCs and mEPSCs could be explained by the reduction of pre-synaptic release probability (Pr) of glutamate. An indirect indication of changes in Pr could be obtained by measuring the ratio of EPSCs during paired-pulse stimulations. A paired-pulse facilitation (PPF) of EPSCs is a most common form of short-term synaptic plasticity observed in central excitatory synapses (Zucker & Regehr, 2002). An increase in PPF indicates decreased Pr , while a decrease in PPF indicates an increase in Pr . Therefore, possible effects of NPY on Pr of glutamate in afferent excitatory synapses on

CCK-basket cells were explored by evaluating afferent stimulation-induced PPF.

CCK-basket cells in the dentate gyrus receive numerous excitatory inputs: from granule cell mossy fiber collaterals on their basal dendrites in the hilus; from perforant path fibers on their apical dendrites in the molecular layer (Freund & Buzsaki, 1996); from hilar mossy cells (Scharfman, 1995), and possibly from CA3 pyramidal cells by axons back-propagating to the dentate gyrus (Scharfman, 2007). Current conventional electrical stimulation techniques do not allow for collective or selective studies on these excitatory inputs and their modulation. Therefore, we used optogenetics to explore excitatory inputs of the CCK basket cells originating from all afferent synapses. To achieve this goal we used an optogenetic approach with Channelrhodopsin-2 (ChR2). ChR2 is a microbial light-sensitive cation channel, which when

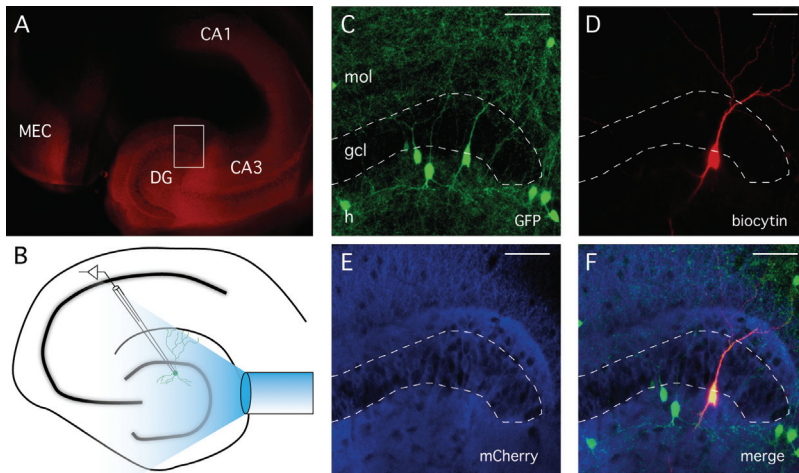


Figure 3. Expression of AAV-CamKIIa-ChR2-mCherry in GAD65-GFP mice and experimental design.

A, Immunostaining against mCherry showing the extent of ChR2 expression in the hippocampus of virus-injected mice. Transgene expression was highest in the dentate gyrus (DG) and CA3 areas, but spread to CA1 and Medial Entorhinal Cortex (MEC). **B**, Schematic diagram depicting the experimental approach. A 400 μm thick core optical fiber connected to a 460 nm blue LED light source was placed on top of the apex of the dentate gyrus to activate ChR2-expressing cells and fibers, while recordings were performed from GFP-positive CCK-basket cells. **C-F**, Confocal stacks showing immunostaining against GFP (**C**), biocytin (**D**), mCherry (**E**) and merged images (**F**). Scale bars are 50 μm . *mol*, molecular layer; *gcl*, granule cell layer; *h*, hilus.

expressed in the membrane of neurons and exposed to ~ 470 nm blue light, is able to depolarize the cell membrane and generate action potentials in a very timely-precise and controllable manner (Boyden *et al.*, 2005). Using AAV vectors, we expressed the ChR2 gene under the CamKIIa promoter in all populations of neurons producing afferent excitatory inputs onto the CCK basket cells, as CamKIIa is selectively expressed in excitatory principal neurons in the hippocampus (CA1-CA3, dentate granule cells) and mossy cells in the dentate gyrus (Monory *et al.*, 2006). Thus, when activated by blue light, ChR2 generates synchronous action potentials in all these populations of neurons at millisecond temporal precision. This results in EPSCs generated in CCK basket cells from all excitatory inputs at the same time, a scenario that could very well be similar to what takes place during highly synchronized seizure activity in the hippocampus.

By using two injection sites targeting the ventral hippocampus, we could achieve robust and long-lasting expression of ChR2 in CA3 pyramidal cells, hilar mossy cells and dentate gyrus granule cells (Figure 3A). In addition, fibers in the middle third of the molecular layer in the dentate gyrus and their cell bodies in layers II/III of the medial entorhinal cortex were also expressing ChR2 (Figure 3, A and

E). The latter was consistent with the findings that AAV vectors can be transported retrogradely to the entorhinal cortex neurons by their axons in the molecular layer of the dentate gyrus (perforant path) (Kaspar *et al.*, 2002). This pattern of expression ensured that exclusively excitatory synapses onto the CCK basket cells were activated by blue light illumination of the entire slice. Such selective stimulation of excitatory inputs would not be possible without optogenetic approach.

To activate ChR2, we used a 400 μm core optical fiber connected to a 460 nm wavelength LED light source, and placed it on the apex of the dentate gyrus, above the molecular layer (a schematic drawing of the experimental setup is depicted in Figure 3B). We then recorded from CCK-basket cells in voltage-clamp configuration at -70 mV. Two brief light stimulations, 1–2 ms duration and 50 ms inter-stimulation-interval (ISI), could reliably and efficiently generate action potentials in ChR2-positive cells (Figure 4A, top) and evoke synaptic currents (light-evoked excitatory post-synaptic currents, leEPSCs) in the post-synaptic CCK basket cells. All recorded paired leEPSCs exhibited PPF (Figure 4A, bottom). Application of 1 M NPY (Figure 4B) caused more pronounced decrease in the amplitude of the first leEPSC (by 22.3 %

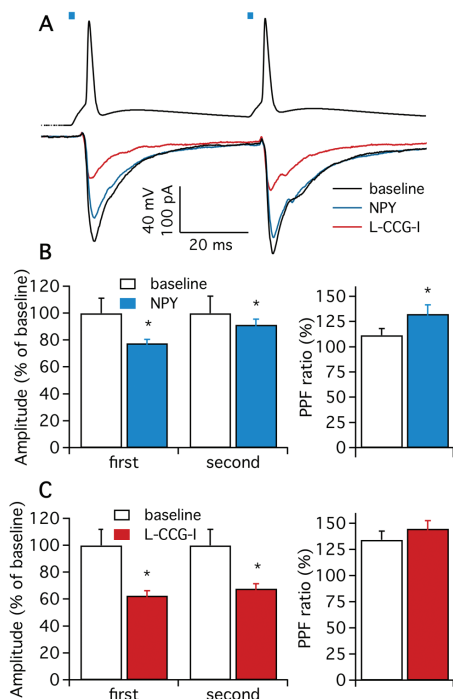


Figure 4. Effects of NPY on light-evoked EPSCs recorded from CCK-basket cells.

A, top, representative trace (average of 16) showing the action potentials evoked by two paired 1 ms blue light pulses with 50 ms ISI in a Chr2-positive granule cell (blue lines on top indicate the moment of light stimulation); **bottom,** representative post-synaptic responses (average of 16) to blue light stimulations recorded in a CCK-basket cell in the presence of 100 μ M PTX, during baseline (black trace), after NPY application (blue trace), and after application of 10 μ M L-CCG-I (red trace). Action potentials and post-synaptic responses were not recorded simultaneously. **B, left,** mean amplitude of light-evoked EPSCs (leEPSCs). Both the first and second response of the pair were significantly reduced by application of NPY (blue bars) compared to baseline (white bars) (* P <0.05); **right,** the PPF ratio was significantly increased after NPY application (* P <0.05). **C, Subsequent L-CCG-I application (red bars) further decreased the amplitude of leEPSCs (left, * P <0.05), but left the PPF ratio unchanged (right, P >0.05).**

from baseline, $n=13$, $P=0.0001$, two-tailed Student's paired t -test) than of the second one (by 8.4 % from baseline, $n=13$, $P=0.047$, two-tailed Student's paired t -test), resulting in increase of the PPF (from 111.7 ± 6.7 % before to 132.7 ± 9.3 % after NPY application, $n=13$, $P=0.002$, two-tailed Student's paired t -test). NPY application did not affect the

ability of Chr2 to induce action potentials in the pre-synaptic cells by light illumination ($n=6$, $P>0.05$, two-tailed Student's paired t -test, data not shown). These results indicate overall decreased Pr of glutamate release from afferent synapses of CCK basket cells.

To evaluate the relative contribution of granule cell mossy fiber-related excitatory inputs in the gross leEPSCs recorded in CCK-basket cells, we subsequently applied the selective mGluR II agonist L-CCG-I, which can suppress glutamate release selectively in mossy fibers of mice (Kokaia *et al.*, 1998; Armstrong *et al.*, 2002; Marchal & Mulle, 2004). The amplitude of both the first and the second leEPSCs of the pair was markedly decreased by L-CCG-I application (62.7 ± 3.7 % of baseline for the first response, $P<0.001$, and 68.0 ± 3.7 % for the second, $P<0.001$, $n=11$, two-tailed Student's paired t -test, Figure 4C) but the PPF ratio was unaltered (134.3 ± 8.4 % before and 144.8 ± 7.7 % after NPY application, $n=11$, $P=0.19$, two-tailed Student's paired t -test), indicating that mossy fiber contribution to the total leEPSCs was approximately 35%.

NPY decreases the frequency of spontaneous and miniature IPSCs onto CCK-basket cells

Next we investigated whether NPY can modulate inhibitory synaptic transmission onto CCK-basket cells in hyper-excitable hippocampus. We started by recording spontaneous IPSCs in voltage-clamp configuration at -70 mV with NBQX and D-AP5 in the perfusion solution to block AMPA and NMDA glutamate receptors and isolate GABAergic transmission. Figure 5A shows representative traces of sIPSCs recordings, before and after NPY application. The mean frequency of sIPSCs was significantly decreased by application of NPY (from 5.9 ± 0.9 Hz before to 3.9 ± 0.8 after NPY application, $n=9$, $P=0.046$, two-tailed Student's paired t -test, Figure 5B left) but the mean amplitude was not affected (56.5 ± 6.4 pA before and 58.1 ± 5.7 pA after NPY application, $n=9$, $P=0.54$, two-tailed Student's paired t -test, Figure 5B right). The K -S analysis of cumulative fraction confirmed that the sIPSC frequency was significantly decreased (as shown by the increase of IELs, $n=9$, $P<0.001$, K -S test, Figure 5C), while the amplitudes were not changed (Figure 5D, $n=9$, $P>0.01$, K -S test).

To determine whether this effect of NPY was attributable to decrease in action potential firing of presynaptic GABAergic interneurons synapsing on

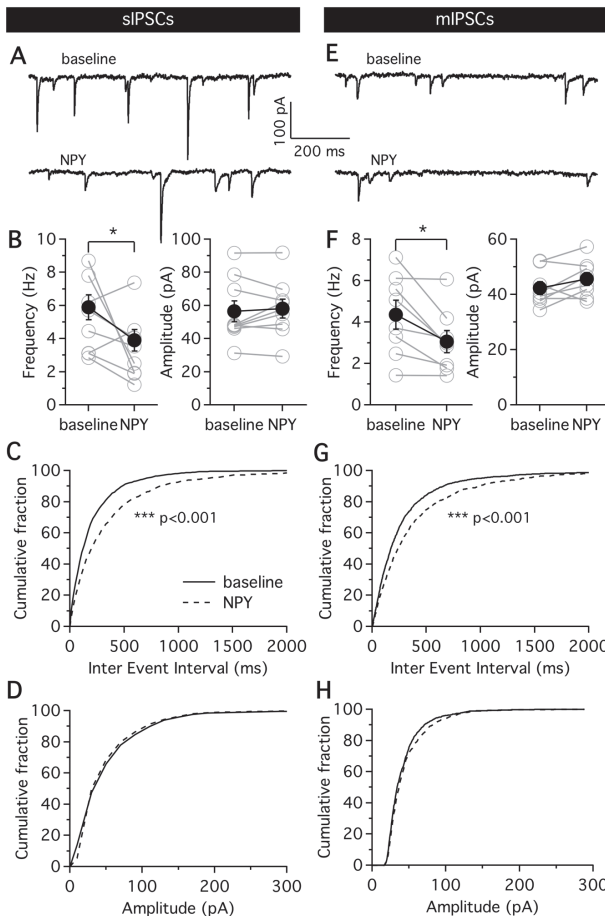


Figure 5. NPY reduces the frequency of sIPSCs and mIPSCs recorded from CCK-basket cells.

A, Representative traces showing sIPSCs recorded during baseline (*top*) and after NPY application (*bottom*). **B**, The mean frequency of sIPSCs was significantly decreased by NPY application (*left*, $*P < 0.05$), but the amplitude was not affected (*right*, $P > 0.05$). Grey lines and open circles represent individual recordings, black lines and solid circles represent mean values. **C**, Cumulative fraction analysis showing an increase in the IELs of sIPSCs after NPY application (*dashed line*) compared to baseline (*solid line*, $***P < 0.001$). **D**, Amplitudes of sIPSCs were not affected ($P > 0.01$). **E**, Representative traces of mIPSCs recorded in the presence of 1 μ M TTX during baseline (*top*) and after NPY application (*bottom*). Notice the lower frequency and smaller amplitudes of mIPSCs compared to sIPSCs in **A**. **F**, NPY application significantly decreased the mean frequency of mIPSCs (*left*, $*P < 0.05$), but did not affect the mean amplitude (*right*, $P > 0.05$). **G**, Cumulative fraction analysis confirming the observed decrease in mIPSCs frequency after NPY application (increase of IELs, $***P < 0.001$), while amplitudes were not affected (**H**, $P > 0.01$).

CCK-basket cells, we blocked action potentials by adding TTX in the perfusion solution and recorded miniature IPSCs in CCK basket cells (Figure 5E, note the smaller amplitudes of mIPSCs compared to sIPSCs in Figure 5A). In these conditions, NPY application still decreased the frequency of mIPSCs (from 4.3 ± 0.7 Hz before to 3.0 ± 0.5 Hz after NPY application, $n=8$, $P=0.017$, two-tailed Student's paired t -test, Figure 5F left) without affecting the mIPSC amplitudes (42.3 ± 2.3 pA before and 45.5 ± 2.3 pA after NPY application, $n=8$, $P=0.23$, two-tailed Student's paired t -test, Figure 5F right). The K -S analysis of cumulative fraction confirmed these results (Figures 5G and H).

Taken together, these data suggest that NPY

decreases pre-synaptic release of GABA, independently from action potentials, in afferent GABAergic synapses of CCK-basket cells.

NPY preferentially affects peri-somatic inhibitory synapses onto CCK-basket cells
CCK-basket cells receive inhibitory afferents from several different classes of GABAergic interneurons, including other CCK-basket cells, PV-positive basket cells and Calretinin-positive interneuron-specific interneurons (CR-IS), at synapses across the entire dendritic tree (Nunzi *et al.*, 1985; Freund & Buzsaki, 1996; Gulyas *et al.*, 1996). The NPY-mediated decrease in the frequency of sIPSCs and mIPSCs described above does not indicate whether peri-somatic or distal dendritic inhibitory synapses

are differentially modulated by NPY. Peri-somatic inhibitory synapses are thought to exert much stronger control over the ability of neurons to generate action potentials due to spatial shunting of excitatory currents originating mostly from the remote dendritic tree. Therefore, preferential modulation of peri-somatic inhibitory synapses by NPY would have stronger consequences for ability of the CCK basket cells to generate action potentials. To address this question, we analyzed relative contribution of spontaneous and miniature IPSCs with fast and slow rise-time kinetics to the overall inhibitory drive onto the CCK basket cells. Assuming that all IPSCs are generated by GABA_A receptors which have similar activation-deactivation kinetics, and that GABA release kinetics in the synapses are also similar, a faster rise time of IPSCs would indicate that the current is generated by peri-somatic inhibitory synapses

close to the recording electrode (placed on the cell soma), while a slower rise time of IPSCs would indicate dendritic localization farther away from the electrode (e.g. distal apical dendrites) (Kobayashi & Buckmaster, 2003). Frequency distribution histograms for sIPSCs indicated that the percentage of events with fast rise times (10-90 %) were markedly decreased by NPY application (Figure 6A), while for mIPSCs the curves for baseline and NPY application appeared largely overlapping (Figure 6B). Quantitative K-S analysis of cumulative fraction showed that both sIPSC and mIPSC rise-times were significantly increased after NPY application compared to baseline (Figure 6C and 6D, $n=9$ for sIPSCs and $n=8$ for mIPSCs, $P<0.001$, *K-S test*), indicating that NPY might

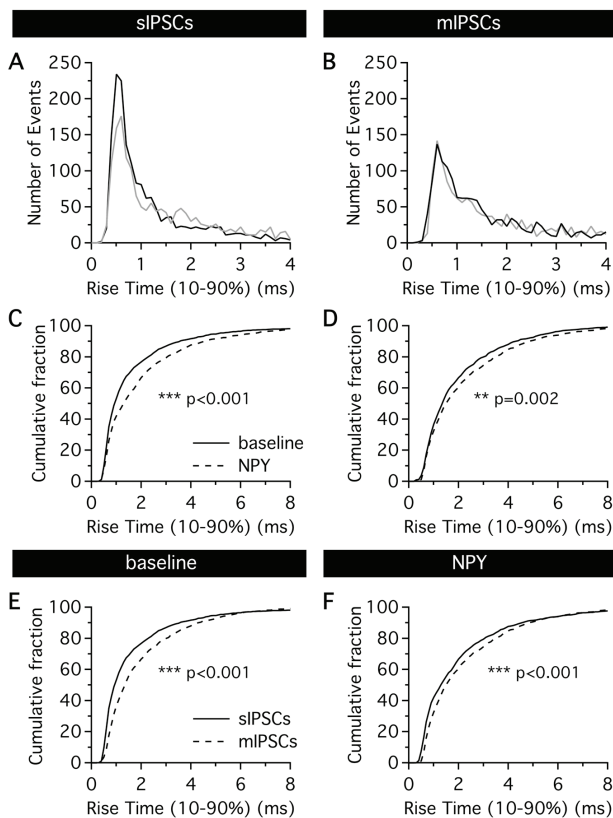


Figure 6. NPY preferentially acts on peri-somatic inhibitory synapses onto CCK-basket cells.

A-B, Frequency distribution histograms of sIPSCs (**A**) and mIPSCs (**B**), before and after NPY application. NPY (gray traces) decreased the number of sIPSCs with fast rise time values compared to baseline (black traces), but curves for mIPSCs are largely overlapping. Also, notice the smaller peak during baseline in **B** compared to **A**. **C-D,** Cumulative fraction analysis reveals that rise time values of both sIPSCs (**C**, *** $P<0.001$) and mIPSCs (**D**, ** $P<0.001$) are significantly increased by NPY application. **E-F,** mIPSCs (gray traces) are significantly slower than sIPSCs (black traces), as indicated by larger rise time values, both during baseline (**E**, *** $P<0.001$) and after NPY application (**F**, *** $P<0.001$).

preferentially act on peri-somatic afferent inhibitory synapses of the CCK-basket cells. The detailed analysis also revealed that rise-times of mIPSCs were slower than sIPSCs (notice the smaller peak during baseline in Figure 6C compared to the same peak in Figure 6A, black traces). Comparison of rise time values of sIPSCs and mIPSCs confirmed that mIPSCs were significantly slower, both during baseline conditions (Figure 6E, $n=9$ for sIPSCs and $n=8$ for mIPSCs, $P<0.001$, *K-S test*) and after NPY

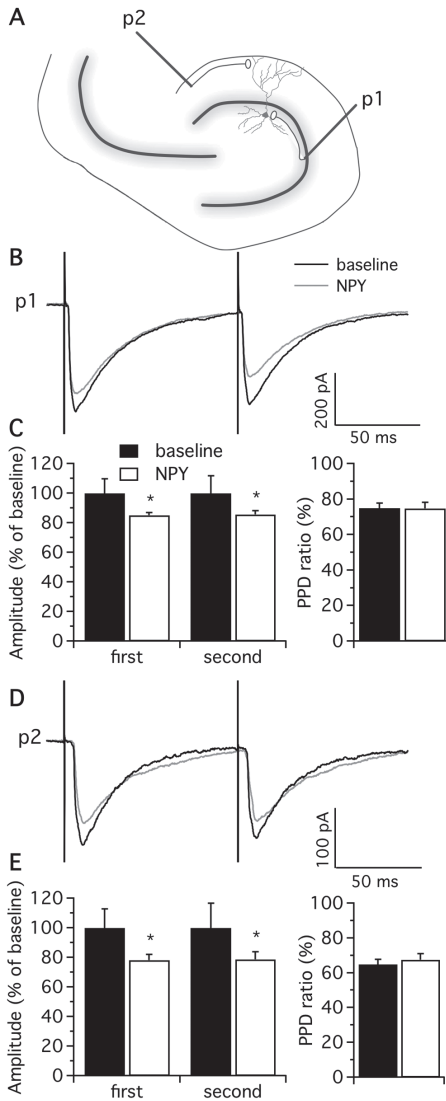


Figure 7. NPY decreases the amplitude of peri-somatic and dendritic stimulation-induced IPSCs.

A, Schematic illustration of the experimental setup. Bipolar stimulating electrodes were placed in the granule cell layer (GCL, p1), to activate peri-somatic inhibitory synapses, and in the outer molecular layer (OML, p2), to activate dendritic inhibitory synapses, while recording from CCK-basket cells in the presence of 5 μ M NBQX and 50 μ M D-AP5. Paired pulses were delivered in both pathways with 100 ms ISI. **B**, Representative traces (average of 16) showing paired post-synaptic responses evoked by p1 stimulation, during baseline (black trace) and after NPY application (grey trace). **C**, Left, the amplitudes of both responses of the pair were significantly decreased by NPY application (white bars, * $P < 0.05$) compared to baseline (black bars); right, PPD ratio was unchanged ($P > 0.05$). **D**, Representative traces (average of 16) showing paired responses evoked by p2 stimulation, during baseline (black trace) and after application of NPY (grey trace). **E**, Application of NPY significantly decreased the amplitude of both the first and the second responses of the pair (left, * $P < 0.05$), but the PPD ratio was not altered (right, $P > 0.05$).

NPY decreases the amplitude of stimulation-evoked IPSCs

Since the data described above suggest that NPY predominantly affects peri-somatic inhibitory synapses onto CCK-basket cells, we explored whether NPY was able to act also on distal/dendritic inhibitory synapses. To address this question, we placed stimulating electrodes in the granule cell layer (GCL, p1) of the dentate gyrus to stimulate peri-somatic inhibitory afferent fibers to CCK-basket cells, and in the outer molecular layer (OML, p2) to stimulate distal dendritic afferent fibers (a schematic illustration of the experimental setup is depicted in Figure 7A). In the presence of NBQX and D-AP5 to block glutamate receptors and isolate monosynaptic GABAergic transmission, paired stimulations with 100 ms ISI were delivered in both pathways, eliciting paired IPSCs, which expressed PPD (representative traces are shown in Figure 7B and 7C). Application of NPY caused a significant and proportional decrease in the amplitude of IPSC pairs (for GCL stimulation, 85.2 ± 1.7 % of baseline for the first response, $P = 0.018$, and 85.5 ± 2.7 % of baseline for the second response, $P = 0.031$, Figure 7C left, $n = 11$; for OML stimulation, 78.2 ± 3.8 % of baseline for the first response, $P = 0.001$, and 78.6 ± 5.0 % of baseline for the second response, $P = 0.011$, Figure 7E left, $n = 10$; two-tailed Student's paired t -test). The PPD ratio was not altered (for GCL stimulation, 74.9 ± 2.7 % during baseline and 74.8 ± 3.5 % after NPY application, $n = 11$, $P = 0.98$, two-tailed Student's paired t -test, Figure 7C right; for OML stimulation, 67.9 ± 4.9 % during baseline and $67.9 \pm$

application (Figure 6F, $n = 9$ for sIPSCs and $n = 8$ for mIPSCs, $P < 0.001$, K - S test), suggesting that those inhibitory interneurons, which form peri-somatic synapses on CCK basket cells, are relatively more spontaneously active. Taken together, these data suggest that in the hyper-excitable hippocampus NPY primarily acts on those inhibitory synapses that are close to the cell soma of CCK-basket cells compared to those on the dendrites.

5.3 % after NPY application, $n=10$, $P=0.99$, two-tailed Student's paired t -test, Figure 7E right). The analysis of the rise times (10–90%) of the stimulation-evoked IPSCs revealed that the mean rise time of GCL-evoked IPSCs was significantly faster compared to that of OML-evoked IPSCs (for GCL stimulation, 4.7 ± 0.7 ms for the first response of the pair and 4.7 ± 0.6 ms for the second response, $n=11$; for OML stimulation, 7.0 ± 0.9 ms for the first response and 6.8 ± 1.2 ms for the second response, $n=10$; $P<0.05$ in both cases, two-tailed Student's t -test, data not shown), confirming the spatial segregation of two different sets of afferent inhibitory synapses on CCK-basket cells (peri-somatic and dendritic, respectively) activated by this particular stimulation paradigm.

Y2 receptor expression is up-regulated after recurrent seizures

One possible explanation for the preferential action of NPY on peri-somatic inhibitory afferent synapses of CCK basket cells could be a re-distribution of presynaptic NPY receptors in these terminals caused by hyper-excitable conditions of the hippocampus. Between the three NPY receptors highly expressed in the hippocampus (Y1, Y2 and Y5), we chose to study the distribution of Y2 receptors, that we have previously shown to be involved in the regulation of inhibitory synapses onto CCK-basket cells by NPY (Ledri *et al.*, 2011).

We performed immunohistochemistry for Y2 receptor distribution in slices from hyper-excitable animals and age-matched controls, and analyzed the immunoreactive fiber density in the inner and outer molecular layers of the dentate gyrus. Representative immunostainings of slices from both groups are shown in Figure 8A and 8B. Immunoreactive fiber density (optical densitometry) analysis revealed that Y2 expression in hyper-excitable animals was significantly increased in the inner molecular layer of the dentate gyrus (34.6 ± 3.2 A.U. in the normal, $n=14$, and 60.2 ± 8.6 A.U. in the kindling animals, $n=11$, corresponding to an increase of 74.0 ± 12.0 %, Figure 8C IML; $P<0.001$, two-tailed Student's t -test). Overall Y2 expression was lower in the outer molecular layer of the control animals, and the increase tended to be slightly less pronounced in hyper-excitable animals (19.6 ± 1.5 A.U. in normal, $n=14$, and 33.7 ± 2.4 A.U. in kindled animals, $n=11$, corresponding to 71.5 ± 10.2 % increase, Figure 8C OML; $P<0.001$, two-tailed Student's t -test). Comparisons between the reference optical density values measured in the fimbria showed no difference

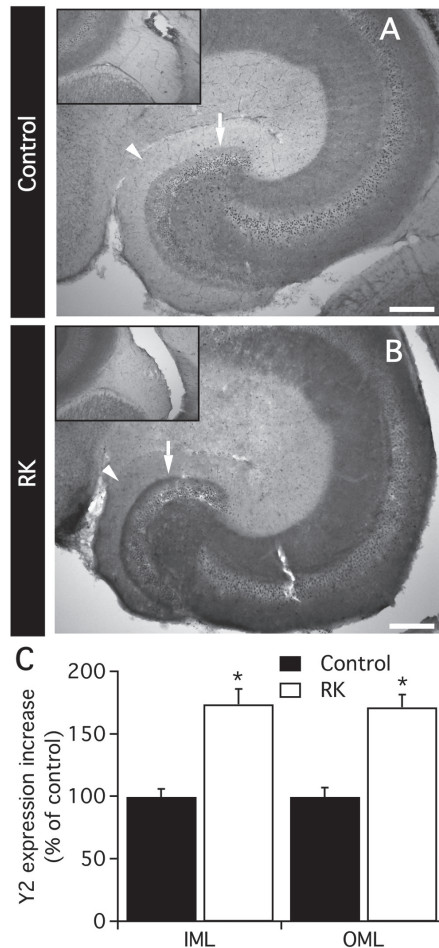


Figure 8. Y2-immunopositive fiber density is increased in the hyper-excitable hippocampus.

A–B, Microphotographs showing the distribution of Y2-positive fibers in the hippocampus of a control (**A**) and an animal that has been subjected to rapid kindling (RK, **B**). Arrow is pointing to the inner molecular layer (IML), arrowhead to the outer molecular layer (OML). Insets on top-left show the fimbria, used as reference in the optical density measurements. Scale bar is 100 μ m. **C,** Y2-positive fiber density in RK animals is significantly increased in both IML and OML of the dentate gyrus, compared to age-matched controls (* $P<0.05$).

between the two groups (Figure 8A and 8B, insets, $P>0.05$, two-tailed Student's t -test, data not shown).

Discussion

Here, using optogenetic and two-pathway stimulation approaches, we demonstrate that in hyper-excitable hippocampus, afferent synapses on CCK-basket cells are altered and respond to the excitability modulator neuropeptide Y, by decreased probability of glutamate release and decreased inhibitory drive on peri-somatic area. This effect of NPY may impact action potential generation probability in CCK-basket cells, and thereby downstream inhibition of principal cells.

Generation of hyper-excitable and identification of CCK-basket cells

In this study we explored whether hyper-excitable state of hippocampus alters afferent synapses to CCK-basket cells, which play a major role in modulating frequency oscillations and dentate gyrus excitability. To reveal such possible modifications, we challenged CCK-basket cell afferent synapses by endogenous excitability modulator NPY, which is upregulated in and released from granule cells by seizure activity (Marksteiner *et al.*, 1990; Schwarzer *et al.*, 1998). We induced hyper-excitable state in the hippocampus by exposing animals to a well-established rapid kindling stimulation protocol. The resulted hyper-excitable was assessed by stimulation-induced seizure susceptibility. Four weeks after the initial rapid kindling stimulations, at the time point of electrophysiological investigations, the animals displayed an increase in duration of afterdischarges elicited by threshold stimulations and an increased number of stage 3-5 seizures, which was consistent with previous results (Elmer *et al.*, 1996) demonstrating hyper-excitable.

To identify CCK-basket cells for electrophysiological recordings in GAD65-GFP mice, we used morphological criteria as previously described (Ledri *et al.*, 2011). Electrophysiological and morphological evidence convincingly demonstrated the CCK-basket cell identity of the recorded cells. Cells displayed regular-spiking phenotype and strongly accommodating action potential trains, and the distribution of their axonal process was mostly confined to the granule cell and inner molecular layers, as previously described (Hefft & Jonas, 2005).

Moreover, we have shown earlier that cells selected with these criteria express functional $\alpha 7$ nicotinic acetylcholine receptors and are immunoreactive for CCK (Ledri *et al.*, 2011).

Excitatory input onto CCK-basket cells

Application of NPY decreased the frequency of spontaneous and miniature EPSCs recorded from CCK-basket cells. Changes in the frequency of spontaneous currents, and not in their amplitude, is usually indicative of processes affecting the pre-synaptic site, and therefore suggest NPY-induced decrease of glutamate release in excitatory synapses onto CCK-basket cells. Supporting decreased glutamate release, the PPF ratio of EPSCs induced by optogenetic stimulation of afferents onto CCK-basket cells was increased by application of NPY, indicating a decreased glutamate P_r .

CCK-basket cells receive excitatory inputs from mossy fiber collaterals on their basal dendrites in the hilus, perforant path and associational-commissural fibers (from mossy cells) on their apical dendrites in the molecular layer (Scharfman, 1995; Freund & Buzsaki, 1996). Some inputs also possibly arise from CA3 pyramidal cell axons back-projecting to the dentate gyrus (Scharfman, 2007). Our data show that at least some of these inputs are affected by NPY. Mossy fibers express Y2 receptors, as previously demonstrated by electrophysiology and immunohistochemistry (McQuiston & Colmers, 1996; Stanic *et al.*, 2006), and contribute to approximately 35% of the total excitatory input to CCK-basket cells (Figure 4C). On the other hand, perforant path and associational fibers are thought to lack Y2 receptors, as NPY failed to alter stimulation-induced EPSPs and EPSCs recorded in the granule cell layer and in single granule cells, respectively (Klapstein & Colmers, 1993). However, it is not known whether associational fiber synapses on interneurons differ from those on principle cells. The inner molecular layer, where associational fibers are arriving, do express Y2 receptors (Tu *et al.*, 2006) (Figure 8), therefore it cannot be excluded that NPY may act on these synapses as well.

Inhibitory input to CCK-basket cells

In the present study, NPY reduced the frequency of spontaneous and miniature IPSCs recorded from CCK-basket cells in the hyper-excitable hippocampus. Such changes are attributable to a pre-synaptic site of action (Behr *et al.*, 2002). CCK-basket cells receive inhibitory input on their apical dendrites in the molecular layer, from HICAP and HIPP cells, and peri-somatically from PV- and CCK-basket cells (Nunzi *et al.*, 1985; Freund & Buzsaki, 1996). In addition, they receive inhibitory input in the inner molecular layer from a subtype of

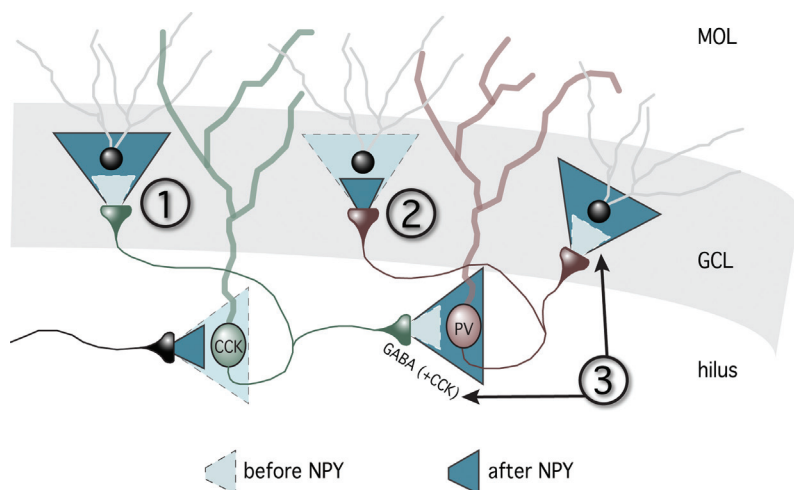


Figure 9. Possible functional implications of NPY effect on CCK-basket cells afferents. Light blue and dashed lines represent baseline conditions, before NPY application. Dark blue and solid lines represent NPY-induced effects. Peri-somatic inhibitory inputs to CCK-basket cells are decreased by NPY application. This effect could result in three different scenarios: 1, GABA release from CCK-basket cells to dentate gyrus granule cells is increased; 2, Increased inhibition of PV-basket cells by CCK-basket cells results in lowered granule cell inhibition by PV-basket cells; 3, Increased CCK release from CCK-basket cells causes depolarization of PV-basket cells and increased synchronization of granule cells.

interneuron-specific interneurons positive for Calretinin (CR-IS) (Gulyas *et al.*, 1996). Y2 receptor immunohistochemistry together with electrophysiological evidence suggests that synapses from CCK-basket cells and from CR-IS cells, both of which terminate in the inner molecular layer, may be affected by NPY, since this region seems to contain more Y2-immunoreactive fibers compared to the outer part of the molecular layer (Figure 8A and 8B). In support, NPY shifted the rise-time values of sIPSCs recorded from CCK-basket cells to slower values. The observed decrease in the frequency of sIPSCs does not seem to be exclusively related to inhibition of HIPP cells by NPY (Paredes *et al.*, 2003), since in our study the effect persisted in the presence of TTX.

Functional implications

CCK-basket cells are proposed to act as fine-tuning devices of network activity, partly due to the variety of modulatory receptors they selectively express. In particular, CCK-basket cells seem to be important in the regulation of learning-related gamma-frequency oscillations, which are thought to be generated by PV-basket cells and have been shown to convert into higher-frequency epileptiform activity (Traub *et al.*, 2005). Taken together, our data support the idea that CCK-basket cells may

play an important role in this frequency conversion. In support of this notion, we demonstrate that afferents to CCK-basket cells in hyper-excitable hippocampus are modulated by NPY, which is upregulated and/or is *de novo* expressed in some neuron populations (see below) by seizure activity, and is one of the most effective modulators of hippocampal excitability.

The hyper-excitable states of the brain, including epilepsy, are associated with massive changes in neuronal networks. Some interneuron subtypes undergo cell death, while synaptic connections to surviving interneurons are rearranged (Bausch, 2005). The expression of NPY and its receptors is also dramatically altered. NPY and Y2 receptor are up-regulated in granule cells, mossy fibers and hilar interneurons (Marksteiner *et al.*, 1990; Schwarzer *et al.*, 1998; Vezzani *et al.*, 1999), while Y1 expression is down-regulated in granule cell dendrites (Kofler *et al.*, 1997). Since NPY acts as a volume transmitter, alterations in its expression and release patterns may change local access of CCK-basket cells to NPY, and thereby change the way they react to NPY released during high-frequency activity. This in turn would influence overall impact of CCK-basket cells on the network, and possibly their modulatory action on network oscillations.

The observed effects of NPY on CCK-basket cell

afferent synapses in the hyper-excitable environment can result in three possible scenarios.

(i) Since peri-somatic inhibitory synapses are strategically located to efficiently control the output of the post-synaptic neuron, the NPY-mediated decrease of peri-somatic inhibitory input onto CCK-basket cells might increase the probability of action potential generation by CCK-basket cells, counteracting the parallel decrease in dendritic excitatory inputs. In case decreased inhibitory perisomatic drive prevails, it will result in increased output (and GABA release) from CCK-basket cells to pyramidal neurons (Figure 9-1). Such action of NPY would favor normalization of increased excitability of the network.

(ii) Inhibitory action on the network excitability exerted by release of GABA may not be the only mechanism by which inhibitory interneurons could regulate epileptiform activity and seizures (Avoli & de Curtis, 2011). Excessive synchrony of certain populations of interneurons, e.g. PV-basket cells, promoted by their highly synchronized GABA release, could support generation of epileptiform discharges. The CCK-basket cell axons are known to target not only granule cells but also PV-basket cells (Karson *et al.*, 2009). Therefore, increased inhibitory influence of CCK-basket cells on PV-basket cells due to NPY action would diminish PV-basket cells contribution in synchronizing pyramidal cell ensembles (Figure 9-2). This could be an additional NPY-related mechanism by which CCK-basket cells would counteract development of high-frequency epileptiform activity.

Another alternative scenario could be envisaged in relation to release of CCK from CCK-basket cells during high frequency activity in the hippocampus (Ghijssen *et al.*, 2001). In CA1, CCK has been shown to depolarize PV-basket cells, and increase their synchronizing impact onto CA1 pyramidal cells (Foldy *et al.*, 2007). Similarly, CCK has been shown to increase firing of hilar interneurons (Deng & Lei, 2006). In this scenario, higher probability of CCK-basket cell activation induced by NPY may lead to increased release of CCK, which consequently would depolarize PV-basket cells. This in turn could promote granule cell synchronization and development of epileptiform activity (Figure 9-3). Finally, further studies are needed to explore whether altered synaptic responsiveness of CCK-basket cells to NPY in hyper-excitable states is a *cause* or an *adaptive* response of the network to the hyper-excitability.

References

- Armstrong, J.N., Brust, T.B., Lewis, R.G. & MacVicar, B.A. (2002) Activation of presynaptic P2X7-like receptors depresses mossy fiber-CA3 synaptic transmission through p38 mitogen-activated protein kinase. *J Neurosci*, **22**, 5938-5945.
- Avoli, M. & de Curtis, M. (2011) GABAergic synchronization in the limbic system and its role in the generation of epileptiform activity. *Prog Neurobiol*, **95**, 104-132.
- Bausch, S.B. (2005) Axonal sprouting of GABAergic interneurons in temporal lobe epilepsy. *Epilepsy & behavior: E&B*, **7**, 390-400.
- Behr, J., Gebhardt, C., Heinemann, U. & Mody, I. (2002) Kindling enhances kainate receptor-mediated depression of GABAergic inhibition in rat granule cells. *Eur J Neurosci*, **16**, 861-867.
- Bischofberger, J., Engel, D., Li, L., Geiger, J.R. & Jonas, P. (2006) Patch-clamp recording from mossy fiber terminals in hippocampal slices. *Nat Protoc*, **1**, 2075-2081.
- Boyden, E.S., Zhang, F., Bamberg, E., Nagel, G. & Deisseroth, K. (2005) Millisecond-timescale, genetically targeted optical control of neural activity. *Nature neuroscience*, **8**, 1263-1268.
- Brager, D.H., Luther, P.W., Erdelyi, F., Szabo, G. & Alger, B.E. (2003) Regulation of exocytosis from single visualized GABAergic boutons in hippocampal slices. *J Neurosci*, **23**, 10475-10486.
- Cobb, S.R., Buhl, E.H., Halasy, K., Paulsen, O. & Somogyi, P. (1995) Synchronization of neuronal activity in hippocampus by individual GABAergic interneurons. *Nature*, **378**, 75-78.
- Colmers, W.F., Lukowiak, K. & Pittman, Q.J. (1987) Presynaptic action of neuropeptide Y in area CA1 of the rat hippocampal slice. *J Physiol*, **383**, 285-299.
- Deng, P.Y. & Lei, S. (2006) Bidirectional modulation of GABAergic transmission by cholecystokinin in hippocampal dentate gyrus granule cells of juvenile rats. *J Physiol*, **572**, 425-442.
- Elmer, E., Kokaia, M., Kokaia, Z., Ferencsik, I. & Lindvall, O. (1996) Delayed kindling development after rapidly recurring seizures: relation to mossy fiber sprouting and neurotrophin, GAP-43 and dynorphin gene expression. *Brain Res*, **712**, 19-34.
- Eslamboli, A., Georgievska, B., Ridley, R.M., Baker, H.F., Muzyczka, N., Burger, C., Mandel, R.J., Annett, L. & Kirik, D. (2005) Continuous low-level glial cell line-derived neurotrophic factor delivery using recombinant adeno-associated viral vectors provides neuroprotection and induces behavioral recovery in a primate model of Parkinson's disease. *J Neurosci*, **25**, 769-777.
- Ferezou, I., Cauli, B., Hill, E.L., Rossier, J., Hamel, E. & Lambolez, B. (2002) 5-HT₃ receptors mediate serotonergic fast synaptic excitation of neocortical vasoactive intestinal peptide/cholecystokinin interneurons. *J Neurosci*, **22**, 7389-7397.
- Foldy, C., Lee, S.Y., Szabadics, J., Neu, A. & Soltesz, I. (2007) Cell type-specific gating of perisomatic inhibition by cholecystokinin. *Nature neuroscience*, **10**, 1128-1130.
- Freedman, R., Wetmore, C., Stromberg, I., Leonard, S. & Olson, L. (1993) Alpha-bungarotoxin binding to hippocampal interneurons: immunocytochemical characterization and effects on growth factor expression. *J Neurosci*, **13**, 1965-1975.
- Freund, T.F. (2003) Interneuron Diversity series: Rhythm and mood in perisomatic inhibition. *Trends Neurosci*, **26**, 489-

- 495.
- Freund, T.F. & Buzsaki, G. (1996) Interneurons of the hippocampus. *Hippocampus*, **6**, 347-470.
- Freund, T.F. & Katona, I. (2007) Perisomatic inhibition. *Neuron*, **56**, 33-42.
- Ghijzen, W.E., Leenders, A.G. & Wiegant, V.M. (2001) Regulation of cholecystokinin release from central nerve terminals. *Peptides*, **22**, 1213-1221.
- Gruber, B., Greber, S., Rupp, E. & Sperk, G. (1994) Differential NPY mRNA expression in granule cells and interneurons of the rat dentate gyrus after kainic acid injection. *Hippocampus*, **4**, 474-482.
- Gulyas, A.I., Hajos, N. & Freund, T.F. (1996) Interneurons containing calretinin are specialized to control other interneurons in the rat hippocampus. *The Journal of neuroscience : the official journal of the Society for Neuroscience*, **16**, 3397-3411.
- Hefft, S. & Jonas, P. (2005) Asynchronous GABA release generates long-lasting inhibition at a hippocampal interneuron-principal neuron synapse. *Nature neuroscience*, **8**, 1319-1328.
- Karson, M.A., Tang, A.H., Milner, T.A. & Alger, B.E. (2009) Synaptic cross talk between perisomatic-targeting interneuron classes expressing cholecystokinin and parvalbumin in hippocampus. *J Neurosci*, **29**, 4140-4154.
- Kaspar, B.K., Erickson, D., Schaffer, D., Hinh, L., Gage, F.H. & Peterson, D.A. (2002) Targeted retrograde gene delivery for neuronal protection. *Mol Ther*, **5**, 50-56.
- Katona, I., Sperlagh, B., Sik, A., Kafalvi, A., Vizi, E.S., Mackie, K. & Freund, T.F. (1999) Presynaptically located CB1 cannabinoid receptors regulate GABA release from axon terminals of specific hippocampal interneurons. *J Neurosci*, **19**, 4544-4558.
- Klapstein, G.J. & Colmers, W.F. (1993) On the sites of presynaptic inhibition by neuropeptide Y in rat hippocampus in vitro. *Hippocampus*, **3**, 103-111.
- Kobayashi, M. & Buckmaster, P.S. (2003) Reduced inhibition of dentate granule cells in a model of temporal lobe epilepsy. *The Journal of neuroscience : the official journal of the Society for Neuroscience*, **23**, 2440-2452.
- Kofler, N., Kirchmair, E., Schwarzer, C. & Sperk, G. (1997) Altered expression of NPY-Y1 receptors in kainic acid induced epilepsy in rats. *Neurosci Lett*, **230**, 129-132.
- Kokaia, M., Asztely, F., Olofsson, K., Sindreu, C.B., Kullmann, D.M. & Lindvall, O. (1998) Endogenous neurotrophin-3 regulates short-term plasticity at lateral perforant path-granule cell synapses. *J Neurosci*, **18**, 8730-8739.
- Ledri, M., Sorensen, A.T., Erdelyi, F., Szabo, G. & Kokaia, M. (2011) Tuning afferent synapses of hippocampal interneurons by neuropeptide Y. *Hippocampus*, **21**, 198-211.
- Marchal, C. & Mulle, C. (2004) Postnatal maturation of mossy fibre excitatory transmission in mouse CA3 pyramidal cells: a potential role for kainate receptors. *J Physiol*, **561**, 27-37.
- Marksteiner, J., Ortler, M., Bellmann, R. & Sperk, G. (1990) Neuropeptide Y biosynthesis is markedly induced in mossy fibers during temporal lobe epilepsy of the rat. *Neurosci Lett*, **112**, 143-148.
- McQuiston, A.R. & Colmers, W.F. (1996) Neuropeptide Y2 receptors inhibit the frequency of spontaneous but not miniature EPSCs in CA3 pyramidal cells of rat hippocampus. *J Neurophysiol*, **76**, 3159-3168.
- Miles, R., Toth, K., Gulyas, A.I., Hajos, N. & Freund, T.F. (1996) Differences between somatic and dendritic inhibition in the hippocampus. *Neuron*, **16**, 815-823.
- Monory, K., Massa, F., Egertova, M., Eder, M., Blaudzun, H., Westenbroek, R., Kelsch, W., Jacob, W., Marsch, R., Ekker, M., Long, J., Rubenstein, J.L., Goebels, S., Nave, K.A., Düring, M., Klugmann, M., Wolfel, B., Dodt, H.U., Zieglgansberger, W., Wotjak, C.T., Mackie, K., Elphick, M.R., Marsicano, G. & Lutz, B. (2006) The endocannabinoid system controls key epileptogenic circuits in the hippocampus. *Neuron*, **51**, 455-466.
- Nunzi, M.G., Gorio, A., Milan, F., Freund, T.F., Somogyi, P. & Smith, A.D. (1985) Cholecystokinin-immunoreactive cells form symmetrical synaptic contacts with pyramidal and nonpyramidal neurons in the hippocampus. *J Comp Neurol*, **237**, 485-505.
- Paredes, M.F., Greenwood, J. & Baraban, S.C. (2003) Neuropeptide Y modulates a G protein-coupled inwardly rectifying potassium current in the mouse hippocampus. *Neurosci Lett*, **340**, 9-12.
- Porter, J.T., Cauli, B., Tsuzuki, K., Lambolez, B., Rossier, J. & Audinat, E. (1999) Selective excitation of subtypes of neocortical interneurons by nicotinic receptors. *J Neurosci*, **19**, 5228-5235.
- Racine, R.J. (1972) Modification of seizure activity by electrical stimulation. II. Motor seizure. *Electroencephalogr Clin Neurophysiol*, **32**, 281-294.
- Scharfman, H.E. (1995) Electrophysiological evidence that dentate hilar mossy cells are excitatory and innervate both granule cells and interneurons. *J Neurophysiol*, **74**, 179-194.
- Scharfman, H.E. (2007) The CA3 "backprojection" to the dentate gyrus. *Progress in brain research*, **163**, 627-637.
- Schwarzer, C., Kofler, N. & Sperk, G. (1998) Up-regulation of neuropeptide Y-Y2 receptors in an animal model of temporal lobe epilepsy. *Mol Pharmacol*, **53**, 6-13.
- Somogyi, P. & Klausberger, T. (2005) Defined types of cortical interneurone structure space and spike timing in the hippocampus. *J Physiol*, **562**, 9-26.
- Sorensen, A.T., Nikitidou, L., Ledri, M., Lin, E.J., Düring, M.J., Kanter-Schlifke, I. & Kokaia, M. (2009) Hippocampal NPY gene transfer attenuates seizures without affecting epilepsy-induced impairment of LTP. *Exp Neurol*, **215**, 328-333.
- Stanic, D., Brumovsky, P., Fetisov, S., Shuster, S., Herzog, H. & Hokfelt, T. (2006) Characterization of neuropeptide Y2 receptor protein expression in the mouse brain. I. Distribution in cell bodies and nerve terminals. *J Comp Neurol*, **499**, 357-390.
- Traub, R.D., Pais, I., Bibbig, A., Lebeau, F.E., Buhl, E.H., Garner, H., Monyer, H. & Whittington, M.A. (2005) Transient depression of excitatory synapses on interneurons contributes to epileptiform bursts during gamma oscillations in the mouse hippocampal slice. *J Neurophysiol*, **94**, 1225-1235.
- Tu, B., Jiao, Y., Herzog, H. & Nadler, J.V. (2006) Neuropeptide Y regulates recurrent mossy fiber synaptic transmission less effectively in mice than in rats: Correlation with Y2 receptor plasticity. *Neuroscience*, **143**, 1085-1094.
- Vezzani, A., Sperk, G. & Colmers, W.F. (1999) Neuropeptide Y: emerging evidence for a functional role in seizure modulation. *Trends Neurosci*, **22**, 25-30.
- Ylinen, A., Soltesz, I., Bragin, A., Penttonen, M., Sik, A. & Buzsaki, G. (1995) Intracellular correlates of hippocampal theta rhythm in identified pyramidal cells, granule cells, and basket cells. *Hippocampus*, **5**, 78-90.
- Zucker, R.S. & Regehr, W.G. (2002) Short-term synaptic plasticity. *Annual review of physiology*, **64**, 355-405.

Paper III

Optogenetics reveal enhanced GABA release at afferent perisomatic inhibitory synapses of dentate gyrus granule cells in hyperexcitable hippocampus

Marco Ledri¹, Litsa Nikitidou¹, Marita Grønning Madsen¹, Deniz Kirik², Karl Deisseroth³ and Merab Kokaia¹

¹Experimental Epilepsy Group, Division of Neurology, Wallenberg Neuroscience Centre, Lund University Hospital, Sweden; ²Brain Repair and Imaging in Neural Systems (BRAINS) Unit, Department of Experimental Medical Sciences, Lund University Hospital, Sweden;

³Department of Bioengineering, Department of Psychiatry and Behavioral Sciences, Stanford University, Stanford, USA

Abstract

Perisomatic inhibitory interneurons constitute a class of GABAergic cells specialized in innervating target neurons in the perisomatic area, a region that includes cell soma, proximal dendrites and axon initial segment. The strategic location of their synapses allows them to efficiently control the output and synchronize oscillatory activity of large numbers of principal cells. Two classes of so-called basket cells, PV- and CCK-containing, comprise the most abundant perisomatic interneurons of the hippocampus. PV-basket cells are important for the generation of gamma frequency (30-90 Hz) oscillations, while CCK-basket cells act as fine-tuning devices that modulate hippocampal network activity by conveying information from extrahippocampal afferents. Gamma frequency oscillations can convert into higher frequency epileptiform activity, therefore perisomatic inhibitory cells could play an important role in this process. In addition, recent evidence suggests that perisomatic inhibition provided by PV cells is preserved in conditions where other interneuron subtypes die, such as hyperexcitable states associated with epilepsy, but whether this functions as compensatory or epileptogenic mechanism is still unclear. Here, using selective optogenetic activation of PV cells in the hippocampus, we show that hyperexcitability, induced by rapid kindling stimulations, enhances GABA release from PV cells onto dentate gyrus granule cells. PV-GC synapses did not differ between controls and kindled animals in terms of GABA release probability and sensitivity to neuropeptide Y, one of the major hippocampal excitability modulators. However, when challenged by repetitive high-frequency optogenetic stimulations, PV synapses responded with enhanced GABA release onto granule cells, unveiling a mechanism that might possibly contribute to the generation of the abnormal synchrony and maintenance of epileptic seizures observed in hyperexcitable states and epilepsy.

Introduction

Perisomatic inhibition comprises a variety of different GABAergic cell types that innervate target cells in the region that includes the cell soma, axon initial segment and proximal dendrites. As opposed to dendritic inhibition, which regulates the efficacy and plasticity of incoming glutamatergic inputs, perisomatic inhibition is important for controlling the output of its targets, and the synchrony of large principal cell populations, due to the strategic location of its contacts (Cobb et al., 1995; Miles et al., 1996). The most abundant perisomatic inhibitory GABAergic cell types are the so-called basket cells. There are two major subpopulations of basket cells in the hippocampus, the Parvalbumin (PV-) and the Cholecystokinin (CCK-) containing basket cells (Somogyi and Klausberger, 2005). Although their location and morphology are similar, their electrical

properties and roles in the hippocampal network are remarkably different (Freund and Katona, 2007). PV-basket cells fire high-frequency non-accomodating action potentials, receive three times more local glutamatergic input (Gulyas et al., 1999), release GABA with higher synchrony (Hefft and Jonas, 2005), and are thought to act as clockworks that generate learning-related gamma-frequency (30-90 Hz) oscillations (Freund, 2003), by functioning as an ensemble connected via chemical and electrical synapses (Galarreta and Hestrin, 1999; Traub et al., 2001). On the other hand, CCK-basket cells fire accomodating action potentials, express a variety of modulatory receptors (e. g., 5-HT₃, nicotinic alpha4 and alpha7, and CB1 receptors) (Freedman et al., 1993; Katona et al., 1999; Porter et al., 1999; Ferezou et al., 2002), and are thought to be fine-tuning devices of network activity (Freund, 2003). Since gamma-frequency oscillations have been shown to convert

into higher-frequency epileptiform activity (Traub et al., 2005), in conditions associated with hyperexcitable states, perisomatic inhibitory cell types could play an important role in this process.

The appearance of hyperexcitable states, and epilepsy, is associated with a number of dramatic changes in the network, such as cell death, inflammation, alterations in neurogenesis and synaptogenesis. In particular, hyperexcitable states underlie several changes in the expression of various factors, and especially of powerful endogenous excitability regulators such as neuropeptide Y (NPY). In the hippocampus, the expression of NPY and one of its receptors (Y2) is up-regulated in hilar interneurons, granule cells and mossy-fibers (Marksteiner et al., 1990; Gruber et al., 1994; Schwarzer et al., 1998; Vezzani et al., 1999), while expression of Y1 receptor seem to be down-regulated (Kofler et al., 1997; Gobbi et al., 1998). Moreover, NPY has been shown to modulate neurotransmission at afferents to CCK-basket cells in the dentate gyrus (Ledri et al., 2011), possibly changing the impact CCK-cells have on regulating hippocampal activity, but it remains to be determined whether NPY can directly modulate the output of perisomatic inhibitory cells.

Together with changes in expression of different factors, hyperexcitability is associated with a massive reorganization of inhibitory networks, as various interneuron subtypes undergo cell death and others alter their connectivity (Bausch, 2005). However, recent evidence suggests that perisomatic inhibition provided by PV cells is to some extent preserved. In animal models of epilepsy, a selective reduction in CA1 pyramidal cell innervation from CCK-basket cell, but not from PV-basket cells, has been observed (Wyeth et al., 2010). Similarly, PV-positive axons seem to be preserved in CA1 and dentate gyrus of the human epileptic hippocampus (Wittner et al., 2001; Wittner et al., 2005), suggesting that PV cells might contribute to the generation of abnormal synchrony and maintenance of epileptic seizures.

In this study, we first wanted to determine whether NPY could directly modulate the output from PV cells onto dentate granule cells. Secondly, we aimed to examine whether hyper-excitable conditions affect the strength of inhibition mediated by the whole PV cell ensemble.

Materials and Methods

Animals

For experiments involving expression of Chr2 in PV-positive cells, PV-Cre mice (Hippenmeyer et al., 2005), age of 6–8 weeks at the beginning of the experimental procedures, were used. Control experiments where

the effect of NPY was tested in afferent synapses onto PV-positive cells were conducted in 17–23 days old PV-tdTomato mice, generated by crossing homozygote PV-Cre mice with homozygote CAG-lox-STOP-lox-tdTomato (Ai14) mice (Madisen et al., 2010). All experiments were conducted according to international guidelines on the use of experimental animals, as well as the Swedish Animal Welfare Agency guidelines, and were approved by the local Ethical Committee for Experimental Animals.

Production of recombinant Adeno-Associated Viral vectors

AAV-Ef1a-DIO-ChR2(H134R)-mCherry viral vector production was essentially performed as previously described (Eslamboli et al., 2005), with minor modifications. Briefly, the transfer vector and the packaging plasmid, pDG5, were transfected into 293 cells. Seventy hours after transfection the cells were harvested and lysed using one freeze-thaw cycle. The crude lysate was clarified by centrifugation at 4,500g for 20 minutes and the vector-containing supernatant was purified using a iodixanol gradient and ultracentrifugation (1.5 hours at 350,000g). The virus-containing iodixanol gradient fraction was further purified using an Acrodisc Mustang Q device (Pall Life Sciences, Port Washington, New York). For further concentration, desalting, and buffer exchange, the purified vector suspension was centrifuged in an Amicon Ultra device (Millipore). The AAV vector was produced as serotype 5. The final number of AAV particles was determined using qPCR and was 1.4×10^{13} genomic particles/ml.

Electrode implantation and virus injection

Animals were anesthetized by inhalation of isoflurane (2.5%, Baxter Chemical AB) and fixed onto a stereotaxic frame (David Kopf Instruments, Tujunga, CA). A bipolar stainless steel stimulation/recording electrode (Plastics One, Roanoke, VA) was stereotaxically implanted in the ventral right hippocampus at the following coordinates (in mm): AP -2.9, ML 3.0, DV -3.0. A reference electrode was placed in the temporal muscle. Electrodes were placed into a pedestal (Plastics One Roanoke, VA) and fixed on the skull with dental cement (Kemdent).

In a subset of animals, during the same surgery, AAV-Ef1a-DIO-ChR2(H134R)-mCherry viral vector suspension was injected through a glass capillary in the left hippocampus (contra-lateral to the electrode) at the following coordinates (in mm): AP -3.2, ML -3.1, DV -3.6 and -3.2. 0.5 μ l of viral suspension were injected at 0.1 μ l/minute in each location in the DV plane. The glass pipette was left in place for 5 minutes after each injection, to avoid back-flow of viral particles through the injection tract. Reference points

for stereotaxic surgery were bregma for the AP axis, midline for the ML axis, and dura for the DV axis.

Electrical rapid kindling

At 7 days after electrode implantation and virus injection, the animals were subjected to electrical rapid kindling in the hippocampus, as previously described (Elmer et al., 1996; Sorensen et al., 2009). The individual threshold was determined by delivering stimulations (1 sec train consisting of 1 ms bipolar square wave pulses at 100 Hz) of increasing current in 10 μ A steps until a focal epileptiform afterdischarge (AD) of more than 5 sec duration was detected by electroencephalographic (EEG) recording. During rapid kindling induction, EEG activity was continuously recorded on a MacLab system (ADInstruments, Bella Vista, Australia) for 200 min except during stimulations, which consisted of 40 suprathreshold stimulation trains (10 s, 1 ms square wave pulses at 50 Hz, 400 μ A intensity) separated by 5 min interval between stimulations. Behavioral seizures were scored according to the Racine scale (Racine, 1972): grade 0, arrest, normal behavior; grade 1, facial twitches (nose, lips, eyes); grade 2, chewing, head nodding; grade 3, forelimb clonus; grade 4, rearing, falling on forelimbs; grade 5, imbalance and falling on side or back. Only animals that developed at least 6 stage 3-5 seizures were subsequently used for electrophysiology.

Slice preparation

Four to six weeks after stimulations, animals were briefly anesthetized with isoflurane and decapitated. The head was quickly immersed in chilled sucrose-based cutting solution, containing (in mM): sucrose 75, NaCl 67, NaHCO₃ 26, glucose 25, KCl 2.5, NaH₂PO₄ 1.25, CaCl₂ 0.5, MgCl₂ 7 (pH 7.4, osmolality 305-310 mOsm). The brain was removed and placed in a Sylgard-coated petri dish containing chilled sucrose-based solution, the cerebellum was discarded and the two hemispheres divided using a razor blade. The left hemisphere, contra-lateral to the stimulating electrode, was then positioned lying on the medial side and a "magic-cut" was performed on the dorsal cortex (Bischofberger et al., 2006). The tissue was subsequently glued "magic-cut" side down on a pedestal and transferred to a cutting chamber containing sucrose-based solution maintained at 2-4 °C and constantly oxygenated with carbogen (95% O₂/5% CO₂). Transverse slices of 300 μ m thickness, comprising the hippocampus and entorhinal cortex, were cut on a vibrating microtome (VT1200S, Leica Microsystems, advancing speed was set at 0.05 mm/sec and amplitude at 1.7 mm), and immediately transferred to an incubation chamber containing sucrose-based solution constantly oxygenated with

carbogen (95% O₂/5% CO₂) and maintained at 34 °C in a water bath. Slices were allowed to rest for 30 minutes before being transferred to room temperature and processed for electrophysiology.

Whole-cell patch-clamp electrophysiology

Individual slices were placed in a submerged recording chamber constantly perfused with gassed artificial cerebro-spinal fluid (aCSF) containing, in mM: NaCl 119, NaHCO₃ 26, glucose 25, KCl 2.5, NaH₂PO₄ 1.25, CaCl₂ 2.5 and MgSO₄ 1.3 (pH 7.4, osmolality 305-310 mOsm). The temperature in the recording chamber was maintained at 32-34 °C, unless otherwise noted.

TdTomato-positive cells were visualized under fluorescent light and infrared differential interference contrast microscopy was used for visual approach of the recording pipette.

Recording pipettes (2.5-5 M Ω resistance) were pulled from thick-walled (1.5 mm outer diameter, 0.86 mm inner diameter) borosilicate glass with a Flaming-Brown horizontal puller (P-97, Sutter Instruments, CA), and contained (in mM): K-Gluconate 122.5, KCl 12.5, KOH-HEPES 10, KOH-EGTA 0.2, MgATP 2, Na₃GTP 0.3, NaCl 8 (pH 7.2-7.4, mOsm 300-310) for measurements of spiking patterns in PV-TdTomato-positive cells; Cs-Gluconate 117.5, CsCl 17.5, NaCl 8, CsOH-HEPES 10, CsOH-EGTA 0.2, MgATP 2, Na₃GTP 0.3, QX-314 5 (pH 7.2-7.4, mOsm 300-310) for recordings of spontaneous excitatory post-synaptic currents in dentate gyrus granule cells (sEPSCs); CsCl 135, CsOH 10, CsOH-EGTA 0.2, MgATP 2, Na₃GTP 0.3, NaCl 8, QX-314 5 (pH 7.2-7.4, mOsm 300-310) for light-evoked inhibitory post-synaptic currents recordings (I_{IPSC}s). Biocytin (3-5 mg/ml) was routinely added to the pipette solution on the day of the recording. Recordings typically lasted 20-30 minutes, and biocytin was allowed to diffuse for additional 10 minutes at the end to assure complete diffusion in the axonal arbor of PV-TdTomato-positive cells. Uncompensated series resistance (typically 8-30 M Ω) was constantly monitored via -5 mV voltage steps and recordings were discontinued after changes of >20% or if the resting membrane potential was more positive than -50 mV.

Cells were held at -70 mV in voltage clamp and at 0 pA in current clamp recordings. Firing pattern was investigated by applying a single 1 sec, 500-1000 pA depolarizing current step.

sEPSCs were recorded in the presence of 100 μ M Picrotoxin (PTX, Tocris Bioscience, Ellisville, MI) to block Gamma-aminobutyric acid A (GABA_A) receptors. 50 μ M DL-2-amino-5-phosphonovaleic acid (D-AP5, Tocris) and 5 μ M 2,3-dihydroxy-6-

nitro-7-sulfamoyl-benzo[f]quinoxaline-2,3-dione (NBQX, Tocris) were used during leIPSC recordings to block N-Methyl-D-Aspartate (NMDA) and α -amino-3-hydroxy-5-methylisoxazole-4-propionic acid (AMPA) receptors, respectively.

For leIPSC recordings, a 400 μ m thick optical fiber was positioned above the apex of the dentate gyrus. Light was generated by a 460 nm wavelength LED light source (Prizmatix, Modiin Ilite, Israel) and stimulation of pre-synaptic PV-ChR2-expressing cells was achieved via 1 ms width light pulses. Paired stimulations with 100, 250 and 500 ms Inter Stimulus Interval (ISI) were used to assess paired pulse depression (PPD). Trains of 10 light pulses at 10 and 20 Hz frequency were used to study GABA release efficiency from PV-positive cells ensembles.

NPY (Schafer-N, Copenhagen, Denmark) was dissolved in distilled water, stored in concentrated aliquots, diluted to 1 μ M concentration in the perfusion solution immediately before use and allowed to diffuse in the recording chamber for 7 min before the continuation of the recordings. Silicon-coated tubing and bottles were used to prevent the peptide from adhering to the tubing and container walls. PTX or D-AP5 and NBQX were applied at the end of the experiments to verify that the synaptic currents were generated by respective receptor activation.

Data were sampled at 20 kHz with an EPC-10 amplifier (HEKA Elektronik, Lambrecht, Germany) and stored on a G4 Macintosh computer using PatchMaster software (HEKA) for offline analysis.

Immunohistochemistry and axonal arbor reconstruction

For identifying the cells recorded in this study, slices after electrophysiology were fixed in 4% Paraformaldehyde (PFA) in phosphate buffer (PB) for 12–24 hours and then stored in anti-freeze solution (ethylenglycol and glycerol in PB buffer) at -20°C until processed. For immunohistochemical staining against, mCherry/tdTomato and biocytin, slices were rinsed three times with KPBS and pre-incubated for 1 hour in blocking solution (10% normal donkey serum and 0.25% Triton X-100 in KPBS, T-KPBS). Sections were then incubated overnight with 1:1000 rat anti-mRFP (5F8, Chromotek, Germany) in 5% serum blocking solution, rinsed three additional times in T-KPBS and incubated for 2 hours in Cy3-conjugated donkey anti-rat secondary antibody (1:400, Jackson ImmunoResearch, Suffolk, UK) and Alexa 488-conjugated avidin-D (1:200, Molecular Probes) in 5% serum blocking solution. Slices were finally rinsed three times in KPBS, mounted on coated slides and cover-slipped with DABCO.

For reconstruction of the axonal arborization of

PV-tdTomato-positive neurons, labeled cells were examined with a confocal laser-scanning microscope (Leica). Confocal Z-stacks were obtained along the entire dendritic and axonal tree of the cells.

Data analysis and statistics

For recordings from PV-tdTomato-positive cells, only cells resembling PV basket cells morphology with axonal arborization confined to the granule cell layer/hilus regions were accepted for analysis. For leIPSCs recordings, only granule cells showing mature morphology with apical dendrites extending to the outer molecular layer were accepted. Off-line analysis was performed using FitMaster (HEKA Elektronik), IgorPro (Wavemetrics, Lake Oswego, OR), MiniAnalysis (Synaptosoft Inc., Decatur, GA), and GraphPad Prism (GraphPad software, San Diego, CA) softwares.

Paired-pulse depression was expressed as the ratio between the amplitude of the second and the first response of the pair, in percentage. To quantify GABA release efficiency, traces were averaged and the amplitude of each leIPSC in a train was measured from the baseline directly preceding the rising phase.

Before and after NPY application differences in sEPSCs frequency and amplitude mean values and PPD were assessed with Student's paired t-test. Comparison of PPD and high-frequency stimulation leIPSCs between control and kindled animals were assessed with Student's un-paired t-test. Inter-event-intervals (IEIs) and amplitude of sEPSCs were analysed using MiniAnalysis software and differences between the groups were calculated with cumulative fraction curves combined with Kolmogorov-Smirnov (K-S) test. Events were automatically recognized by the software and included in the analysis if their magnitude was at least 5 times bigger than the calculated average root mean square (RMS) noise. Only the last 150 events before start of NPY application and the first 150 events after equilibration of NPY (7 min after start of NPY application) were included in the analysis. Values are presented as means \pm SEM. Differences are considered significant with $p < 0.05$ for paired t-test and $p < 0.01$ for K-S test.

Results

Expression of ChR2 in PV+ cells

The first objective of the present study was to evaluate whether NPY, a known modulator of excitability and neurotransmitter release in the hippocampus, affects GABA release from PV cells onto dentate gyrus granule cells (GC). The properties of Parvalbumin- to granule cell (PV-GC) synapses have been extensively studied using paired recordings in normal

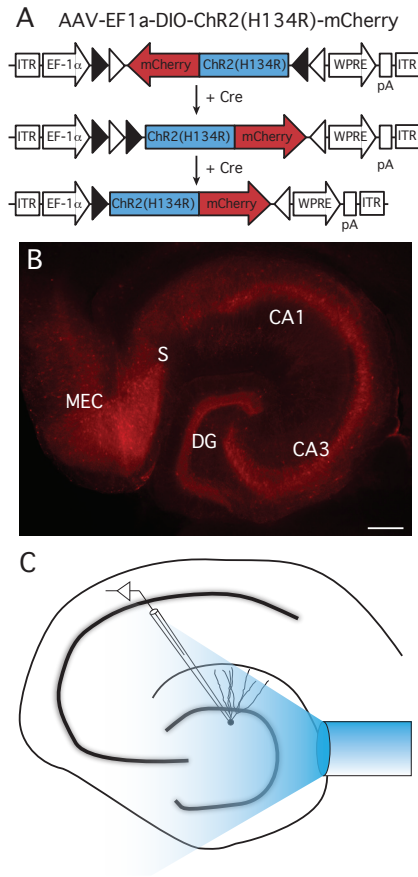


Figure 1. Expression of ChR2(H134R)-mCherry in PV cells and experimental setup.

A, AAV-EF1a-DIO-ChR2(H134R)-mCherry recombination in Cre-expressing cells. In the presence of Cre, ChR2(H134R)-mCherry is inverted in the sense orientation and expressed under the control of the EF1a promoter. ITR, Inverted Terminal Repeats; WPRE, Woodchuck Post-Regulatory Element; pA, poly(A). **B**, ChR2(H134R)-mCherry was highly expressed in all area of the hippocampus; CA, Cornu Ammonis; DG, Dentate Gyrus; MEC, Medial Entorhinal Cortex; S, Subiculum; scale bar is 200 μ m. Note the preferential location of mCherry expression in all hippocampal cell layers. **C**, Schematic experimental setup for lIPSCs recordings. A 400 μ m optical fiber connected to a 460 nm wavelength LED light source was placed above the apex of the dentate gyrus to activate ChR2(H134R)-mCherry expressing cells and fibers, while recordings were performed from granule cells.

(Kraushaar and Jonas, 2000; Hefft and Jonas, 2005), and epileptic animals (Zhang and Buckmaster, 2009). However, PV cells form ensembles via gap junctions that function synergistically to control oscillatory activity of principal cells (Galarreta and Hestrin, 1999). Therefore, more holistic and perhaps more physiological approach would be to explore post-synaptic responses in single granule cells evoked by stimulation of multiple interconnected PV cells at the same time. To achieve this goal, we used an optogenetic approach and expressed ChR2 selectively in PV cells of the hippocampus. ChR2 is a light-sensitive cation channel able to depolarize neuronal membranes with millisecond precision when exposed to ≈ 470 nm blue light (Boyden et al., 2005). To express ChR2 in PV-positive cells, we injected a Cre-dependent Adeno-Associated viral vector (AAV-Ef1a-DIO-ChR2(H134R)-mCherry), carrying a ChR2 variant (H134R) (Nagel et al., 2005) -mCherry fusion construct under the control of the general Elongation Factor 1 alpha (EF1a) promoter, in PV-Cre mice, a strategy previously used in the barrel (Cardin et al., 2009) and infralimbic pre-frontal cortices (Sohal et al., 2009). In the AAV-Ef1a-DIO-ChR2(H134R)-mCherry construct, the direction of the ChR2(H134R)-mCherry transgene is inverted, and flanked by two nested pairs of incompatible lox sites (loxP and lox2722, (Atasoy et al., 2008)). In Cre-expressing cells, the transgene is first reversibly flipped into the sense orientation using either pair of lox sites (Figure 1A), allowing gene expression; subsequently, an irreversible excision occurs between the other lox site pair, preventing further recombination (Figure 1A).

Using two injection sites in the ventral and medial hippocampus, we achieved high level of ChR2(H134R)-mCherry expression in all areas of the hippocampus, including dentate gyrus, CA3 and CA1 (Figure 1B).

PV-GC synapses are not affected by NPY in normal animals

To assess whether NPY affects PV-GC synapses, we recorded from granule cells in the presence of NBQX and D-AP5 to block glutamate receptors and isolate GABAergic synaptic transmission. Granule cells were held in voltage clamp at -70 mV. In order to activate ChR2(H134R)-mCherry expressing PV cells in the slices, we placed an optical fiber above the apex of the dentate gyrus, at a vertical distance of approximately 50 μ m from the tissue, and delivered 1 ms blue light flashes (schematic experimental setup is shown in Figure 1C). In these conditions, paired light pulses with 100 ms Inter Stimulus Interval (ISI) evoked synaptic currents (light-evoked inhibitory

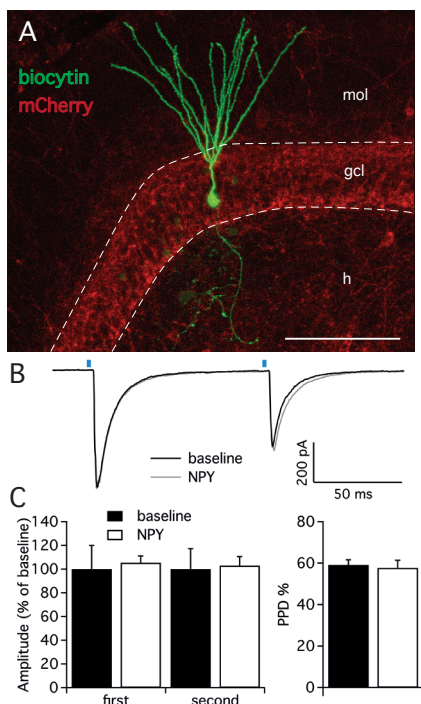


Figure 2. NPY does not alter leIPSCs recorded from granule cells in normal animals.

A, Confocal stacks showing immunostaining against biocytin (green) and mCherry (red). Cells for leIPSCs recordings showed typical mature granule cell morphology. The density of ChR2(H134R)-mCherry fibers was highest in the granule cell layer, preferential location of PV-positive axons. mol, molecular layer; gcl, granule cell layer; h, hilus; scale bar is 100 μm . **B**, Representative traces of leIPSCs recorded from granule cells, before (black trace) and after NPY application (gray trace). Average of 16 consecutive traces. The blue dots represent the time of the light pulse application. **C**, NPY does not affect the amplitudes of leIPSCs (left, $n=5$), and the PPD ratio is unchanged (right).

post-synaptic currents, leIPSCs) in post-synaptic granule cells that exhibited paired-pulse depression (a representative trace is shown in Figure 2B). Application of 1 μM NPY did not alter the amplitude of neither the first ($105.5 \pm 5.7\%$ of baseline, $p>0.05$, Student's paired t-test) nor the second ($103.0 \pm 7.5\%$ of baseline, $p>0.05$, Student's paired t-test) response of the pair (Figure 2C, left). Similarly, the PPD ratio was also unchanged (from $59.2 \pm 2.5\%$ during baseline to $57.7 \pm 3.7\%$ after NPY application, $p>0.05$, Student's paired t-test, Figure 2C, right). Taken together, these data indicate that NPY does not affect peri-somatic

inhibitory synapses from PV cells onto granule cells in the dentate gyrus of normal animals.

NPY decreases sEPSCs recorded from PV-cells. The lack of effect by NPY on PV-GC leIPSCs could be explained by an absence of pre-synaptic NPY receptors on PV terminals, or a low biological activity of the peptide when applied in our recording conditions. It has been previously shown that NPY can decrease the frequency of mossy-fiber mediated spontaneous excitatory post-synaptic currents (sEPSCs) recorded from CA3 pyramidal cells (McQuiston and Colmers, 1996) and CCK-basket cells (Ledri et al., 2011). Since PV cells receive one of their major excitatory inputs from mossy fibers (Blasco-Ibanez et al., 2000), as part of their feedback inhibitory function, we sought to investigate whether NPY could decrease the frequency of sEPSCs recorded from PV cells in the dentate gyrus. To identify PV cells for recordings, we used a transgenic mouse line created by crossing PV-Cre mice with the reporter mouse line CAG-lox-STOP-lox-tdTomato (Ai14) (Madisen et al., 2010). In the resulting offspring, the red fluorescent protein tdTomato is expressed in PV cells, and allows prospective identification of PV cells for electrophysiological recordings. To confirm the identity of the recorded cells, we examined the morphological and electrophysiological properties of PV/tdTomato+ cells. Biocytin staining revealed that the axonal arborization was largely confined to the granule cell layer/hilar regions (Buhl et al., 1994; Hefft and Jonas, 2005) (Figure 3A), and cells responded with high-frequency firing upon depolarization induced by current injection (Figure 3B), confirming the identity of the recorded cells.

We then recorded sEPSCs from PV/tdTomato+ cells in voltage clamp configuration at -70 mV , with PTX in the perfusion solution to block GABAA receptors and isolate glutamatergic synaptic transmission, before and after application of NPY. The mean frequency of sEPSCs was significantly decreased by NPY application (from $8.6 \pm 1.4\text{ Hz}$ during baseline to $6.6 \pm 1.3\text{ Hz}$ after NPY application, $p<0.05$, Student's paired t-test, Figure 3C), but their mean amplitude was not affected ($22.8 \pm 2.6\text{ pA}$ during baseline, $20.1 \pm 3.0\text{ pA}$ after NPY application, $p>0.05$, Student's paired t-test, Figure 3E). The following K-S analysis of cumulative fraction of sEPSCs confirmed that the frequency was decreased (increase of IEL, $p<0.01$, Figure 3D) and the amplitude was unaffected ($p>0.01$, Figure 3F).

These data show that the frequency of sEPSCs recorded from PV cells is decreased by NPY, and demonstrate that the applied peptide is biologically active in our recording conditions.

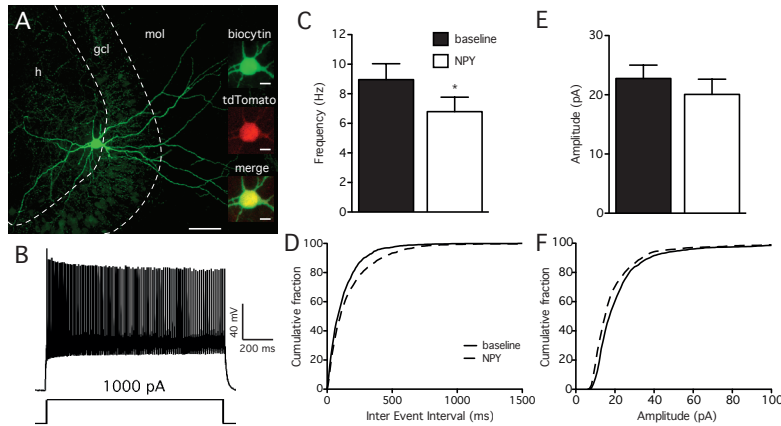


Figure 3. NPY reduces the frequency of sEPSCs recorded from PV cells.

A, Biocytin staining showing the axonal arborization of a PV cell, localized to the granule cell layer and hilus. Insets are showing co-localization (*bottom*) of biocytin (green, *top*) with tdTomato (red, *middle*). Scale bars are 100 μ m and 10 μ m for the insets. **B**, Typical fast-spiking response of a PV cell to a 1 s, 1000 pA depolarizing pulse injected via the patch pipette. **C**, The mean frequency of sEPSCs recorded from PV cells is decreased by NPY application (* $p < 0.05$, $n = 8$). **D**, Cumulative fraction analysis showing an increase in the IELs of sEPSCs after NPY application (*dashed line*) compared to baseline (*solid line*), *** $p < 0.001$, $n = 8$. **E-F**, Mean amplitude and cumulative fraction analysis of sEPSCs amplitudes before and after NPY application do not reveal significant differences.

NPY does not affect PV-GC synapses in hyperexcitable conditions

Since NPY failed to alter PV-GC lEPSCs in normal animals, PV terminals onto granule cells may not express NPY pre-synaptic receptors. However, the expression of NPY and its receptors is highly regulated by seizures and hyperexcitable states, and therefore we hypothesized that PV-GC synapses might become sensitive to NPY in hyperexcitable conditions where NPY receptors are up-regulated. To induce hyperexcitability, we used a well-characterized rapid kindling (RK) protocol, consisting of 40 electrical stimulations, one every five minutes (Elmer et al., 1996; Sorensen et al., 2009), on the same day. During the rapid kindling stimulations, animals developed behavioral seizures ranging from stage 0 to 5, with an average of 13 ± 0.2 stage 3-5 seizures per animal (data not shown). Electrophysiological investigations were performed four weeks later, at the time point where animals have reached the peak of hyperexcitability (Elmer et al., 1996).

We then recorded lEPSCs from granule cells in the hyperexcitable hippocampus, before and after application of NPY. Two brief, 1 ms light pulses with 100 ms ISI evoked large amplitude lEPSCs in granule cells that exhibited PPD (representative traces are shown in Figure 4A). Similarly to what was previously seen in normal animals, application of NPY did not change the amplitude of neither response of

the pair (98.5 ± 3.5 % of baseline for the first response, 97.5 ± 4.7 % for the second response, $p > 0.05$ in both cases, Student's paired t-test, Figure 4B), and did not alter the PPD ratio (from 63.6 ± 2.3 during baseline to 62.5 ± 1.3 after NPY application, $p > 0.05$, Student's paired t-test, Figure 4B).

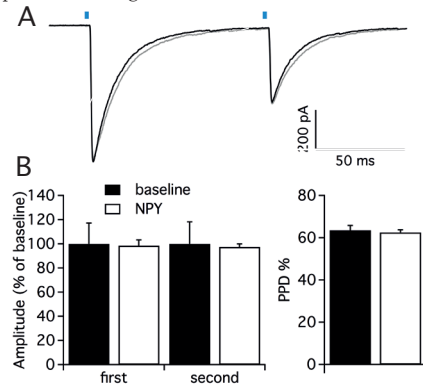


Figure 4. NPY does not affect PV-GC lEPSCs in hyperexcitable animals.

A, Representative traces of lEPSCs recorded from granule cells, before (*black trace*) and after NPY application (*gray trace*). Average of 16 consecutive traces. The blue dots represent the time of the 1 ms light pulse application. **B**, NPY does not affect the amplitudes of lEPSCs (*left*, $n = 8$), and the PPD ratio is unchanged (*right*).

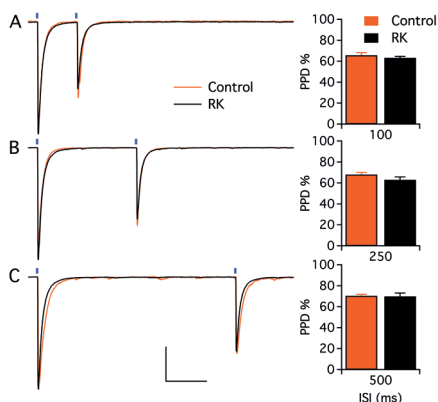


Figure 5. Paired-pulse short-term plasticity at PV-GC synapses is not affected by hyperexcitability.

A-C, Representative traces of leIPSCs evoked by paired blue light stimulation (blue dots) with 100 (*A*), 250 (*B*) and 500 ms (*C*), in control (orange trace) and RK animals (black trace). Traces are average of 16 consecutive responses and normalized to peak amplitudes. *D-F*, the mean PPD ratio at all ISI is not different in control and RK animals ($p > 0.05$, $n = 9$ for controls and $n = 6$ for RK).

These data demonstrate that NPY does not affect PV-GC synapses in hyperexcitable conditions, and indicate that PV terminals onto granule cells might not express pre-synaptic NPY receptors.

Hyper-excitability increases GABA release at PV-GC synapses

The second objective of this study was to investigate whether hyperexcitable conditions alone could alter the properties of PV-GC synapses. We recorded from granule cells in both normal and hyperexcitable animals, and first stimulated pre-synaptic PV cells by paired 1 ms light pulses at 100, 250 and 500 ms ISI (representative traces are shown in Figure 5). Granule cells were held at -70 mV in voltage clamp configuration, in the presence of NBQX and D-AP5 to block glutamate receptors and pharmacologically isolate GABA_A-mediated currents. To investigate short-term plasticity at PV-GC synapses, and more specifically GABA release probability (Pr) (Baldelli et al., 2005), we analyzed the PPD ratio at the different ISI and found no difference between the groups (65.7 ± 2.4 % in control and 63.2 ± 1.4 in RK animals for 100 ms ISI, Figure 5A; 68.1 ± 2.7 in control and 70.4 ± 3.2 in RK animals for 250 ms ISI, Figure 5B; 69.9 ± 1.4 % in control and 70.4 ± 3.2 in RK animals for 500 ms ISI; $p > 0.05$ in all cases, Student's unpaired t-test, Figure 5C).

Since alterations in paired-pulse ratios are a very crude measure of release probability for GABA, and may be

masked by activation of presynaptic GABAB receptors, we sought to adopt repetitive stimulations by trains of pulses, which may reveal changes in GABA release over longer time due to altered release or changes in releasable pool of GABA vesicles. We delivered a train of 10 light pulses at 10 Hz (Figure 6B), and quantified the extent of depression of each response by analyzing the leIPSC_n/leIPSC₁ ratio. We found that the ratio at the 10th stimulation was significantly lower in controls compared to RK animals (28.2 ± 5.9 % in control and 42.9 ± 3.2 in RK animals, $p < 0.05$, Student's unpaired t-test, Figure 6A), but the ratios at all other stimulations were not significantly different ($p > 0.05$, Student's unpaired t-test, Figure 6A). We speculated that increasing the stimulation frequency, and therefore the speed of depression, would unveil and strengthen further differences between the two groups. We then delivered a train of 10 light pulses at 20 Hz (Figure 6D), and found that the leIPSC_n/leIPSC₁ ratio was significantly decreased in control animals compared to RK from the 5th stimulation onwards (34.9 ± 4.2 in control and 43.0 ± 1.9 in RK for leIPSC5/leIPSC1; 35.7 ± 4.4 in control and 44.1 ± 2.6 in RK for leIPSC6/leIPSC1; 26.2 ± 4.2 in control and 40.2 ± 3.7 in RK for leIPSC7/leIPSC1; 25.4 ± 4.8 in control and 40.2 ± 3.0 in RK for leIPSC8/leIPSC1; 25.9 ± 4.6 in control and 39.2 ± 3.1 in RK for leIPSC9/leIPSC1; 23.8 ± 3.8 in control and 38.2 ± 3.1 in RK for leIPSC10/leIPSC1; $p < 0.05$ in all cases, Student's unpaired t-test, Figure 6C).

Taken together, these data indicate increased endurance of GABA release in hyperexcitable states.

Discussion

The main finding of this study shows that synchronous GABA release from the PV cell ensembles onto granule cells is not altered by NPY in the hyperexcitable hippocampus, suggesting that NPY does not directly regulate inhibitory inputs from multiple PV cells to granule cells in these conditions. Of particular interest is though the discovery of increased endurance of GABA release from PV cells in hyperexcitable states of the hippocampus induced by recurrent seizures. Such strengthening of GABA release at high frequency activity may promote synchronization of granule cell – PV cell based oscillations in the dentate gyrus, and thereby contribute to the generation of seizures.

Selective stimulation of PV cells

Here we used an optogenetic approach to selectively and synchronously stimulate PV cells of the hippocampus as an interconnected network, in a way that may represent more a physiological pattern of hippocampal activity. Such approach has been made possible the injection of a Cre-dependent AAV carrying

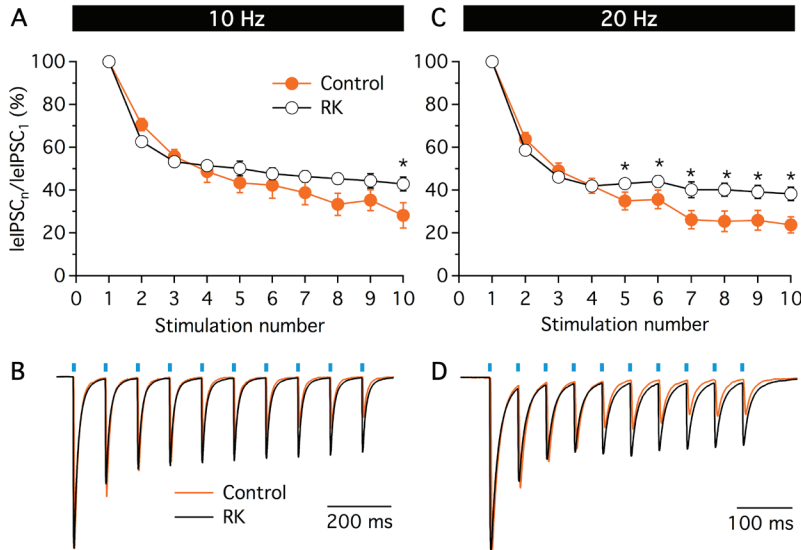


Figure 6. Hyperexcitability reduces the degree of PV-GC leIPSCs depression during sustained stimulation. **A-B,** XY plots summarizing leIPSCs recorded from granule cells evoked by trains of 10 light pulses at 10 (**A**) and 20 Hz (**B**), in control (orange trace) and RK animals (black trace). The ratio between the amplitude of any given response in the train and the first (leIPSC_n/leIPSC₁) is plotted against the response number. The degree of leIPSC depression is reduced in RK animals (**p* < 0.05, *n* = 9 for controls and *n* = 6 for RK). **C-D,** Representative traces showing leIPSCs evoked by trains of light pulses (blue dots) at 10 (**C**) and 20 Hz (**D**), in control (orange trace) and RK (black trace) animals. Traces are averages of 20 consecutive responses and normalized to peak amplitudes.

Chr2 in PV-Cre mice. Two subclasses of perisomatic interneurons express PV in the hippocampus: basket cells and axo-axonic (or chandelier) cells. Basket cells innervate an area comprising the cell soma and proximal dendrites of target cells, while chandelier cells are specialized in innervating the axon initial segment of principal cells. It has been previously shown that the large amplitude inhibitory post-synaptic potentials evoked in pyramidal cells by the stimulation of these two cell types are indistinguishable from each other (Buhl et al., 1994), and that they share similar spiking pattern during gamma oscillations (Tukker et al., 2007) and theta activity (Klausberger et al., 2003) recorded in vivo. However, it has also been reported that GABAergic inputs targeting the axon initial segment have a more depolarized reversal potential compared to those targeting the soma and proximal dendrites (Szabadics et al., 2006). Thus, axo-axonic cells may fulfill a different function as compared to PV-basket cells, but this needs further clarifications. In our experimental conditions, both subclasses express Chr2, since recombination is driven by the PV promoter, and light stimulation would therefore induce action potentials in both basket cells and chandelier cells.

Effects of NPY on PV-GC synapses

Inhibitory post-synaptic currents evoked by optogenetic stimulation of PV cells ensembles recorded from granule cells were not affected by NPY in normal animals, as well as in animals where hyperexcitability was induced by RK. The failure of NPY to affect inhibitory transmission onto granule cells in the normal hippocampus has been described previously (Klapstein and Colmers, 1993), though the relatively unspecific electrical stimulation approach used in the previous studies could have masked possible changes in specific inputs. Here, the optogenetic stimulation of selective PV expressing inhibitory neurons did not reveal any effect of NPY on these synaptic inputs either. Low biological activity of the applied peptide does not seem to be a likely explanation, since NPY could efficiently decrease sEPSCs recorded from PV cells. Therefore, lack of expression of NPY receptors in PV-GC presynaptic terminals could account for the absence of NPY effect. Among all NPY receptors, Y1 and Y2 are the most abundant in the hippocampus, and NPY acting via Y2 receptors have been already shown to modulate GABAergic transmission in the dentate gyrus (Ledri et al., 2011). Although moderate levels of Y2 expression have been demonstrated in

the granule cell layer of the hippocampus (Stanic et al., 2006), the area where most PV cell axons are present, our present data suggest that cell types other than PV might be responsible for Y2 expression, e.g. CCK-basket cells. Nevertheless, despite the fact that NPY does not affect PV-GC synapses directly, its modulation of incoming afferent excitatory synapses onto PV cells might alter their excitability and therefore potentially influence overall inhibition of granule cells.

Hyperexcitability enhances GABA release at PV-GC synapses

The second finding of this study is increased endurance of GABA release from PV-GC synapses in hyperexcitable conditions during high frequency optogenetic stimulations. Some insights on basic release mechanisms of GABA, such as release probability (P_r), can be obtained by measuring the ratio between two responses evoked by paired stimulation with brief (50–800 ms) ISI (Baldelli et al., 2005). We found no differences in PPD of leIPSCs at 100, 250 and 500 ms ISI between RK and control animals, indicating that P_r of GABA is not altered by hyperexcitable conditions. Another measure of efficacy of GABA release is usually obtained by analyzing the amplitude and degree of depression of 10 or more consecutive responses at 10–50 Hz (Baldelli et al., 2005; Hefft and Jonas, 2005). At a stimulation frequency of 10 Hz, we found that only leIPSC10/leIPSC1 was different between controls and RK animals, but stimulating PV cells at 20 Hz unveiled an increase in the leIPSCn/leIPSC1 from the 5th stimulation onwards, indicating that, during periods of sustained high frequency activity in hyperexcitable conditions, PV cells respond with increased GABA release over time of stimulation. This finding suggests that the readily released pool (RRP) of GABA may be higher in hyperexcitable animals. However, quantifying RRP is not possible in our conditions, since the amplitudes of leIPSCs cannot be directly compared between different recordings. The amplitude of a given leIPSC is directly proportional to the number of pre-synaptic PV cells or their fibers activated by the light pulses, which is to some extent dependent on the precision and efficiency of viral infection in the particular slice and is not quantifiable.

A possible explanation underlying the increased GABA release observed here during repetitive stimulation could be an increased expression of ChR2 in RK animals compared to controls. After Cre-mediated recombination, which reaches the maximum at 7 days from viral injection (Kaspar et al., 2002), the expression levels of ChR2 are controlled by the strength of the EF1a promoter, therefore

differences in the expression of PV, and consequently activity of PV promoter, would not account for a change in ChR2 expression. Moreover, expression of PV seems to be decreased rather than increased in animal models of epilepsy and tissue from epilepsy patients (Sloviter et al., 2003; Wittner et al., 2005), and a hyperexcitability-mediated modulation of the strength of the general EF1a promoter seems unlikely, although it cannot be completely excluded.

An alternative explanation could be due to differences in GABAB receptor expression between controls and kindled animals. In fact, activation of pre-synaptic GABAB receptors induces inhibition of GABA release, and selective blockade of GABAB receptors reduces PPD (Davies et al., 1990), therefore decreased levels of GABAB receptor expression in RK animals could be responsible for the decreased depression of leIPSCs observed here during repetitive stimulations. Although GABAB receptor expression is highly modulated by seizures (Furtinger et al., 2003a; Furtinger et al., 2003b; Straessle et al., 2003), they are not expressed by PV cell terminals (Sloviter et al., 1999), and therefore it seems unlikely that changes in GABAB expression could explain the difference in leIPSCs depression at high frequencies described here.

The present findings seem to be in contrast with what was previously described in the pilocarpine model of epilepsy, where transmission at PV-GC synapses has been shown to be impaired, as measured by a trend towards decreased RRP and increased failure rate using paired recordings between PV-basket cell and granule cell (Zhang and Buckmaster, 2009). However, the differences in design of the two studies might explain this controversy. First, systemic pilocarpine injection produces high levels of cell death and inflammation (Voutsinos-Porche et al., 2004), along with hyperthermia and ischemic damage (Fabene et al., 2007), and therefore alterations in synaptic transmission observed in this model might not only be dependent on increased excitability. On the contrary, the RK model used here induces hyperexcitability with minimal cell death and inflammation (Wood et al., 2011). Second, paired recordings only allow to study the interaction between two cells, while the optogenetic approach used here permits to investigate the effect of stimulating the entire PV ensemble, in a more physiological, and more sensitive manner (Galarreta and Hestrin, 1999).

Functional implications

Here we show that hyperexcitability induces an increase in GABA release endurance at PV-GC synapses during sustained activity. This observation might result in two possible scenarios. (i) Overall

inhibitory drive of granule cells seems to be decreased in animal models of epilepsy, as measured by a decrease in the frequency of spontaneous and miniature IPSCs (Kobayashi and Buckmaster, 2003; Jakubs et al., 2006), but new evidence suggests that perisomatic inhibitory input is preserved, and that PV cells might be resistant to seizure-induced cell death (Wyeth et al., 2010). Therefore, increased GABA release from PV cells could partially respond to the loss of inhibition from other cell types and counteract the increased excitability of the network.

(ii) On the other hand, inhibitory action exerted by GABA is not the only mechanism by which inhibitory interneurons could regulate epileptiform activity and seizures (Avoli and de Curtis, 2011). Due to the strategic location of their inhibitory synapses, onto the soma, proximal dendrites and axon initial segment of principal cells, perisomatic interneurons are highly suited to control synchrony of principal cells ensembles. Therefore, an increased GABA release from PV cells onto granule cells would consequently support more efficient synchronization of high number of granule cells, and promote the development of epileptiform discharges. In addition, collaterals of aberrant sprouted mossy fibers, that develop in hyperexcitable environments (Elmer et al., 1996; Nadler, 2003), make synaptic contacts with both granule cells and PV cells (Kotti et al., 1997; Sloviter et al., 2006), and might further increase the intrinsic resonance of the oscillatory network.

References

- Atasoy D, Aponte Y, Su HH, Sternson SM (2008) A FLEX switch targets Channelrhodopsin-2 to multiple cell types for imaging and long-range circuit mapping. *J Neurosci* 28:7025-7030.
- Avoli M, de Curtis M (2011) GABAergic synchronization in the limbic system and its role in the generation of epileptiform activity. *Progress in neurobiology* 95:104-132.
- Baldelli P, Hernandez-Guijo JM, Carabelli V, Carbone E (2005) Brain-derived neurotrophic factor enhances GABA release probability and nonuniform distribution of N- and P/Q-type channels on release sites of hippocampal inhibitory synapses. *J Neurosci* 25:3358-3368.
- Bausch SB (2005) Axonal sprouting of GABAergic interneurons in temporal lobe epilepsy. *Epilepsy & behavior* : E&B 7:390-400.
- Bischofberger J, Engel D, Li L, Geiger JR, Jonas P (2006) Patch-clamp recording from mossy fiber terminals in hippocampal slices. *Nat Protoc* 1:2075-2081.
- Blasco-Ibanez JM, Martinez-Guijarro FJ, Freund TF (2000) Recurrent mossy fibers preferentially innervate parvalbumin-immunoreactive interneurons in the granule cell layer of the rat dentate gyrus. *Neuroreport* 11:3219-3225.
- Boyden ES, Zhang F, Bamberg E, Nagel G, Deisseroth K (2005) Millisecond-timescale, genetically targeted optical control of neural activity. *Nature neuroscience* 8:1263-1268.
- Buhl EH, Halasy K, Somogyi P (1994) Diverse sources of hippocampal unitary inhibitory postsynaptic potentials and the number of synaptic release sites. *Nature* 368:823-828.
- Cardin JA, Carlen M, Meleis K, Knoblich U, Zhang F, Deisseroth K, Tsai LH, Moore CI (2009) Driving fast-spiking cells induces gamma rhythm and controls sensory responses. *Nature* 459:663-667.
- Cobb SR, Buhl EH, Halasy K, Paulsen O, Somogyi P (1995) Synchronization of neuronal activity in hippocampus by individual GABAergic interneurons. *Nature* 378:75-78.
- Davies CH, Davies SN, Collingridge GL (1990) Paired-pulse depression of monosynaptic GABA-mediated inhibitory postsynaptic responses in rat hippocampus. *The Journal of physiology* 424:513-531.
- Elmer E, Kokaia M, Kokaia Z, Ferencz I, Lindvall O (1996) Delayed kindling development after rapidly recurring seizures: relation to mossy fiber sprouting and neurotrophin, GAP-43 and dynorphin gene expression. *Brain Res* 712:19-34.
- Eslamboli A, Georgievska B, Ridley RM, Baker HF, Muzyczka N, Burger C, Mandel RJ, Annett L, Kirik D (2005) Continuous low-level glial cell line-derived neurotrophic factor delivery using recombinant adeno-associated viral vectors provides neuroprotection and induces behavioral recovery in a primate model of Parkinson's disease. *J Neurosci* 25:769-777.
- Fabene PF, Merigo F, Galie M, Benati D, Bernardi P, Farace P, Nicolato E, Marzola P, Sbarbati A (2007) Pilocarpine-induced status epilepticus in rats involves ischemic and excitotoxic mechanisms. *PLoS one* 2:e1105.
- Ferezou I, Cauli B, Hill EL, Rossier J, Hamel E, Lambolez B (2002) 5-HT₃ receptors mediate serotonergic fast synaptic excitation of neocortical vasoactive intestinal peptide/cholecystokinin interneurons. *J Neurosci* 22:7389-7397.
- Freedman R, Wetmore C, Stromberg I, Leonard S, Olson L (1993) Alpha-bungarotoxin binding to hippocampal interneurons: immunocytochemical characterization and effects on growth factor expression. *J Neurosci* 13:1965-1975.
- Freund TF (2003) Interneuron Diversity series: Rhythm and mood in perisomatic inhibition. *Trends in neurosciences* 26:489-495.
- Freund TF, Katona I (2007) Perisomatic inhibition. *Neuron* 56:33-42.
- Furtinger S, Bettler B, Sperk G (2003a) Altered expression of GABAB receptors in the hippocampus after kainic-acid-induced seizures in rats. *Brain research Molecular brain research* 113:107-115.
- Furtinger S, Pirker S, Czech T, Baumgartner C, Sperk G (2003b) Increased expression of gamma-aminobutyric acid type B receptors in the hippocampus of patients with temporal lobe epilepsy. *Neurosci Lett* 352:141-145.
- Galarreta M, Hestrin S (1999) A network of fast-spiking cells in the neocortex connected by electrical synapses. *Nature* 402:72-75.
- Gobbi M, Gariboldi M, Piwko C, Hoyer D, Sperk G, Vezzani A (1998) Distinct changes in peptide YY binding to, and mRNA levels of, Y1 and Y2 receptors in the rat hippocampus associated with kindling epileptogenesis. *Journal of neurochemistry* 70:1615-1622.
- Gruber B, Greber S, Rupp E, Sperk G (1994) Differential NPY mRNA expression in granule cells and interneurons of the rat dentate gyrus after kainic acid injection. *Hippocampus* 4:474-482.
- Gulyas AI, Megias M, Emri Z, Freund TF (1999) Total number and ratio of excitatory and inhibitory synapses converging onto single interneurons of different types in the CA1 area of the rat hippocampus. *J Neurosci* 19:10082-10097.
- Hefft S, Jonas P (2005) Asynchronous GABA release generates long-lasting inhibition at a hippocampal interneuron-principal neuron synapse. *Nature neuroscience* 8:1319-1328.
- Hippenmeyer S, Vrieseling E, Sigrist M, Portmann T, Laengle

- C, Ladle DR, Arber S (2005) A developmental switch in the response of DRG neurons to ETS transcription factor signaling. *PLoS biology* 3:e159.
- Jakubs K, Nanobashvili A, Bonde S, Ekdahl CT, Kokaia Z, Kokaia M, Lindvall O (2006) Environment matters: synaptic properties of neurons born in the epileptic adult brain develop to reduce excitability. *Neuron* 52:1047-1059.
- Kaspar BK, Vissel B, Bengoechea T, Crone S, Randolph-Moore L, Muller R, Brandon EP, Schaffer D, Verma IM, Lee KF, Heinemann SF, Gage FH (2002) Adeno-associated virus effectively mediates conditional gene modification in the brain. *Proceedings of the National Academy of Sciences of the United States of America* 99:2320-2325.
- Katona I, Sperlagh B, Sik A, Kafalvi A, Vizi ES, Mackie K, Freund TF (1999) Presynaptically located CB1 cannabinoid receptors regulate GABA release from axon terminals of specific hippocampal interneurons. *J Neurosci* 19:4544-4558.
- Klapstein GJ, Colmers WF (1993) On the sites of presynaptic inhibition by neuropeptide Y in rat hippocampus in vitro. *Hippocampus* 3:103-111.
- Klausberger T, Magill PJ, Marton LF, Roberts JD, Cobden PM, Buzsaki G, Somogyi P (2003) Brain-state- and cell-type-specific firing of hippocampal interneurons in vivo. *Nature* 421:844-848.
- Kobayashi M, Buckmaster PS (2003) Reduced inhibition of dentate granule cells in a model of temporal lobe epilepsy. *The Journal of neuroscience : the official journal of the Society for Neuroscience* 23:2440-2452.
- Koffler N, Kirchmair E, Schwarzer C, Sperk G (1997) Altered expression of NPY-Y1 receptors in kainic acid induced epilepsy in rats. *Neurosci Lett* 230:129-132.
- Kotti T, Riekkinen PJ, Sr., Miettinen R (1997) Characterization of target cells for aberrant mossy fiber collaterals in the dentate gyrus of epileptic rat. *Exp Neurol* 146:323-330.
- Kraushaar U, Jonas P (2000) Efficacy and stability of quantal GABA release at a hippocampal interneuron-principal neuron synapse. *J Neurosci* 20:5594-5607.
- Ledri M, Sorensen AT, Erdelyi F, Szabo G, Kokaia M (2011) Tuning afferent synapses of hippocampal interneurons by neuropeptide Y. *Hippocampus* 21:198-211.
- Madisen L, Zwingman TA, Sunkin SM, Oh SW, Zariwala HA, Gu H, Ng LL, Palmiter RD, Hawrylycz MJ, Jones AR, Lein ES, Zeng H (2010) A robust and high-throughput Cre reporting and characterization system for the whole mouse brain. *Nature neuroscience* 13:133-140.
- Marksteiner J, Ortler M, Bellmann R, Sperk G (1990) Neuropeptide Y biosynthesis is markedly induced in mossy fibers during temporal lobe epilepsy of the rat. *Neurosci Lett* 112:143-148.
- McQuiston AR, Colmers WF (1996) Neuropeptide Y2 receptors inhibit the frequency of spontaneous but not miniature EPSCs in CA3 pyramidal cells of rat hippocampus. *Journal of neurophysiology* 76:3159-3168.
- Miles R, Toth K, Gulyas AI, Hajos N, Freund TF (1996) Differences between somatic and dendritic inhibition in the hippocampus. *Neuron* 16:815-823.
- Nadler JV (2003) The recurrent mossy fiber pathway of the epileptic brain. *Neurochemical research* 28:1649-1658.
- Nagel G, Brauner M, Lieuwald JF, Adeishvili N, Bamberg E, Gottschalk A (2005) Light activation of channelrhodopsin-2 in excitable cells of *Caenorhabditis elegans* triggers rapid behavioral responses. *Current biology : CB* 15:2279-2284.
- Porter JT, Cauli B, Tsuzuki K, Lambolez B, Rossier J, Audinat E (1999) Selective excitation of subtypes of neocortical interneurons by nicotinic receptors. *J Neurosci* 19:5228-5235.
- Racine RJ (1972) Modification of seizure activity by electrical stimulation. II. Motor seizure. *Electroencephalogr Clin Neurophysiol* 32:281-294.
- Schwarzer C, Koffler N, Sperk G (1998) Up-regulation of neuropeptide Y-Y2 receptors in an animal model of temporal lobe epilepsy. *Mol Pharmacol* 53:6-13.
- Sloviter RS, Zappone CA, Harvey BD, Frotscher M (2006) Kainic acid-induced recurrent mossy fiber innervation of dentate gyrus inhibitory interneurons: possible anatomical substrate of granule cell hyper-inhibition in chronically epileptic rats. *The Journal of comparative neurology* 494:944-960.
- Sloviter RS, Ali-Akbadian L, Elliott RC, Bower BJ, Bower NG (1999) Localization of GABA(B) (R1) receptors in the rat hippocampus by immunocytochemistry and high resolution autoradiography, with specific reference to its localization in identified hippocampal interneuron subpopulations. *Neuropharmacology* 38:1707-1721.
- Sloviter RS, Zappone CA, Harvey BD, Bumanglag AV, Bender RA, Frotscher M (2003) "Dormant basket cell" hypothesis revisited: relative vulnerabilities of dentate gyrus mossy cells and inhibitory interneurons after hippocampal status epilepticus in the rat. *The Journal of comparative neurology* 459:44-76.
- Sohal VS, Zhang F, Yizhar O, Deisseroth K (2009) Parvalbumin neurons and gamma rhythms enhance cortical circuit performance. *Nature* 459:698-702.
- Somogyi P, Klausberger T (2005) Defined types of cortical interneurone structure space and spike timing in the hippocampus. *The Journal of physiology* 562:9-26.
- Sorensen AT, Nikitidou L, Ledri M, Lin EJ, During MJ, Kanter-Schiffke I, Kokaia M (2009) Hippocampal NPY gene transfer attenuates seizures without affecting epilepsy-induced impairment of LTP. *Exp Neurol* 215:328-333.
- Stanic D, Brumovsky P, Fetisov S, Shuster S, Herzog H, Hokfelt T (2006) Characterization of neuropeptide Y2 receptor protein expression in the mouse brain. I. Distribution in cell bodies and nerve terminals. *The Journal of comparative neurology* 499:357-390.
- Straessle A, Loup F, Arabadzisz D, Ohning GV, Fritschy JM (2003) Rapid and long-term alterations of hippocampal GABAB receptors in a mouse model of temporal lobe epilepsy. *The European journal of neuroscience* 18:2213-2226.
- Szabadics J, Varga C, Molnar G, Olah S, Barzo P, Tamas G (2006) Excitatory effect of GABAergic axo-axonic cells in cortical microcircuits. *Science* 311:233-235.
- Traub RD, Kopell N, Bibbig A, Buhl EH, LeBeau FE, Whittington MA (2001) Gap junctions between interneuron dendrites can enhance synchrony of gamma oscillations in distributed networks. *J Neurosci* 21:9478-9486.
- Traub RD, Pais I, Bibbig A, LeBeau FE, Buhl EH, Garner H, Monyer H, Whittington MA (2005) Transient depression of excitatory synapses on interneurons contributes to epileptiform bursts during gamma oscillations in the mouse hippocampal slice. *Journal of neurophysiology* 94:1225-1235.
- Tukker JJ, Fuentealba P, Hartwich K, Somogyi P, Klausberger T (2007) Cell type-specific tuning of hippocampal interneuron firing during gamma oscillations in vivo. *J Neurosci* 27:8184-8189.
- Vezzani A, Sperk G, Colmers WF (1999) Neuropeptide Y: emerging evidence for a functional role in seizure modulation. *Trends in neurosciences* 22:25-30.
- Voutsinos-Porche B, Koning E, Kaplan H, Ferrandon A, Guenounou M, Nehlig A, Motte J (2004) Temporal patterns of the cerebral inflammatory response in the rat lithium-pilocarpine model of temporal lobe epilepsy. *Neurobiology of disease* 17:385-402.
- Wittner L, Eross L, Czirjak S, Halasz P, Freund TF, Maglóczy Z (2005) Surviving CA1 pyramidal cells receive intact perisomatic inhibitory input in the human epileptic

Manuscript

- hippocampus. *Brain : a journal of neurology* 128:138-152.
- Wittner L, Magloczky Z, Borhegyi Z, Halasz P, Toth S, Eross L, Szabo Z, Freund TF (2001) Preservation of perisomatic inhibitory input of granule cells in the epileptic human dentate gyrus. *Neuroscience* 108:587-600.
- Wood JC, Jackson JS, Jakubs K, Chapman KZ, Ekdahl CT, Kokaia Z, Kokaia M, Lindvall O (2011) Functional integration of new hippocampal neurons following insults to the adult brain is determined by characteristics of pathological environment. *Exp Neurol* 229:484-493.
- Wyeth MS, Zhang N, Mody I, Houser CR (2010) Selective reduction of cholecystokinin-positive basket cell innervation in a model of temporal lobe epilepsy. *J Neurosci* 30:8993-9006.
- Zhang W, Buckmaster PS (2009) Dysfunction of the dentate basket cell circuit in a rat model of temporal lobe epilepsy. *J Neurosci* 29:7846-7856.